



University of HUDDERSFIELD

University of Huddersfield Repository

Woods, Louis

The Measurement of Audio Transformer Colouration

Original Citation

Woods, Louis (2019) The Measurement of Audio Transformer Colouration. Masters thesis, University of Huddersfield.

This version is available at <http://eprints.hud.ac.uk/id/eprint/35000/>

The University Repository is a digital collection of the research output of the University, available on Open Access. Copyright and Moral Rights for the items on this site are retained by the individual author and/or other copyright owners. Users may access full items free of charge; copies of full text items generally can be reproduced, displayed or performed and given to third parties in any format or medium for personal research or study, educational or not-for-profit purposes without prior permission or charge, provided:

- The authors, title and full bibliographic details is credited in any copy;
- A hyperlink and/or URL is included for the original metadata page; and
- The content is not changed in any way.

For more information, including our policy and submission procedure, please contact the Repository Team at: E.mailbox@hud.ac.uk.

<http://eprints.hud.ac.uk/>

The Measurement of Audio Transformer Colouration

By

Louis Woods

A Thesis Submitted to the University of Huddersfield in Partial
Fulfilment of the Requirements for the degree of

MSc by Research (Engineering)

School of Computing and Engineering
The University of Huddersfield
Queensgate
Huddersfield
HD1 3DH

January 2019

Copyright Statement

- i. The author of this thesis (including any appendices and/ or schedules to this thesis) owns any copyright in it (the “Copyright”) and s/he has given The University of Huddersfield the right to use such Copyright for any administrative, promotional, educational and/or teaching purposes.
- ii. Copies of this thesis, either in full or in extracts, may be made only in accordance with the regulations of the University Library. Details of these regulations may be obtained from the Librarian. Details of these regulations may be obtained from the Librarian. This page must form part of any such copies made.
- iii. The ownership of any patents, designs, trademarks and any and all other intellectual property rights except for the Copyright (the “Intellectual Property Rights”) and any reproductions of copyright works, for example graphs and tables (“Reproductions”), which may be described in this thesis, may not be owned by the author and may be owned by third parties. Such Intellectual Property Rights and Reproductions cannot and must not be made available for use without permission of the owner(s) of the relevant Intellectual Property Rights and/or Reproductions.

Abstract

This thesis presents and discusses research undertaken into the detection and measurement of colouration produced by audio transformers. It is common for transformers to be subjectively described by audio professionals as ‘warm’, ‘fat’, ‘smooth’, etc. however there is little evidence to show if there is an audible difference and if there is a correlation between these levels of perceptual attributes and the performance of the device. Therefore, the research question was defined as: is there an audible difference with a transformer?

A review of the objective and subjective elements of the study was conducted. First the history, application and operation of the audio transformer with an aim to understand the objective measures and performance of the device with focus on the nonlinear distortion response. This also includes the design and testing of a suitable test circuit used in the measurement method. The subjective review concerns perception of distortion and testing methodologies for investigating audible differences. The conclusion of the review is that few pieces of research exist showing the relationship between device, distortion and perception.

The testing of each transformer involved the use of a specially designed test circuit using a variety of measures including THD+N and frequency domain analysis, to provide the most information about the operation of the device. Using the same setup, the device responses to a variety of samples were recorded and implemented in a double-blind triple-stimulus with hidden reference test using trained listeners in accordance with the ITU-R BS.1116-3 recommendation. The test results were then analysed for a random distribution using a 1-tailed binomial test. The results of the analysis show a high likelihood that the bass samples were audibly different shown by the significant p-values of all 3 samples at less than 0.001. A slight correlation seems to exist with THD+N, 3rd harmonic distortion and level however with no other obvious trends, it was concluded that the distortion and therefore the audibility is programme dependent.

It was concluded that transformers are likely to produce a level of distortion deemed audible although the effect is considered to be programme dependent.

Table of Contents

ABSTRACT	3
LIST OF FIGURES	5
LIST OF TABLES	7
ACKNOWLEDGEMENTS.....	8
ABBREVIATIONS/ NOMENCLATURE	9
CHAPTER 1: INTRODUCTION	11
CHAPTER 2: LITERATURE REVIEW	13
2.1 ELECTROMAGNETIC INDUCTION AND THE TRANSFORMER.....	13
2.2 USE OF TRANSFORMERS IN AUDIO APPLICATIONS.....	17
2.3 TRANSFORMER OPERATION	19
2.4 TRANSFORMER MATERIALS AND CONSTRUCTION	27
2.5 PERCEPTION OF DISTORTION	34
2.6 TEST CIRCUIT DESIGN.....	38
2.7 LISTENING TEST DESIGN	46
CHAPTER 3: OBJECTIVE TESTING	51
3.1 TRANSFORMERS.....	51
3.2 METHOD.....	54
3.3 RESULTS	71
CHAPTER 4: SUBJECTIVE ANALYSIS	91
4.1 STIMULI	91
4.2 LISTENING SUBJECTS.....	93
4.3 LISTENING ENVIRONMENT AND PLAYBACK SYSTEM	94
4.4 METHOD.....	96
4.5 RESULTS	100
CHAPTER 5: DISCUSSION	111
CHAPTER 6: CONCLUSION.....	115
6.1 FUTURE WORK	117
REFERENCES	118
APPENDIX A- DSCOPE SIGNAL ANALYSER MEASURES	124
APPENDIX B- TEST CIRCUIT MEASURES	127
APPENDIX C- LUNDAHL LL1582 MEASURES	131
APPENDIX D- CARNHILL VTB1148 MEASURES	135
APPENDIX E- SPECTROGRAM ANALYSIS	141

List of Figures

Figure 1. Michael Faraday's Induction Ring-Coil Apparatus (The Faraday Museum- The Royal Institution, 2014)	15
Figure 2. Operation of an Ideal Transformer (“Transformer,” 2006).....	19
Figure 3. Iron-Cored Transformer Electronic Symbol (“Transformer Iron Core,” 2006).....	20
Figure 4. Hysteresis Loop - B-H Plot (NDT Education Resource Center, 2018)	22
Figure 5. Rotation of Magnetic Domains in a Magnetic Material (“Dominios,” 2004).....	23
Figure 6. Transformer Equivalent Circuit (Reeder, 2005)	24
Figure 7. C Core Half (“C Core,” 2007)	30
Figure 8. Laminated E-I Transformer Core Design (right) (“Transformer Core Interleaved,” 2007)	31
Figure 9. Test Circuit Schematic	40
Figure 10. AD8429 Simplified Schematic (Analog Devices, 2017)	41
Figure 11. Lundahl LL1582 Line Output Transformer.....	51
Figure 12. Carnhill VTB1148 Line Output Transformer	52
Figure 13. A Total Harmonic Distortion Plus Noise (THD+N) versus Frequency Graph	56
Figure 14. A Total Harmonic Distortion Plus Noise (THD+N) versus Amplitude Graph	57
Figure 15. Test Circuit- THD+N vs Frequency- 0dB Gain.....	65
Figure 16. Test Circuit- THD+N vs Amplitude- 0dB Gain	66
Figure 17. Measurement methods for Primary and Secondary Inductance (a. left), Leakage Inductance (b. centre) and Winding Capacitance (c. right) (Hioki, 2017).....	68
Figure 18. Mutual Inductance Measurement Methods: Aiding (left) and Opposing (right) (Hioki, 2017)	69
Figure 19. Test Circuit and Lundahl LL1582- Frequency Response- 0dB Gain	72
Figure 20. Test Circuit and Lundahl LL1582- Phase Response- 0dB Gain.....	73
Figure 21. Test Circuit and Lundahl LL1582- THD+N vs Frequency- 0dB Gain.....	74
Figure 22. Test Circuit and Lundahl LL1582- THD+N vs Amplitude- 0dB Gain.....	75
Figure 23. Test Circuit and Lundahl LL1582- FFT at 20Hz -38dBu Input- 0dB Gain	76
Figure 24. Approximate hysteresis measurement of LL1582- 20Vp-p input at 20Hz	77
Figure 25. Test Circuit and Lundahl LL1582- THD+N vs Amplitude- +16dB Gain.....	78
Figure 26. Test Circuit and Lundahl LL1582- FFT at 20Hz +4dBu Input- +16dB Gain	79
Figure 27. Test Circuit and Lundahl LL1582- FFT at 1kHz +4dBu Input- +16dB Gain	80
Figure 28. Test Circuit and Carnhill VTB1148- Frequency Response- 0dB Gain.....	84
Figure 29. Test Circuit and Carnhill VTB1148- Phase Response- 0dB Gain.....	85
Figure 30. Test Circuit and Carnhill VTB1148- THD+N vs Frequency- 0dB Gain	86
Figure 31. Test Circuit and Carnhill VTB1148- THD+N vs Amplitude- 0dB Gain.....	87
Figure 32. Test Circuit and Carnhill VTB1148- FFT at 20Hz -38dBu Input- 0dB Gain	88
Figure 33. The Applied Psychoacoustic Laboratory at The University of Huddersfield (University of Huddersfield, 2019)	94
Figure 34. The Listening Test User Interface Implemented on HULTI-GEN (Gribben & Lee, 2015)	97
Figure 35. Correct Identifications of Each Sample Per Subject- LL1582 Tests	101
Figure 36. Mean Correct Identifications with 95% CI Error Bars for All Subjects- LL1582 Tests	102
Figure 37. Correct Identifications of Each Sample Per Subject- VTB1148 Tests	107
Figure 38. Mean Correct Identifications with 95% CI Error Bars for All Subjects- VTB1148 Tests	108
Figure 39. dScope Series III Self-Test THD+N vs Frequency.....	124
Figure 40. dScope Series III Self-Test THD+N vs Amplitude	125
Figure 41. dScope Series III Self-Test- FFT at 20Hz +4dBu Input.....	126
Figure 42. Test Circuit- Frequency Response- 0dB Gain	127
Figure 43. Test Circuit- Phase Response- 0dB Gain	128
Figure 44. Test Circuit- FFT at 1kHz -38dBu Input- 0dB Gain.....	129
Figure 45. Test Circuit- Jensen MT Test- 0dB Gain	130
Figure 46. Test Circuit and Lundahl LL1582- Jensen MT Test- 0dB Gain.....	131
Figure 47. Test Circuit and Lundahl LL1582- Frequency Response- +6dB Gain	132
Figure 48. Test Circuit and Lundahl LL1582- THD+N vs Amplitude- +6dB Gain	133
Figure 49. Test Circuit and Lundahl LL1582- Frequency Response- +16dB Gain	134
Figure 50. Test Circuit and Carnhill VTB1148- FFT at 1kHz +4dBu Input- 0dB Gain	135
Figure 51. Test Circuit and Carnhill VTB1148- Jensen MT Test- 0dB Gain.....	136
Figure 52. Test Circuit and Carnhill VTB1148- THD+N vs Amplitude- +6dB Gain.....	137
Figure 53. Test Circuit and Carnhill VTB1148- THD+N vs Frequency- +16dB Gain	138
Figure 54. Test Circuit and Carnhill VTB1148- THD+N vs Amplitude- +16dB Gain.....	139
Figure 55. Test Circuit and Carnhill VTB1148- FFT at 20Hz +4dBu Input- +16dB Gain	140

Figure 56. Test Circuit- Bass Sample- 0dB Gain	141
Figure 57. Test Circuit and Lundahl LL1582- Bass Sample- 0dB Gain.....	142
Figure 58. Test Circuit and Lundahl LL1582- Bass Sample- +6dB Gain	143
Figure 59. Test Circuit and Lundahl LL1582- Bass Sample- +16dB Gain	144
Figure 60. Test Circuit- Double Bass Sample- 0dB Gain.....	145
Figure 61. Test Circuit and Lundahl LL1582- Double Bass Sample- 0dB Gain	146
Figure 62. Test Circuit and Lundahl LL1582- Double Bass Sample- +6dB Gain	147
Figure 63. Test Circuit and Lundahl LL1582- Double Bass Sample- +16dB Gain	148
Figure 64. Test Circuit and Carnhill VTB1148- Double Bass Sample- 0dB Gain.....	149
Figure 65. Test Circuit and Carnhill VTB1148- Double Bass Sample- +6dB Gain	150
Figure 66. Test Circuit- Snare Drum Sample- 0dB Gain.....	151
Figure 67. Test Circuit and Carnhill VTB1148- Snare Drum Sample- 0dB Gain	152
Figure 68. Test Circuit and Carnhill VTB1148- Snare Drum Sample- +6dB Gain	153

List of Tables

Table 1. AD8429 and NE5532 IC Specifications.....	39
Table 2. Output Signal Levels with Relation to Input Signal Level.....	44
Table 3. Transformer Specifications.....	53
Table 4. Listening Test Structure Per Subject.....	98
Table 5. Lundahl LL1582 Subjective Statistical Analysis Results- Heatmap (95% & 99% CI).....	103
Table 6. Lundahl LL1582 Subjective Statistical Analysis Results- Significant p-values (95% CI).....	104
Table 7. Lundahl LL1582 Subjective Statistical Analysis Results- Significant p-values (99% CI).....	105
Table 8. Carnhill VTB1148 Subjective Statistical Analysis Results- Heatmap (95% & 99% CI).....	109
Table 9. Carnhill VTB1148 Subjective Statistical Analysis Results- Significant p-values (95% & 99% CI)	109

Acknowledgements

Thank you to my supervisor Dr. Steven Fenton for his support and guidance throughout the research and to the University of Huddersfield for the opportunity to carry out this research through the Vice-Chancellor Scholarship.

A big thank you to Per Lundahl and Lundahl Transformers and Carnhill Transformers Ltd. for generously providing all the transformers used in the study. I would also like to thank all members of the Applied Psychoacoustic Laboratory at the University of Huddersfield for being so welcoming and supportive and to all those who took part in the listening tests.

Thank you to my friends and family especially my mum, dad and sister for their continued love and support over the course of this work and a special thank you to my partner Georgia for her unwavering belief, encouragement and love that has pushed me through.

Abbreviations/ Nomenclature

AC	Alternating Current
AI	Artificial Intelligence
API	Application Programming Interface
A/m	Amperes per metre
<i>B</i>	Magnetic Flux Density
BJT	Bipolar Junction Transistor
<i>C</i>	Capacitance
C.G.S.	Centimetre-Gram-Second
CI	Confidence Interval
CMRR	Common-Mode Rejection Ratio
DAW	Digital Audio Workstation
DC	Direct Current
DIM	Dynamic Intermodulation Distortion
DMM	Digital Multi-Meter
DUT	Device Under Test
DMM	Digital Multi-Meter
EBU	European Broadcasting Union
EMC	Electromagnetic Compatibility
emf	Electromotive Force
EMI	Electromagnetic Interference
FFT	Fast Fourier Transform
GUI	Graphical User Interface
H	Henry
<i>H</i>	Magnetising Force
HULTI-GEN	Huddersfield University Listening Test Interface Generator
IC	Integrated Circuit
IEC	International Electrotechnical Commission
IMD	Intermodulation Distortion
ITU	International Telecommunication Union
<i>k</i>	Mutual Inductance Coupling Coefficient
<i>L</i>	Inductance

L_a	Aiding Inductance
L_o	Opposing Inductance
LCR	Inductance, Capacitance and Resistance
LKFS	Loudness K-rated Full Scale
LUFS	Loudness Units, referenced to Full Scale
M	Mutual Inductance
M.K.S.	Metre-Kilogram-Second
mmf	Magnetomotive Force
MT	Multi-Tone
Ni-Fe	Nickel-Iron
μ	Permeability
μ_0	Permeability of Free Space (Vacuum)
N	Turn Ratio
Op-amp	Operational Amplifier
Φ	Magnetic Flux
R	Resistance
RF	Radio Frequency
R_m	Reluctance
r.m.s.	Root Mean Square
SI	International System of Units
SMPTE	Society of Motion Picture and Television Engineers
SNR	Signal-to-Noise Ratio
SQAM	Sound Quality Assessment Material
SUT	Signal-Under-Test
T	Tesla
THD	Total Harmonic Distortion
THD+N	Total Harmonic Distortion Plus Noise
V_s	Power Supply Voltage
WAET	Web Audio Evaluation Tool
Wb	Weber

Chapter 1: Introduction

Since its invention in the early 1800s (Guarnieri, 2013) the transformer has revolutionised technology across nearly two centuries. From power to audio applications the device has proved a crucial building block in electronic design. Today transformers are fundamental to alternating current (AC) power distribution. However its importance in the audio signal chain has diminished since the invention and widespread use of the transistor, which largely replaced the existing thermionic valve technology (Scafe, 2017). Although audio transformers fell from popularity in modern circuit design they never completely died out and are still used by some audio device manufacturers with many customers showing a preference towards this equipment. A large amount of this equipment described is often microphone preamplifiers which are praised for the impact of their transformers on the sound especially when used creatively to not only amplify the low-level signal from the microphone but to drive the circuit ‘hard’ or at high-levels to produce ‘colouration’. It is known that driving a transformer at high-levels produces a higher level of flux density and therefore distortion as described by Partridge (1942). This distortion is said to give the audio a ‘colour’ or tone with many people proclaiming how the equipment imparts a signature sound or colouration on the audio like that stated by Farmelo and Hampton (2010) who uses a selection of vocabulary to describe the characteristics of the devices as “fat lows, punchy mids and a silky top” with a variety of other descriptors used like ‘smooth’, ‘rich’, ‘bold’, ‘punchy’, ‘round’ etc. The desire for this colour is to creatively affect signals being recorded and mixed to create a track or song.

The explanation for the sonic character or colouration towards transformer-based equipment is vague with minimal written material and research in the area. Most written claims come from quotes in magazine articles and website forums in which many

producers, recording engineers and hobbyists base these observations upon empirical tests or experiences with equipment which contains transformers such as that by Schumacher (2005). To the author's knowledge there is no complete, published research into the sonic characteristics of the devices in isolation therefore it is felt that the observations leading to these claims are not scientifically tested and therefore no complete proof provided. The aim of this research is to discover if there is a perceptible difference when a transformer is present in the signal path and what is the cause of this effect.

Using electrical measurements of the components and psychoacoustic testing, this research aims to investigate if there is a perceptual difference and if so is there a correlation between the two measures. Standard electrical measures such as total harmonic distortion (THD) have been employed to give a broad picture of how the transformers operate under various conditions followed by psychoacoustic testing using ABX testing and finally statistical analysis of the results.

The long-term goal of this research is to further the understanding of electronic components used in the audio signal path, and the related perceptual effects which can then be used to model these characteristics and parameters for use in the design of audio equipment.

Chapter 2: Literature Review

This review covers the background of the transformer through its history, application, operation and construction to provide a concise overview of the device and the role it plays in audio electronics. Following from this, a selection of objective and subjective testing methods are assessed culminating in the design and build of a test circuit and listening test creating the method for testing of the transformers in this research.

2.1 Electromagnetic Induction and The Transformer

In 1820 the Danish scientist Hans Christian Ørsted (also known as Oersted) discovered that by placing a current-carrying wire near a compass, the compass needle was deflected, which showed that there was a relationship between electricity and magnetism (Tretkoff, Ramlagan, Chodos, & Ouellette, 2008). It was also discovered in the early 1800s by André-Marie Ampère that coiling a wire to create, what he called a solenoid, the magnetic field was channelled like that of a magnet with two opposite poles (Blondel & Wolff, 2013). However, it wasn't until later experiments by Michael Faraday in 1831 (Faraday, 1831) and later the mathematical proof by James Clerk Maxwell around 1862, that electromagnetic induction had truly been discovered (Turnbull, 2017). Through the four famous Maxwell's equations (in its modern form shown by equations 1-4) he proved the relationships between electricity, magnetism and light and thus the electromagnetic spectrum. The differential equations are:

$$\nabla \cdot D = \rho \quad (\text{Gauss' Law}) \quad (1)$$

$$\nabla \cdot B = 0 \quad (\text{Gauss' Law for Magnetism}) \quad (2)$$

$$\nabla \times E = -\frac{\partial B}{\partial t} \quad (\text{Faraday's Law}) \quad (3)$$

$$\nabla \times H = J + \frac{\partial D}{\partial t} \quad (\text{Ampère-Maxwell Law}) \quad (4)$$

where:

E is the electric field

ρ is free electric charge density

ϵ_0 is the permittivity of free space

B is the magnetic flux

t is time

H is the magnetising field strength

J is free current density

D is the electric displacement field

The Maxwell-Faraday equation or Faraday's Law (equation 3) is the basis of all electromagnetic induction. As stated by Jordan & Balmain (1968) "Faraday's Law, which states that the electromotive force around a closed path is equal to the negative of the time rate of change of magnetic flux enclosed by the path". It was famously demonstrated by Faraday how an electrical current applied to one coil induced a current in the second coil via a ferromagnetic core, by using his ring-coil apparatus (fig.1). Although Faraday demonstrated the principle by switching a direct current (DC) on and off, he had created the earliest known example of a transformer.



Figure 1. Michael Faraday's Induction Ring-Coil Apparatus (The Faraday Museum- The Royal Institution, 2014)

It would not be until over 40 years later that the idea was advanced further by various engineers and scientists: Sebastian Ziani de Ferranti and Lucien Gaulard in the 1880s and then a major development came with the suggestion of a closed-core transformer design by the Hungarian electrical engineer Ottó Bláthy in 1884 (Whelan, Rockwell, & Normandin, 2014). In 1885 the American, William Stanley, worked on the design of a more practical transformer which was then later used commercially in the USA in the transmission of power in 1886. It was also in 1890 when Sir James Alfred Ewing coined the term hysteresis to describe the resistance of a magnetic material to a changing magnetic field (Encyclopedia Britannica, 2019).

During the late 1800s and early 1900s the transformer design was utilised in telecommunications with the creation of the telephone hybrid (Sescom, 2019) which allowed two-way transmission of audio over telephone networks. This is one of the first commercial implementations of a transformer used to carry audio frequency AC. Following the invention of the first amplifying thermionic valve, the 'Audion' by Lee de Forest between 1906 and 1908 and later known as the triode (Fielding, 2018), there became a growing need to interface the high impedance valve with lower impedance circuits or components such as loudspeakers. The first application of the triode valve was in 1912 when de Forest used it for the amplification of radio waves containing speech and

music by cascading the valves and interfacing each stage with a transformer (Fielding, 2018).

With a new industry of communication growing and the outbreak of the first world war new devices were being created for applications such as radio communications which lead to a growing broadcast industry post-war and with the invention of 'talking pictures' in the 1920s, a drive for the goal of better audio quality such as a broader frequency range and lower distortion furthering the design of the transformer (Sescom, 2019). Sowter (1987) mentions how improvements with analogue disk and tape recording after 1945 continued to drive the development of the transformer bandwidth to operating between 40Hz to 16kHz and eventually 20Hz to 20kHz as is standard today.

With the growth of industries such as television broadcast, radio broadcast, high fidelity recording and live sound reinforcement in the 1950s came the need for higher quality components. It is also notable that the telephone industry was the primary user of audio transformers and continued to be so for many years with large companies such as Western Electric as industry leaders in the development of all aspects of the devices and methods of production (Sescom, 2019). With the invention of the transistor began the start of a gradual decrease in the importance of the audio transformer across a period of over 10 years and then a further decline with the invention and eventual wide spread use of the IC leading to the consequent removal of audio transformers from most circuit designs in the 1970/80s onwards due to expense and factors like weight and size (Sescom, 2019).

2.2 Use of Transformers in Audio Applications

The transformer has largely fallen from popularity in modern circuitry most likely due to expense, size and weight when compared with alternatives. Most of the applications of audio transformers have been replaced with RC (resistor-capacitor) filter circuits and IC op-amps more frequently in small signal designs. As mentioned in section 2.1: transformers are still fundamental to the clear majority of valve circuitry offering the most practical way of interfacing the high impedance valves to lower impedance circuits, whilst also providing galvanic isolation for safety, however they are still used in some transistor-based and even in some IC operational amplifier-based circuits.

Some professional audio equipment manufacturers still use transformers in their designs with many of their revered pieces of equipment containing transformers. Effects units such as the famed Teletronix LA-2A levelling amplifier and Urei 1176 limiting amplifier manufactured by Universal Audio use transformers at the input and output- although it is a salient fact that the LA-2A also contains thermionic valves which also play a role in the characteristic sound. The same is true for a selection of microphone preamplifiers such as the Neve 1073, api 512c and Golden Age Project pre-73. Although it is claimed that these devices colour the sound, the most information provided by manufacturers about the sonic qualities of a device such as “warmth” (AMS Neve, 2018) and “rich-sounding” (API, 2018), tends to be in the form of a written marketing profile for the piece of equipment in question, not in the form of a specification due to there being few standardised methods to quantify these qualities.

The transformer, although expensive and labour intensive to make, still offers the unique properties of both galvanic isolation and signal balancing reducing CMRR whilst

matching impedances of the two or more circuits it connects which cannot be done with any other single component.

The primary research is to discover if transformers could be the cause of an audible difference however the question arose during the course of this study to whether capacitor-based circuits could affect the circuit in a way that transformer-based circuits do not. This could then explain a possible cause of why a proportion of people feel that there is a difference with transformer-based. Papers such as that by Duncan, Dodds, and Williams (2008), Bateman (2002), Gaskell (2011) and van der Veen and van Maanen, (2008) discuss the distortions measured in capacitors. It must be noted that even in the perceptual-based studies there was not an immediate significant difference. In the paper by Gaskell (2011) it is concluded that there seemed to be a perceived effect caused by the capacitor distortion which has a non-linear, frequency-dependant performance. Although the perceived sound quality was not investigated further it was suggested that colouration was likely to occur. It is also concluded by van der Veen & van Maanen, (2008) that there are significant audible effects caused by the non-linear behaviour of the capacitor distortion with one major cause identified as the mechanical resonance of the device also found by Duncan et al. (2008).

2.3 Transformer Operation

The basic principle of a transformer's operation is to 'transform' a changing electric current in one coil of wire (the primary winding) into a changing magnetic field in the coil which creates magnetic flux (Φ) in the ferromagnetic core material which induces a changing electric current in a second coil of wire (the secondary winding) (fig.2). The purpose of this change between electrical and magnetic energy provides a method for balanced connection, increased common-mode rejection, galvanic isolation and supports different coils or windings of different specifications. Different winding configurations allow the preceding and succeeding circuits to match impedances removing the effects of loading either circuit. The electronic symbol for a simple transformer is shown in figure (3).

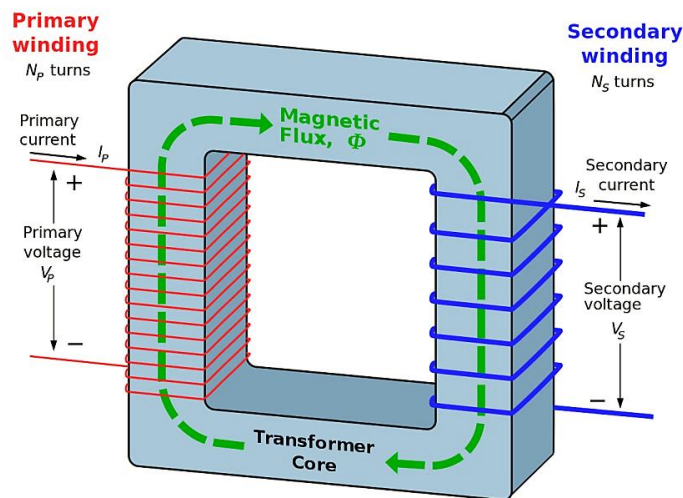


Figure 2. Operation of an Ideal Transformer ("Transformer," 2006)

A transformer can be categorised into two types of circuit: the electrical and the magnetic. As mentioned briefly in section 2.1, a wire passing current produces a magnetic field perpendicular to the flow of current. By placing two of the same conductors parallel to

each other the magnetic fields add therefore doubling the field intensity, so by coiling the conducting wire the magnetic field density greatly increases. Coiling the wire also changes the shape of the field to that of a bar magnet which helps to direct the magnetic flux in the magnetic core.

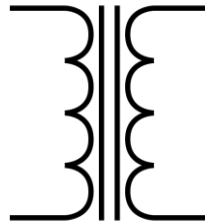


Figure 3. Iron-Cored Transformer Electronic Symbol (“Transformer Iron Core,” 2006)

Transformers often consist of more than a single primary and secondary winding, which offers the flexibility of different winding ratios. Through the different combinations of the primary to the secondary, by connecting them in parallel or series which determines the effective gain and impedance matching properties. This property of transformers allows the device to match impedances by ‘reflecting’ the impedance of each winding and connecting circuit to the opposite side. The windings also introduce some parasitic elements such as the wire material resistance, leakage inductance and a distributed or self-capacitance due to the proximity of adjacent wires. This stray capacitance can impact the high frequency response of transformer, but this is a compromise of having higher ratios to give better SNR whilst keeping the number of turns to minimum as the stray/interwinding capacitance will increase.

The magnetic core can be thought of as the magnetic circuit analogous to an electronic circuit. Equation 5 presents the formula for magnetomotive force (mmf) the equivalent to electromotive force (emf) in magnetics.

$$mmf = NI \quad (5)$$

where:

N is the number of turns

I is the current

The core is used to channel the magnetic flux from the primary winding to the secondary as efficiently as possible. As most of the flux produced by the primary is confined to the core (except for leakage inductance) this helps to further couple the two windings by providing a high-permeability path which can be thought of as offering a ‘path of least resistance’. However, there is a point when the core cannot contain anymore flux called saturation. After the this point the coil will revert back to reacting as though it was air-cored (McLyman, 2004) although the saturation results in an increase in harmonic distortion at the secondary winding.

The permeability of a material is a measure of its ability to conduct magnetic flux. The permeability of a vacuum (μ_0) is presented in equation 6 this also has a relative permeability of 1.0 with most ferromagnetic materials relative permeability over 4000 such as mumetal which has a permeability of over 2.5×10^{-2} and relative permeability over 20,000 (Nave, 2018). Equation 7 shows the relationship between permeability (μ), flux density (B) and field strength (H).

$$\mu_0 = 4\pi \times 10^{-7} = 1.257 \times 10^{-6} \quad [Hm^{-1}] \quad (6)$$

$$\mu = \frac{B}{H} \quad [Hm^{-1}] \quad (7)$$

Another property of the core is reluctance (R_m) which is the measure of the material's resistance to magnetic flux, analogous to resistance in an electrical circuit. Reluctance can be controlled with an air gap as most of the reluctance will be due to the high reluctivity of air in the gap compared to the low reluctivity of the core material. By controlling the level of reluctance, the correlation between B and H can be adjusted to create a more linear relationship.

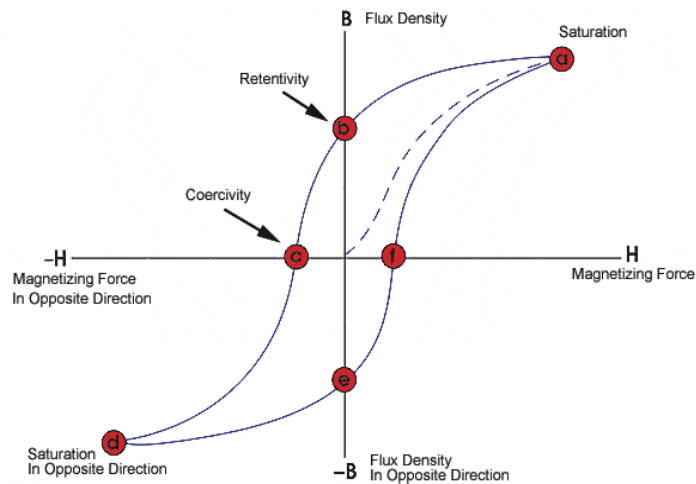


Figure 4. Hysteresis Loop - B-H Plot (NDT Education Resource Center, 2018)

Transformer core materials present a lag also known as Hysteresis (from the Greek word *hústeros* meaning late). Hysteresis is the delay of magnetic flux density (B) behind the magnetising force (H) which depends on the permeability of the magnetic core material. Hysteresis is represented with a hysteresis loop also known as a B-H curve, commonly in

the form a bi-directional sigmoid function (fig.4). The loop depicts how much energy is lost in the core.

The curve can be split into three constituent parts: coercivity, saturation and retentivity. The B-H curve is directly related to the magnetic structure of the core material which is made up of magnetic domains which further consist of magnetic di-poles. Each domain contains magnetic dipoles which can be thought of as miniature bar magnets which change direction when a magnetic field is applied. Each domain is then oriented in the direction of the magnetic field. When a magnetising current flows in the magnetising winding, the di-pole and therefore the domains resist the change of the magnetic field like an inductor, this level is shown by the coercivity having the unit Amperes per metre (A/m). When the current is removed there is a level of magnetism left in the material known as the retentivity, this is due to the lack of energy to force the di-poles/ domains to change orientation, this unit of measurement is the Tesla (T). Both these effects become more of a problem at low-signal levels as stated by van der Veen (2007) the nonlinear effect of these parameters cause a drop in the core's relative permeability and inductance. Finally, when all these di-poles are oriented in the same direction they cannot change any more, so are said to be saturated (fig.5). Transformer saturation, frequency and level will be investigated during the study.

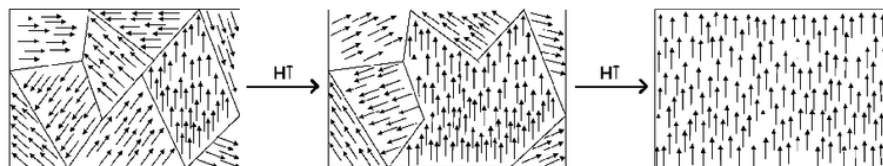


Figure 5. Rotation of Magnetic Domains in a Magnetic Material (“Dominios,” 2004)

A transformer however, is not a perfect electronic device and as mentioned above there are parasitic elements which can be viewed in the equivalent circuit (fig.6). As presented by the circuit diagram, the parasitic elements change at different frequencies and for ease can be categorised into three frequency bands: low, mid and high frequency. The performance of the device is characterised by these elements. These elements comprise of leakage inductance, inter-winding capacitance and winding resistance.

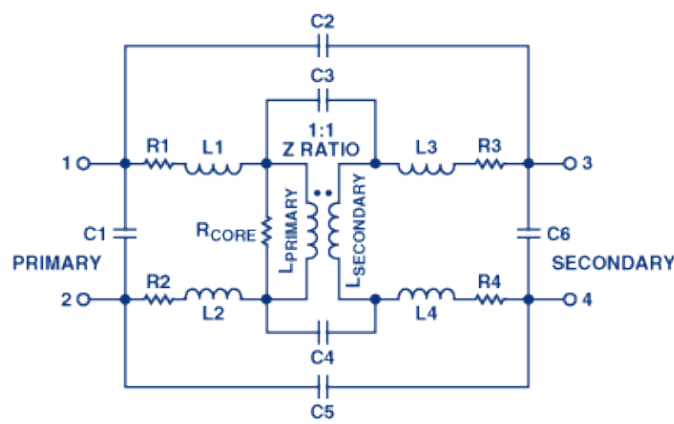


Figure 6. Transformer Equivalent Circuit (Reeder, 2005)

At low frequencies the response is largely determined by the number of turns of the primary winding and the core material and size. The core must be capable of containing the flux, at the maximum desired level at the lowest frequency, without saturating or producing large amounts of distortion. The level of distortion produced by the device is largely determined by the relationship between flux density and the magnetising force.

The winding resistance therefore the wire size must also be considered as this determines the overall impedance of the winding which needs to be kept small enough to avoid a large voltage across it. These parameters tend to determine the overall size of the transformer. The mid-frequency range up to approximately 10kHz poses the least problems due to the

high reactance of the primary which is mainly limited by the winding resistance and excessive iron losses.

At high frequencies the leakage inductance and parasitic capacitances can cause significant issues. The leakage inductance begins to cause a reduction in the amplitude of the signal across the secondary, this problem is normally rectified through the choice of winding format for example interleaving the windings reduces the amount of leakage. The parasitic capacitances consist of the self-capacitance, which is caused by the coils of wire being side-by-side producing a level of capacitance with the turns of wire adjacent, and inter-winding capacitance, that which is between the primary and secondary windings. More stray capacitance exists through the core and the electrostatic and electromagnetic shields which as suggested by Sowter (1987) can be combined to form a single stray capacitance value.

Fringing flux can also cause problems as discussed by McLyman (2004) it reduces the efficiency of the device and can cause eddy currents which in high-signal level devices can cause localised heating such as in the windings and brackets and can even cause premature saturation. Skin effect can also reduce the amount of effective permeability of a material, this predominantly occurs at high frequencies. Sowter (1987) explains how this is often observed with laminated cores and happens when flux concentrates on the outer surface of the laminations which is rectified by using thinner laminations.

There are many applications where this property is useful and often crucial which rely on the principles of galvanic isolation and common mode rejection. The common-mode rejection ratio (CMRR)- the measure of how effective a device is at rejecting concurrent

and in-phase signals on two inputs such as noise -is a principal factor when dealing with microphone and small-signal levels as any electromagnetic interference (EMI) can degrade the quality of the signal. Larger magnetic fields like that caused by substantial amounts of DC or a permanent magnet close to the transformer can cause it to assume a polarised state (magnetised) although as stated by Sowter (1987) this scarcely has a permanent effect, a polarised state does cause higher levels of distortion and a reduced output level. It is explained by Sowter (1987) that it is not easy for most Ni-Fe alloys such as mumetal to acquire a unidirectional magnetisation under normal operating conditions although silicon iron can become slightly polarised if it encounters low frequency AC or high-level transients close to the point of core saturation. The galvanic isolation also provides a level of safety from accidental electric shock in high voltage, high current circuits such as valve circuits. Transformers also block DC however even at a reasonably low-level it can cause asymmetric saturation of the core material affecting the transfer of the audio signal causing an increased level of distortion.

It is common for Zobel networks to be used, when designing with transformers, to control the effects of high frequency 'ringing' on the output signal of the device caused mainly by the parasitic leakage inductance of the transformer and load capacitance. A Zobel network, sometimes known as a damping network is an RC filter consisting of a resistor and capacitor connected together in series which is connected in parallel with the transformer secondary winding. This helps to reduce the resonating effects of the leakage inductance and load capacitance at high frequencies (Whitlock, 2002).

2.4 Transformer Materials and Construction

There are many transformer core designs used for a wide variety of applications however the ones most relevant to this research are those used to make the devices being tested: C-core, E-I core and the U-I core. The main two types of transformer construction are the shell and the core. This relates to the way in which the windings are situated on the core material: either in the centre of the core or surrounding respectively. These two can be split further into the shape and format of the material with common mediums being ferrite powder, laminations and wound which come in various formats such as the E-I core, C-core and U-I Core.

Hysteresis of a material is often measured using the ring method presented in EN IEC 60404-6:2003 (CENELEC, 2018). This involves winding a primary and secondary onto a ring or toroid of the sample material then measuring the current of the primary and the voltage of the secondary across the frequency range 20Hz-100kHz whilst increasing the magnetising current. These values can then be used to plot the B-H curve or AC magnetization curve. Another way to view the B-H plot using the same setup as above but to use an oscilloscope in X-Y mode connecting one channel to the primary winding and the other channel to the secondary winding.

Each material provides distinctive characteristics to the magnetic circuit analogous to a conductor in an electrical circuit. The permeability of the core material is a key factor when designing a transformer and can determine how the transformer performs. The material's permeability is often described as either hard or soft which "...is the measure of the ability of a material to support the formation of a magnetic field" ("Permeability (electromagnetism)," n.d.). Many core materials exist and are used for a wide variety of

applications for instance: grain-oriented silicon steel also known as electrical steel (such as Hi-B steel), Ni-Fe alloys (such as mumetal and Supermalloy), ferrite powder, metallic glass etc. There are also many different constructions of core such as stamped laminations, powder and tape being the most common. Each material offers unique properties which are utilised for different applications however mumetal and grain-oriented silicon steel are two of the most common materials used for audio transformer cores as these have a high permeability (magnetically soft) reducing core losses, lowers leakage inductance and allows for a smaller number of turns on each winding reducing parasitic capacitance. Overall core loss is determined by the hysteresis, magnetic core material resistivity and eddy current loss.

Mumetal which was developed in 1923 for use in submarine telegraph cables as inductive loading, is one of the most used soft magnetic Nickel-Iron (Ni-Fe) alloy composed mostly of nickel (73-80%) and iron however lesser amounts of other elements are added such as molybdenum, silicon, copper, chromium, manganese and carbon being the most common. Mumetal is used by a substantial amount of audio transformers due to the high permeability of the material, the size of the device can be reduced and subsequently the weight. Research by Sowter (1944) shows how the increased permeability of mumetal has a lower distortion coefficient when compared to silicon iron alloys. With transformers designed for larger signal levels the core material is most often a form of grain-oriented silicon steel. The steel is characterised by the silicon content and the processing of the material through cold rolling, annealing at high-temperature (approximately 1200°C) which recrystallises the structure producing large grains that are finally oriented into the final direction by rolling. This process ultimately improves the magnetic qualities as flux will flow in the same direction relative to the grain direction, making toroidal transformers

the optimum shape although C and E cores are often used to retain many of the benefits whilst keeping the size of the device small. Examples of electrical steel such as Hi-B steel are processed in a way that creates larger grains with the addition of a glass surface coating to apply tensile stress to the material increasing the permeability and reduces the overall electrical loss. With all types of core materials, the magnetic properties can be severely reduced by the improper joining of laminations and mounting fixtures such as bolts. Excess amounts of torsion, bending or compression of the material can dramatically reduce the permeability. As pointed out by McLyman (2004) most high-permeability magnetic materials are sensitive to pressure, temperature, frequency and signal voltage. This is further pointed out by Sowter (1987) that the uniformity of flux density in the magnetic circuit is an important factor in the creation of distortion.

The C-core, E-I core and the U-I core rely upon the principle of laminating the material to reduce size and to reduce the effects of eddy currents which can adversely impact the performance of the transformer. Eddy currents, which are proportional to the applied primary winding voltage, produce a force which opposes the direction of the magnetic field created by the primary winding so by creating a core of thin sheets and using a material of higher resistivity the effect is greatly reduced whilst still retaining a high permeability. A way to combat the effect of eddy currents is to use a material that also has a high electrical resistivity so that the currents will be low. Another precaution used is to coat the material with insulating material to further reduce the currents.

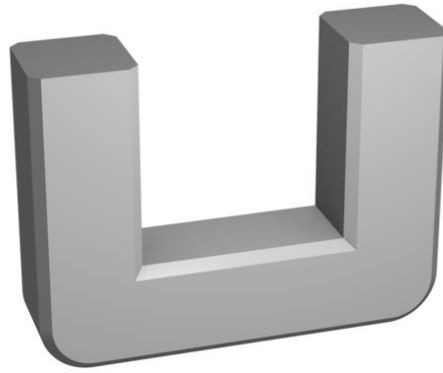


Figure 7. C Core Half (“C Core,” 2007)

Most cut C cores begin by winding a tape of the material around a mandrel in the direction of the magnetic grain, the core is then secured by means of a band and buckle or spot welded. Most cores are then impregnated with resin to provide mechanical strength and then cut in half producing two C-shaped sides (fig.7). The mating surfaces of both sides are then ground and lapped (finely ground commonly together with abrasive) and finally acid-etched to create a smooth surface to minimise the size of the air gap and therefore increase the permeability of the core. As the permeability is affected by each mechanical process that causes stress through tension and torsion, annealing is then used to restore the magnetic properties. This design offers a small core size and high permeability due to the type of material and winding in the direction of the magnetic grain aiding the channelling of magnetic flux. The most common method of E-I core construction uses interleaved alternate stamped laminations such as that shown in figure (8). The alternate method minimises the overall effect of air gaps by stacking the E and I laminations one way then reversing for the next stack, this staggers the gaps. With laminations comes the issue of flux crowding or sometimes known as fringing flux is what happens when the flux in one lamination jumps to the adjacent lamination as this offers a higher permeability than the air gap offering a ‘path of least resistance’. This crowding effect eventually causes the area of crowding to saturate prematurely and finally leads to quicker saturation of the core.

Laminated U-I and laminated C cores offer a compromise between the high permeability of the tape wound C core design and the compact size of the laminated E-I core design.

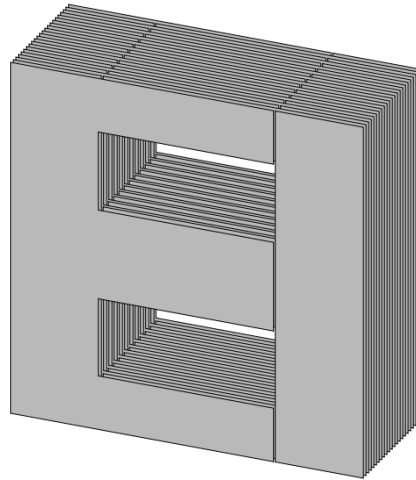


Figure 8. Laminated E-I Transformer Core Design (right) (“Transformer Core Interleaved,” 2007)

Some core materials are processed using special techniques such as annealing, impregnation and glass coating. Annealing is commonly used during the construction of transformer cores after shaping or stamping. When the material is shaped or stamped the structure of the metal/ alloy is changed and this affects the permeability. The annealing process changes the structure by heating the magnetic materials up to a high temperature (the temperature is dependent on the material), then cooling it back to room temperature whilst controlling the conditions of temperature, atmosphere, time and sometimes uses a magnetic field. As discussed by Sowter (1987) glass coating can also be used to provide tensile stress on the material improving permeability such as with Hi-B transformer steel. Impregnating a transformer with wax or resins such as epoxy helps to keep laminations and any other parts from vibrating thus avoiding the effects of mechanical vibration although as stated by Sowter (1987) microphony can be caused by using the wrong

material. It also stops the mechanical movement of the core material and windings so as to not cause damage or adversely change the device's properties.

The windings are mostly made by coiling a length of enamelled copper magnet wire (although aluminium or silver are also used in some designs) around a former such as a plastic bobbin or other insulating material which is then placed around the core material. The winding technique used when constructing the transformer is also vital to the performance of the device. Methods such as bifilar and layering formats are used to increase the coupling between the two windings, this results in an increase of mutual inductance and can reduce the amount of parasitic winding capacitance which impacts the response of the transformer at high-frequencies (McLyman, 2004). This is a fine balance to create the best performance for the size and application of the transformer. Electrostatic screening between the primary and secondary are also frequent additions to reduce the amount of capacitance between windings and RF interference. One implementation of this is by winding a strip of copper foil between the windings although this is dependent on the winding format and design.

Transformers can be affected by surrounding electromagnetic interference and even the effects of ferromagnetic materials in close proximity to the device such as holes for mounting bolts and brackets which can cause issues such as nonuniform concentration of flux. Many transformers are protected using a magnetic shield also known as a Faraday shield to protect from extraneous noise and EMI. A single mumetal shield can provide 30dB-40dB attenuation at 50Hz to the noise and most frequently comes in the form of a can or box around the transformer. Shielding is often used on susceptible components such as small signal devices like microphone input transformers or devices near a power supply

where there is increased level of 50Hz mains which could be superimposed on the audio signal. It is also common practice to double shield the device if there is an increased risk of noise or interference. Shields are typically tested using Helmholtz coils that induce a 50Hz field around the device then the device is measured.

2.5 Perception of Distortion

The perception of distortion is a broad topic that has long been disputed. When examining the performance of a piece of audio equipment it is frequent practice to use the total harmonic distortion (THD) percentage as a gauge of how ‘clean’ or transparent the device is. This is then often wrongly used to determine if the equipment will sound ‘good’ or ‘bad’. The suitability of THD, Intermodulation Distortion (IMD) and Signal-to-Noise Ratio (SNR) to describe a device’s performance, has long been debated in the field of audio quality as this measure only shows how much non-linearity there is in a system and not what the distortion mechanism is (e.g. symmetrical, asymmetrical, etc.) and how this is correlated to the human auditory system. An example is presented by Leinonen & Ojala (1978) a study which compares a selection of metrics such as THD, Society of Motion Picture and Television Engineers Intermodulation Distortion (SMPTE-IM), Dynamic Intermodulation Distortion (DIM), etc. conclude that each metric reacts differently to each individual distortion mechanism. Another reason for the poor correlation is the use of pure tone signals which are periodic compared to complex signals such as music, noise, etc which are statistically random. Research such as that by Voishvillo (2007) has shown that multi-tones and noise are better candidates for test stimuli when concerning auditory perception. Methods such as the one developed by Belcher (1976) uses a pseudo-random test noise signal sequence that covers most of the audio frequency range and later two sets of comb-filters to provide a measurement technique that has improved correlation with the perception.

There is no specific threshold or level of THD that is deemed audible and there is also no explanation of what THD is pleasing to the ear due to the ambiguity of the metric. An example is presented by Lipshitz & Vanderkooy (1981) on testing the audibility of

crossover distortion in relation to THD the amount of distortion was varied and was found that THD reached around 1% at the point at which it became audible when using a musical signal. As stated by Herzog (2009), the threshold of hearing distortion is decreased by signals with multiple harmonics. When compared to sounds with fewer but more dominant spectral components due to masking. Higher order distortion has a lower threshold compared to lower order having a higher threshold. However, some metrics have been developed to produce a means of correlating perception with an objective scale such as the Perceived Audio Quality or PEAQ (International Telecommunication Union, 2001), GedLee (G_m) metric (Lee & Geddes, 2003), Perceptual Nonlinear Distortion Response or PNDR (Minnick, 2012), DS (Tan, Moore, & Zacharov, 2003) and Rnonlin (Tan, Moore, Zacharov, & Mattila, 2004). One feature made clear in the G_m metric is a method of determining the high-order nonlinearity; the frequency content that is above the content frequency range that will be less likely to be masked and the effects of low-level nonlinearity; a higher level of distortion is present at low signal levels. A large amount of research into this area has led to a method of assessing perceived audio quality, proposed in the ITU-R BS.1387-1 (2001). This method uses a reference signal and the signal-under-test along with a combination of FFT and filter bank analysis to model the physiological and psychoacoustic aspects of the human auditory system such as the outer and middle ear transfer characteristic and the Basilar membrane. The aim of these measurement methods is to create a metric that correlates better with the perception of sound quality when compared to those such as THD and reduce the need of subjective testing which can be time consuming and expensive.

In the paper presented by Voishvillo (2007) there is a need to first understand the systems involved in the perception of distortion which can be split into: the nonlinear system, the

human hearing system and the signal. The complexity of all the components produce complex products like low and high-level nonlinearities, low and high order nonlinearities and the distortion spectral content that occurs above and below the spectrum of an undistorted signal compared to content that spreads into the signal's spectrum.

Programme dependence concerns the level, frequency and timing qualities of the stimuli affecting the amount of distortion. The level nonlinearity or level-dependant distortion is an important factor to consider especially when the level range is broad as in the case of the signal across a microphone preamplifier output transformer. It is typical to think of distortion as increasing with signal level however with respect to transformers the effect of an increase in overall distortion at low signal levels is also an issue. Most audio transformers exhibit both phenomena at the extremes of low and high signal level which is due to the core properties in particular the retentivity and the saturation points of the core material. Frequency dependence relates to the level of distortion produced at different frequencies across the operating range which can vary with frequency known as dynamic distortion. Both level and spectral content affect the amount of spectral masking and therefore the perception of the distortion. The timing of the stimuli refers to the effect of the sound's envelope on the amount of temporal masking.

Spectral and temporal masking are significant factors when considering the perception of distortion. As explained by Voishvillo (2007) spectral masking concerns the level of the masker frequency affecting the signals either side; the maskees, this is caused by the fact that low level signals are not processed as fast as higher-levels. Temporal masking manifests when the masker signal which occurs around 10-20ms before (backward masking) or 100-200ms after (forward masking) the maskee signal which is mainly caused

by the suppression of signals from the Basilar membrane to the brain. An example is that of low frequency signals being particularly good at masking higher frequencies therefore distortion components at low frequencies can mask other components. A point made by Voishvillo (2007) is that due to this the hearing system could tolerate higher levels of distortion at low frequencies.

One method of assessing perception is discussed by Liebetrau et al. (2015) through the use of psychoacoustic attributes such as loudness, sharpness, roughness, fluctuation and tonality which can be measured and is believed that the combination of each attribute along with the appropriate weighting is responsible for the perception of the sound. The term annoyance and pleasantness is often used to describe perception in studies such as that by Fastl and Zwicker (2007). It was observed by Liebetrau et al. (2015) that this pleasantness is closely correlated with sharpness and roughness although fluctuation and tonality were shown to have poor if any correlation. As explained by Herzog (2009), sharpness will increase with signals containing low frequency as the distortion products will be higher than the original frequency.

A point made by Lipshitz and Vanderkooy in their paper 'The Great Debate' (1981) discusses how linear differences must be thoroughly excised suggesting an equalisation of linear differences to within 0.1dB before conclusions about the audibility or significance of nonlinear errors can be reached as the human hearing system is acutely sensitive to small linear differences. It was determined by Suzuki, Morita, and Shindo, (1980) that with a phase distortion of 90° the effect was audible although subtle using certain stimuli although it was not likely to be audible with music.

2.6 Test Circuit Design

It was stated by Farmelo (2010) that microphone preamplifiers are often praised for the impact of their transformers on the sound especially when used creatively such as driving the transformer ‘hard’ or at high-levels to produce the desired ‘colouration’ . To test the transformers fairly it was decided to implement them in a close-to ‘real world’ professional audio application whilst creating a transparent testing platform. The test circuit had to be as transparent as possible to have less chance of colouring the sound or affecting the signal whilst still representing a realistic drive circuit for the output transformer. For ease, the Analog Devices AD8429 instrumentation amplifier (Analog Devices, 2017) was chosen rather than a discrete transistor-based circuit. Although the use of an instrumentation amplifier is not considered a realistic example of a circuit design used in professional recording microphone preamplifiers, the AD8429 provides a low-noise, low-distortion, transparent drive to the transformer and presents similar input and output impedances.

It was first thought that a standard audio op-amp, the NE5532, would offer the best option for an applied ‘real-world’ example as the IC is so widely used however it was decided that it would be advantageous to use a more transparent option with a lower overall distortion level to provide an improved chance of capturing any distortions created by the transformer. The advantages of building a low-noise, low-distortion instrumentation amplifier using NE5532s such as the low noise 4-4 configuration presented by Self (2015), were also considered but this option was deemed more tedious and time-consuming to build and to debug any problems if they occurred whereas the AD8429 offered an immediate solution. Table (1) compares some of the important specifications of the two ICs. A disadvantage of using the AD8429 is that the CMRR improves with gain which in

most applications of the NE5532 such as non-inverting and inverting configuration, this would not be the case resulting in a higher level of noise.

	AD8429	NE5532
Input Voltage Noise	$1nV/\sqrt{Hz}$	$5nV/\sqrt{Hz}$
CMRR (Min)	$80dB$	$70dB$
Slew Rate	$22V/\mu S$	$9V/\mu S$
THD	0.0005% ($G = 100$)	0.002%
Peak-to-Peak Output Voltage Swing ($V_S = \pm 15V$)	$27.2V$	$26V$

Table 1. AD8429 and NE5532 IC Specifications

The complete circuit design was split into modular daughter boards utilising pin headers which allowed the components to be swapped between various mother boards which helped to speed up the testing process and importantly minimised the stress on the components which would otherwise cause damage especially true with the shielded transformers. The main circuit design (fig.9) was implemented on the series of mother boards into which the instrumentation amplifier, switched gain resistors and transformer daughter boards connected to complete the circuit.

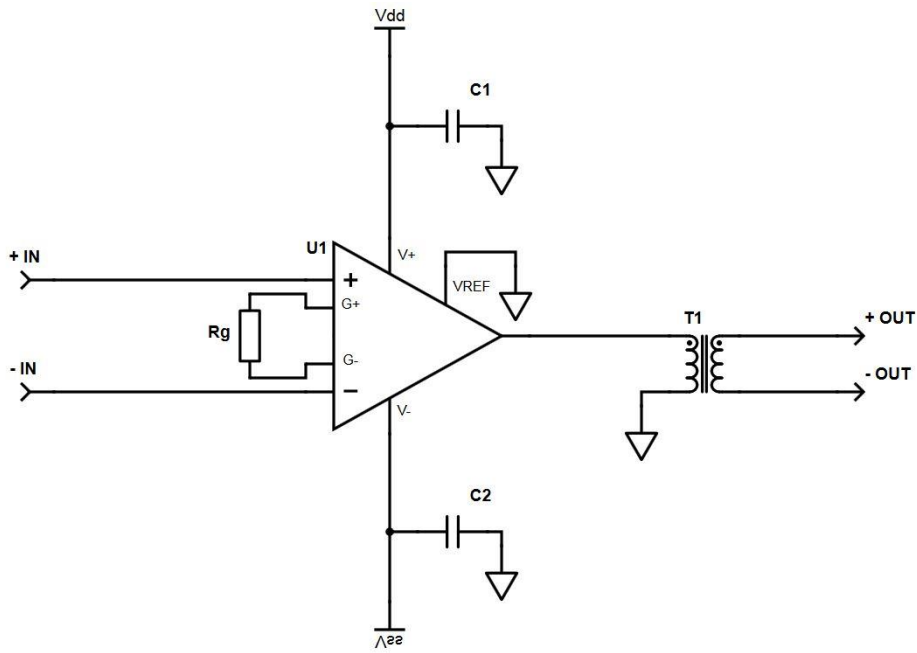


Figure 9. Test Circuit Schematic

By increasing the gain, the CMRR improves which helps when analysing the signal at low levels. The AD8429 uses the standard three op-amp architecture on a single IC (fig.10 simplified schematic). This comprises of two non-inverting amplifiers which both act as buffers; matching the impedance of the circuit connected at the input to the third amplifier which is a differential amplifier. The two input amplifiers share a feedback network which includes the gain setting resistor allowing one resistor to control both gains simultaneously. The differential amplifier provides the high CMRR that is needed to remove any extraneous noise present at the input. The overall transfer of the circuit is presented as equation 8.

$$V_{out} = G (V_{in+} - V_{in-}) + V_{REF} \quad (8)$$

where:

V_{out} is the output voltage

G is the gain

V_{in+} is the non-inverting input voltage

V_{in-} is the inverting input voltage

V_{REF} is the reference offset voltage

The IC also contains overvoltage protection diodes which offer an added level of safety when connecting and disconnecting the test apparatus which may produce momentary voltage spikes which may otherwise cause damage to the instrumentation amplifier. Another feature of the device is the addition of bipolar junction transistors (BJT), arranged as a long-tailed pair, at the inputs of the package to increase the CMRR of the input signal and produce the characteristic high input impedance of an integrated circuit op-amp.

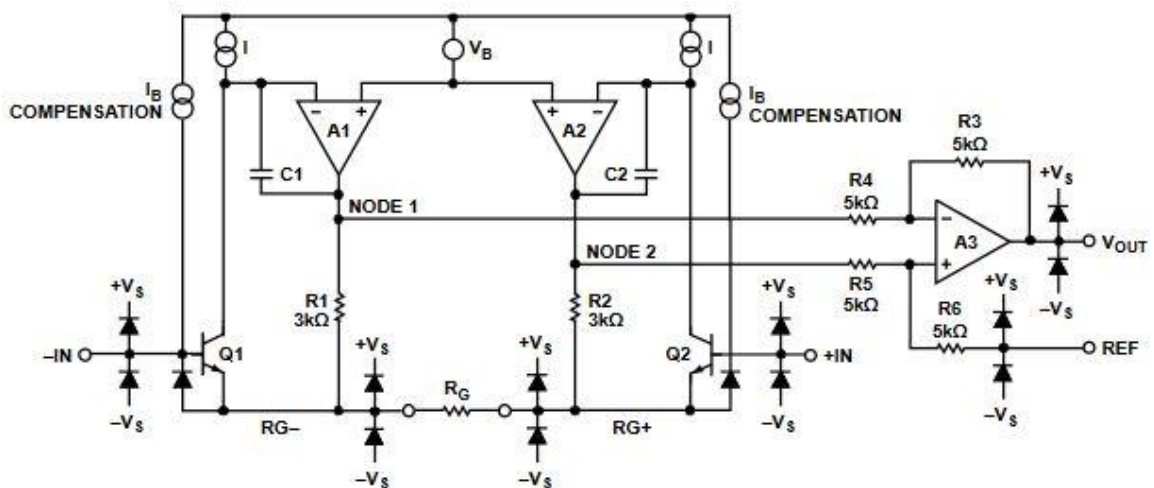


Figure 10. AD8429 Simplified Schematic (Analog Devices, 2017)

By having a pre-existing feedback path on the IC, it can be assumed that the resistors are well matched making the gain of each amplifier more accurate and it also allows quicker design and setup of the gain stage using just a single external resistor connected between the two gain (R_G) pins. The gain resistors were connected to the circuit via a switched daughter board providing 0dB gain with an open-circuit and +6dB and +16dB when a value of 6.2k Ω and 1.1k Ω resistance was individually switched into the circuit respectively calculated using the formulae presented in equations 9 and 10.

$$G = 1 + \frac{6k\Omega}{R_G} \quad (9)$$

$$\therefore R_G = \frac{6k\Omega}{G-1} \quad (10)$$

By switching in the desired gain resistor this gives a more accurate gain control over that provided by a potentiometer. Decoupling capacitors were added to the instrumentation amplifier board, close to the power supply pins to remove any noise or interference on the power rails. The benefits of adding multiple decoupling capacitors in parallel to further reduce the chance of noise affecting the circuit, as suggested by the manufacturer, was examined although the risk posed by the level of noise superimposed on the laboratory power supply unit was not considered a significant one.

The design is powered using a $\pm 16V$ dual rail power supply allowing a 32V peak-to-peak output signal swing which allows for a maximum of +20dBu output and a degree of overhead for signals that may momentarily rise above this level (absolute maximum approximately +22dBu). The instrumentation amplifier also has a discrepancy of how much the output can swing in relation to the rail voltages: -1.1 Vs and +1.7 Vs. The maximum output current of the device is 35mA short-circuit. A reference pin is also

available which gives the option to apply a DC offset to the output which would prove useful for future testing of the effects of phantom power and stray DC however for these series of tests the output was referenced to ground. Horowitz and Hill (2015) explain how adding the two op-amp followers before the differential amplifier in an instrumentation amplifier not only means the input impedance is higher but that the resistors that follow can have a lower value therefore reducing the effect of the inherent Johnson noise. These two op-amps produce the high differential gain which then drives a unity-gain differential amplifier which provides the high CMRR.

There are many variations of professional microphone preamplifiers however, a substantial portion of these designs tend to have a discrete push-pull output whether transistor-based or valve-based. It was decided that this design would take longer to implement and due to the addition of more components into the signal path this would add to the overall noise and distortion level, with crossover distortion being one of the more salient issues.

Voltage noise is specified below $100\text{nV}/\sqrt{\text{Hz}}$ for gain of 10 and 1. Stated THD is flat across 10Hz-1kHz between a gain of 1-10 with an increase from approximately 2kHz-20kHz for a gain of 1 and from approximately 10kHz-20kHz. CMRR is stated between 76-90dB for a gain of 1 and 10 at $5\text{kHz} \pm 10V_{CM}$. As the level across a microphone preamplifier output can vary greatly, the output transformers are presented with a broad range of signal levels with most being designed to handle signals around the standard professional audio level: line-level (+4dBu or $1.228 V_{RMS}$). Table (2) shows the input levels and related output level with respect to the gain. With the range of levels produced using six inputs and three gain levels this should give a better understanding of the

device's operation over a broad span of frequencies covering close to the regions where distortion will be most prominent: the low-level around the retentivity of the core material to the high-levels when the core begins to saturate. Ultimately this helps to better show the effects of level-dependant nonlinearities using signal levels from a real-world context.

Input Signal Level	Output Signal Level (after gain)		
	0dB (G=1)	+6dB (G=2)	+16dB (G=6.3)
-38dBu	-38dBu	-32dBu	-22dBu
-24dBu	-24dBu	-18dBu	-8dBu
-10dBu	-10dBu	-4dBu	+6dBu
-4dBu	-4dBu	+2dBu	+12dBu
0dBu	0dBu	+6dBu	+16dBu
+4dBu	+4dBu	+10dBu	+20dBu

Table 2. Output Signal Levels with Relation to Input Signal Level

It is common for commercial preamplifiers to have THD+N in the region of 0.05% - 1%. These values are generally considered high for professional audio equipment however there is still a substantial demand for this equipment with many end users regarding the 'colouration' to be something admired for creative purposes.

It is not uncommon to find circuit designs which include a step-up, output transformers and, in these cases, the amplifier loop gain is increased. This would provide a wider bandwidth along with lower distortion due to the sharing of the effective voltage gain between the amplifier section and the transformer (equation 11).

$$G_{(U1)} = \frac{G_{total}}{\left(\frac{N_s}{N_p}\right)} \quad (11)$$

where:

G_{total} is the given circuit total gain (transformer and amplifier)

G_{U1} is the gain of the op amp

N_p is the number of turns (primary winding)

N_s is the number of turns (secondary winding)

Another method of reducing distortion is presented by Jung (2005) this explains how mixed feedback drivers can reduce distortion by effectively cancelling the primary winding resistance therefore lowering the output impedance by reflecting the impedance onto the secondary winding.

2.7 Listening Test Design

Subjective testing is crucial to understanding the relationship between objective measures and perceptual differences as stated by Lipshitz & Vanderkooy (1981, p. 483) “Not every audible characteristic of some components... can yet be objectively measured in a way that correlates meaningfully with what is heard.”.

As explained by Bech & Zacharov (2007) the selection of stimuli is crucial to eliciting the perceptual differences of the device-under-test that are trying to be measured and therefore need to be chosen for this purpose. A selection of material is important when considering the issue of programme dependence that can vary with signal frequency, level and duration. It is stated in the ITU-R BS.1116-3 recommendation that for small impairment tests, critical listening material should be used however it is also stated that “there is no universally ‘suitable’ programme material...” (International Telecommunication Union, 2015. p.8). It is also suggested that excerpts should ideally be less than eight seconds as most subjects preserve greater detail using their ultra-short-term memory.

There will inevitably be slight level differences between samples recorded through a DUT and reference signal, and this would also be unavoidable when considering a circuit with voltage gain. It is then important to match the loudness levels of each sample with the corresponding reference signal. One method is the use of LUFS (loudness units, referenced to full scale) to measure the signal and adjust to an equal loudness. Many other methods relate to electrical-based measures whereas the LUFS unit accounts for sound duration and the distribution of frequency (Ronan, Ward, & Sazdov, 2016).

The appropriate testing procedure is dependent upon the hypothesis being tested and therefore the statistical result produced by the test. When testing for a difference or small impairments in audio a test such as that suggested in the ITU-R BS.1116-3 recommendation (International Telecommunication Union, 2015): the double-blind triple-stimulus with hidden reference method also known as a double-blind ABX test is used. The test is forced choice which ‘forces’ an incorrect or correct identification which produces a binomial result that can then be analysed using a binomial statistical test, producing a probability that the subject was guessing or was confidently choosing the right answer. As explained by Boley and Lester (2009) double-blind testing is also used to eliminate the bias produced by subtle cues given by the test administrator.

The listening test software is an important part of the testing method and must be carefully chosen to provide the correct test such as ABX, provide an easy-to-use user interface and eliminate any bias that could be produced by presentation such as the order of the stimuli. There are a variety of testing software available which each have a range of advantages and disadvantages. In a comparison made by Jillings et al. (2016) the Huddersfield University Listening Test Interface Generator (HULTI-GEN) and the Web Audio Evaluation Tool (WAET) offer the most applications and are free to use. HULTI-GEN (Gribben & Lee, 2015) based in Max provides an intuitive design interface and quick setup. WAET which is a Web Audio API-based tool which uses Java Script and HTML offers the most flexibility including: 15 different tests including ABX, remote testing using a server and analytical/ diagnostic tools which can be used to collect data about other parameters such as a timeline showing the length of time a subject takes to answer questions. WAET also provides a comment box function which is useful when trying to understand how each subject perceives a difference and what vocabulary is used to

describe the attributes. Although the comments are useful to help discern what differences can be heard it is not a complete elicitation test and therefore needs more investigation which is beyond the scope of this research.

The length of each trial is dictated by the length of each sample and the average time it takes to compare sample A and sample B with the reference X. It is recommended in the ITU-R BS.1116-3 (International Telecommunication Union, 2015) to use 10-15 trials per session with a break with a length of no less than the length of the session. Randomisation of stimuli and trials removes any bias presented by repetition and can also help with listener fatigue: by changing the order it keeps the listener concentrated. When clicking between the two stimuli A and B, the sample continues to play which removes the distraction of the audio file playing from the beginning each time, but this only works when both stimuli files are time aligned to avoid any clicks or pops caused by the mismatch between the two.

As stated by the ITU-R BS.1116-3 recommendation (International Telecommunication Union, 2015) the listening environment in which the test is to be done is also a factor that must be controlled although this is less of a concern with respect to headphone reproduction. The addition of background noise can cause distraction but all mask audible components in the test. The two choices of playback method are loudspeaker or headphone reproduction. Both methods have pros and cons such as those discussed by Bech & Zacharov (2007) concerning positioning, calibration, etc.

The listening level or playback level is often fixed such as that suggested in the ITU-R recommendation (International Telecommunication Union, 2015) of $78\text{dBA} \pm 0.25$. By

keeping the level fixed this controls the variable and eliminates any possible bias caused by the level changes between subjects. However, it is important to note, as stated in the recommendation, the effects on the audibility of products such as distortion when allowing the subject to choose playback level are not fully known. There is a possibility of hearing distortion at a higher playback level however other issues such as loud playback level could introduce bias in the form of listening subject fatigue and even hearing damage with prolonged exposure.

The statistical analysis starts with the experiment design which considers the procedure for testing the alternative hypothesis to ultimately retain or reject the null hypothesis based on the probability. If the result is completely random i.e. the subjects are guessing the distribution will be binomial. The binomial distribution relies upon two criteria one being the testing software to randomise the test stimuli and the other is when the test subject cannot identify the correct answer, the result is a random choice. As the testing software used is a true random number generator this criterion is fulfilled however human subjects are not truly random which can lead to the introduction of a human bias or sampling error if the listener shows a bias towards A or B when they cannot hear a difference.

$$H_0: p = 0.5$$

$$H_a: p > 0.5$$

As shown by H_a being greater than 0.5, this means the test is directional therefore a one-tailed test is used. With the binomial distribution, the number of test trials and the number of correct answers the probability value or p-value can be determined. The p-values can be calculated by first finding the z-scores using the formulae presented by Harris and Holland

(2009) shown in equations (12 & 13), then looking up the value in the appropriate statistical table in this case one for a normal distribution.

$$Z_{sample} = \frac{(P_s - 0.5) - P_u}{\sqrt{\frac{P_u(100 - P_u)}{n}}} \quad (12)$$

$$P_s = Z_{sample} \sqrt{\frac{P_u(100 - P_u)}{n}} + P_u + 0.5 \quad (13)$$

when $P_s > P_u$

Where:

P_s = sample percentage

P_u = assumed population percentage

N = sample size

Another method would be through the use of a statistical software package such as IBM SPSS. The output of both methods, the p-value, represents the probability of randomly getting more correct identifications with the same conditions. A downside to using a binomial distribution is the results are not valid with a small amount of data points therefore becomes more reliable with more trials.

It is important to note that statistical analysis is a way of presenting how confident the interpretation of the results is and does not determine if there is or isn't a definite audible difference only how likely there is a difference.

Chapter 3: Objective Testing

This section examines the transformers used in the testing starting with the construction and application of the devices. The methods used to test each device, using various metrics including THD+N, are explained and finally, the results of the testing stage are presented and discussed.

3.1 Transformers

The two output transformers used in the testing were the Lundahl LL1582 and the Carnhill VTB1148 which were chosen as both are different in construction so as to provide an insight into the possible differences between materials and designs of devices made for the same application. The Lundahl LL1582 line output transformer (fig.11) is constructed using a wound silicon iron tape cut C-core, with two primary and two secondary copper wire windings wound onto plastic tape, internal electrostatic shielding and all housed in a mumetal shield. The Carnhill VTB1148 (fig.12) is a high voltage output transformer made with grain-oriented silicon steel laminated E-I core with two primary and two secondary copper wire windings contained on a plastic bobbin all fixed together using a channel style bracket. Both devices have also been impregnated with a resin to limit mechanical movement and wear.



Figure 11. Lundahl LL1582 Line Output Transformer



Figure 12. Carnhill VTB1148 Line Output Transformer

The transformer winding ratios used were 1: 1 for the LL1582 and 1: 1.7 for the VTB1148 as this device did not offer a 1: 1 ratio however a ratio of 2: 1.7 was available but it was decided that it was best to connect both transformer windings using the same configuration.

During this study two microphone transformers were also tested: the Lundahl LL1538 and the Carnhill VTB9045. Although these were not used in the subjective testing the results offer a greater understanding of how these designs perform in comparison to the output transformers. The Lundahl LL1538 is made using a mumetal laminated C-core, internal electrostatic shields and a mumetal electromagnetic shield and the Carnhill VTB9045 which is a laminated mumetal U-I core with internal electrostatic shielding and a steel outer case for protection from wear. The specifications of all the transformers are shown in table (3). The winding ratios used were 1:5 for the LL1538 and 1:4 for the VTB9045.

As mentioned in section 2.3, Zobel networks are common in transformer applications, however for testing it was decided that one would not be needed. The reasoning for this is

that the device showed minimal effects of ringing and the added components in the signal path would add noise to the circuit.

	Lundahl LL1582 Line Output	Carnhill VTB1148 Line Output	Lundahl LL1538 Microphone Input	Carnhill VTB9045 Microphone Input
Maximum Level	+30dBu @ 50Hz	-	-	-
Winding/ Turns Ratio (N1: N2)	1 + 1: 1 + 1	1 + 1: 1.7 + 1.7	1 + 1: 5	1 + 1: 2 + 2
Static Resistance of each Primary	45Ω	8Ω	44Ω	25Ω
Static Resistance of each Secondary	45Ω	21Ω	880Ω	140Ω

Table 3. Transformer Specifications

3.2 Method

All devices used in the circuit were measured using a variety of metrics to provide a deeper understanding of how each device performs. This performance can be split into two categories: linear and non-linear distortions. Linear distortion concerns the change of the amplitude and phase of the signal's frequency components which as stated by Tan et al. (2003) that these changes typically cause a change in colouration. Nonlinear distortion is caused by the addition of frequency components that are not part of the original signal and is often described as producing a rough or harsh sound.

The focus of many studies that look at perception of distortion focus on the nonlinear response of the devices which is an extensive part of the problem despite this it is a salient fact that the linear response can have a substantial impact on the perception of distortion, thus both responses are observed. As mentioned previously, Lipshitz and Vanderkooy (1981) discuss how linear differences must be thoroughly excised due to the auditory system's sensitivity to small linear differences however it was decided to not cancel out any linear effects and focus on the transformer response in its entirety. All the measurements taken here are taken using electrical-based metrics such as THD, IMD, etc.

Total Harmonic Distortion (THD) and Total Harmonic Distortion Plus Noise (THD+N) are commonly used to describe the amount of non-linear distortion a device/ system produces. The method involves presenting a sine wave to the DUT then measuring the resulting signal minus the original signal. As shown in the equation 14 below, THD+N is the sum of all the harmonic content plus the RMS level of the noise component whilst discounting the fundamental frequency this is then represented as a percentage.

$$THD + N (\%) = 100 \sqrt{\frac{\sum_{i=2}^{\infty} (V_i^2) + V_n^2}{V_f^2}} \quad (14)$$

where:

V_i is the level of harmonic component (volts)

V_n is the RMS noise voltage

V_f is the level of the fundamental (input signal)

When plotted against frequency and amplitude these graphs can provide a deeper level of insight into the performance of the device as shown in figure 13 and 14.

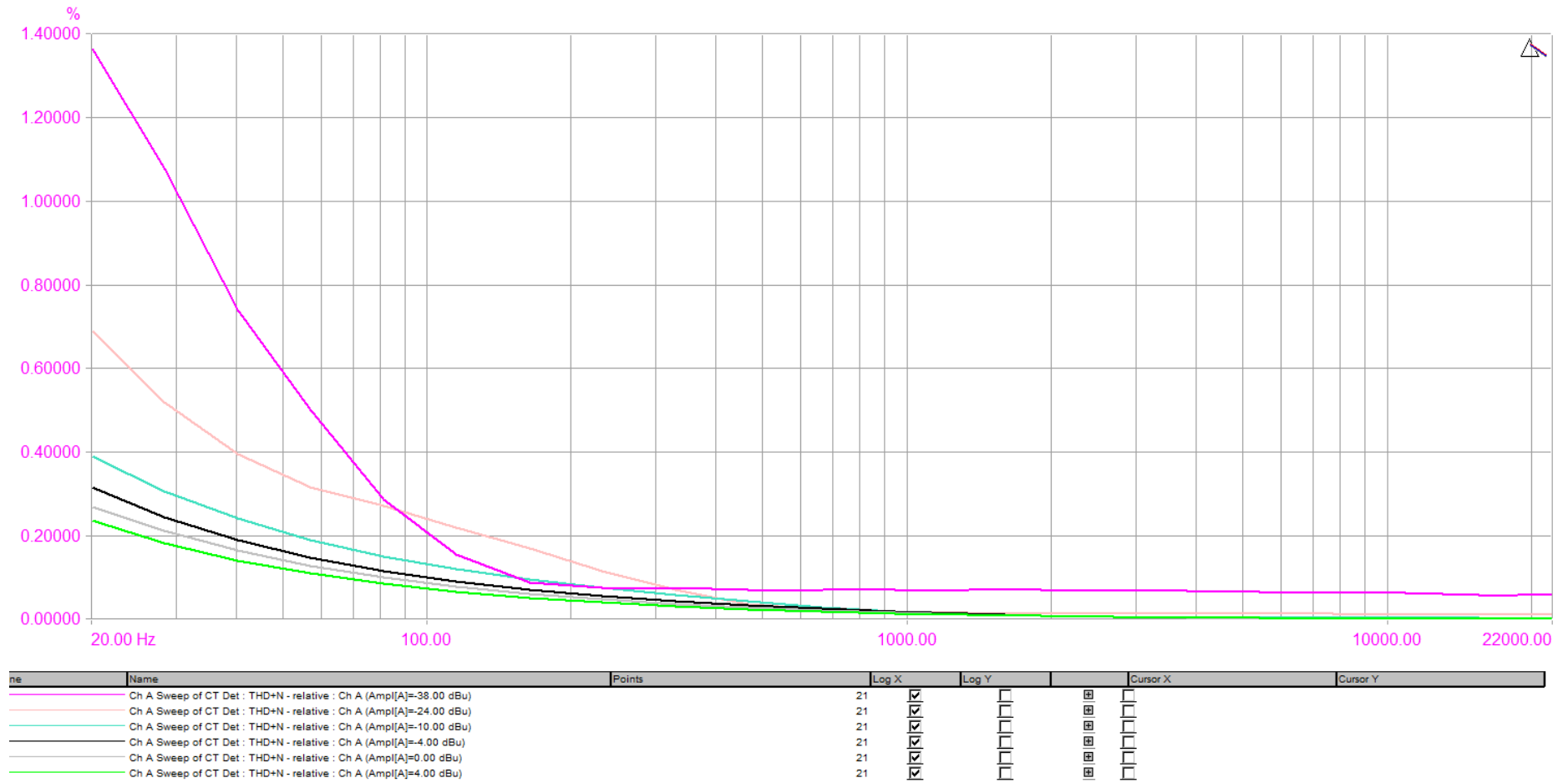
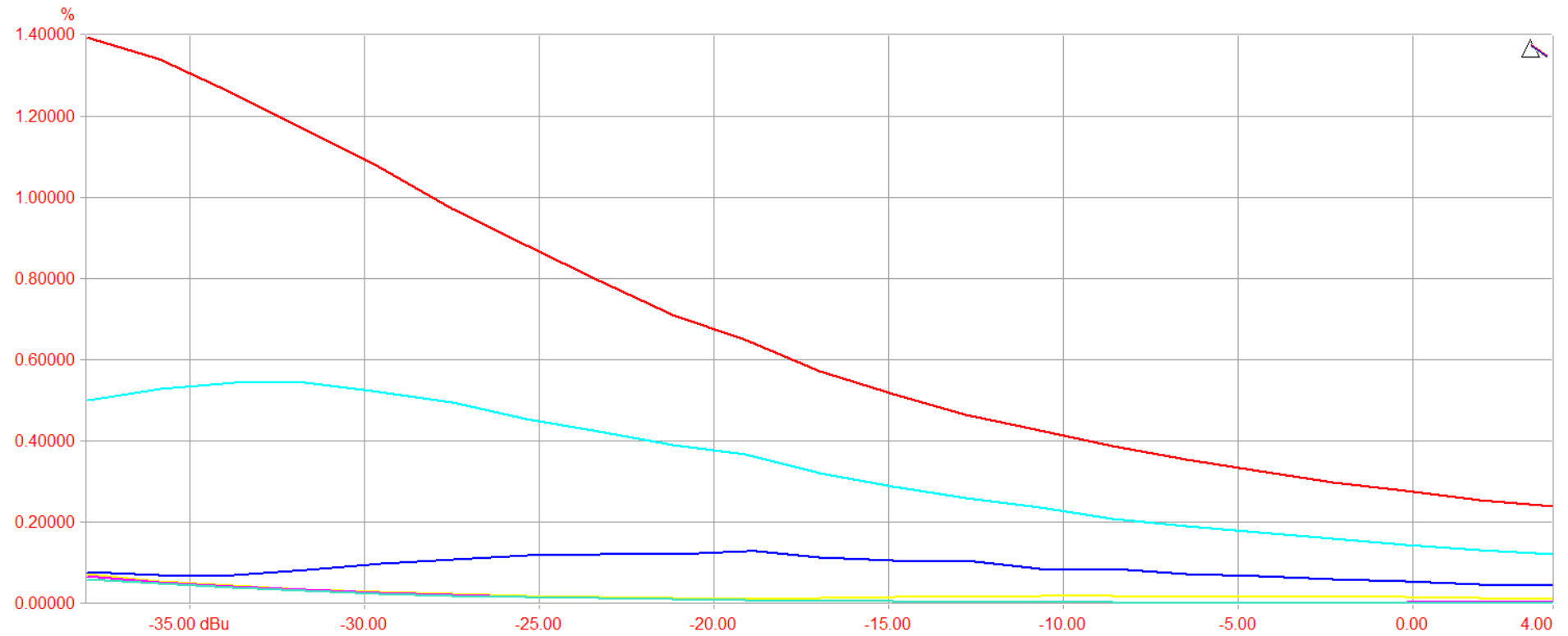


Figure 13. A Total Harmonic Distortion Plus Noise (THD+N) versus Frequency Graph



ne	Name	Points	Log X	Log Y	Cursor X	Cursor Y
	Ch A Sweep of CT Det : THD+N - relative : Ch A (Freq[A]=20.00 Hz)	21	<input checked="" type="checkbox"/>	<input type="checkbox"/>	<input type="checkbox"/>	<input type="checkbox"/>
	Ch A Sweep of CT Det : THD+N - relative : Ch A (Freq[A]=50.00 Hz)	21	<input checked="" type="checkbox"/>	<input type="checkbox"/>	<input type="checkbox"/>	<input type="checkbox"/>
	Ch A Sweep of CT Det : THD+N - relative : Ch A (Freq[A]=200.00 Hz)	21	<input checked="" type="checkbox"/>	<input type="checkbox"/>	<input type="checkbox"/>	<input type="checkbox"/>
	Ch A Sweep of CT Det : THD+N - relative : Ch A (Freq[A]=1000.00 Hz)	21	<input checked="" type="checkbox"/>	<input type="checkbox"/>	<input type="checkbox"/>	<input type="checkbox"/>
	Ch A Sweep of CT Det : THD+N - relative : Ch A (Freq[A]=5000.00 Hz)	21	<input checked="" type="checkbox"/>	<input type="checkbox"/>	<input type="checkbox"/>	<input type="checkbox"/>
	Ch A Sweep of CT Det : THD+N - relative : Ch A (Freq[A]=10000.00 Hz)	21	<input checked="" type="checkbox"/>	<input type="checkbox"/>	<input type="checkbox"/>	<input type="checkbox"/>
	Ch A Sweep of CT Det : THD+N - relative : Ch A (Freq[A]=20000.00 Hz)	21	<input checked="" type="checkbox"/>	<input type="checkbox"/>	<input type="checkbox"/>	<input type="checkbox"/>

Figure 14. A Total Harmonic Distortion Plus Noise (THD+N) versus Amplitude Graph

The total harmonic distortion metric cannot be used on its own however as it does not discriminate between different nonlinear distortion mechanisms and therefore must be used in a broad context to provide an insight into how the entire system performs. It must also be noted that the validity of THD and THD+N when being compared with the perception of distortion has long been debated as detailed in section 2.5. Nonetheless, THD and THD+N are still widely used, and it still provides an effective representation of the amount of non-linearity in a system. A method of elaborating on the THD metric is to look at the 2nd and 3rd harmonic distortion also. This can provide another view of what could be causing the distortion and can also provide a very rudimentary way of assessing the mechanism or cause of the distortion.

Intermodulation distortion (IMD) is also another non-linearity that can be used to analyse a device's performance and occurs when two or more signals interact producing other frequency components that are mathematically related to the original components. Tests for IMD commonly involve presented the device under test (DUT) with two test tones then analysing the resulting output signal for other components mathematically related to the two fundamental frequencies. The most common methods used for IMD measurements are the SMPTE and IMD (ITU-R) (CCIF). The SMPTE method uses two test signals one low-frequency, normally 60Hz and one high-frequency that is not harmonically related, normally 7kHz, summed in a ratio of 4:1 (+4dBu and -8dBu respectively). IMD (ITU-R) also known as CCIF, uses two signals spaced 1kHz apart and an amplitude ratio of 1:1 with common frequencies being 19kHz and 20kHz however there is no standard. For the purpose of the testing in this study the SMPTE standard was used.

A greater improvement in the analysis of distortion is to use a fast Fourier transform (FFT) on the signal so it can be represented in the frequency domain which provides an extremely valuable tool for visualising the entire output signal spectrum. This offers the most practical way of viewing the distortion products and amplitudes with relation to the fundamental signal offering more insight into what type of distortion mechanism is affecting the signal and ultimately what the cause of it is. FFTs do have some discrepancies with respect to the accuracy which is largely dependent upon resolution, sample rate of measurements, windowing and averaging. Another way to visualise the effects of a device's transfer is by using a spectrogram which is often used when a complex input signal is used such as an excerpt of music or multi-tones. With this method the intensity of the heatmap and the complexity can show differences between a processed and an unprocessed signal.

Multi-tone (MT) measurements are used to provide a deeper insight into how the device reacts under a more complex signal at different frequencies. A suggestion presented in a paper by Jensen & Sokolich (1988) was to use a multi-tone signal comprising of frequencies above 10kHz and observe the effects below 10kHz. Some studies have also looked at the use of ultrasonic signals (above 20kHz) but due to the nonlinearity cause issues at lower-frequencies that are in the audible frequency range. Multi-tone signals however correlate to human perception closer than the use of a sine wave signal due to the effects of masking caused by the auditory system as explained by Voishvillo (2007).

The linear measurements of frequency response and phase were also recorded. Although these responses did not drastically depart from a flat response in all the tests it was considered that the linear response can affect the overall perception. For example, the

change in frequency response could result in a boost or a cut increasing the audibility of nonlinear distortion products.

These are the most standard electrical tests for measuring the performance of an electrical device however other methods of distortion measurements exist such as sine-square testing and coherence and incoherence function which uses noise or musical signals. Coherence function as explained by Voishvillo (2007) creates a 'gap' in the input signal noise spectrum revealing the distortion is then swept to create a distortion response.

Each transformer's parasitic elements were also measured and calculated such as winding resistance, inductance, leakage inductance, mutual inductance and interwinding capacitance which show the transformers effect on a more fundamental level. All these measurements were taken using the Keysight DDM and the Rohde & Schwarz LCR Bridge.

The equipment used for all the tests setups were the:

- Keysight 33500B series waveform generator
- Keysight DSOX2004A digital storage oscilloscope
- Prism Sound dScope series III analyser
- Tenma 72-7245 laboratory power supply
- Keysight 34450A Digital Multi-Meter (DMM)
- Rohde & Schwarz HM8118 LCR Bridge

The dScope Series III is an analogue and digital audio analyser which is capable of measuring a variety of circuit properties. The analyser was setup to automatically run a

series of tests and save all the tests to a results file when complete. This save a lot of time when running tests and offered the best way of storing the data. Each test was customised through the software. Unbalanced connection using BNC connectors and balanced connection through XLR connectors are available with the majority of the tests in this study using balanced connections. For unbalanced connections a GW Instek GTP-060A-4 oscilloscope probe was used in x1 mode.

As the analyser has selectable input and output impedances, they were chosen to best interface the circuit but also with the idea of a microphone preamplifier application in mind. The impedances of the dScope were also selected to the most applicable value. There are three available options for impedances: 50 Ω , 150 Ω and 600 Ω at the output of the analyser and 150 Ω , 600 Ω and 100k Ω at the input. It was decided that the output would be 50 Ω due to the high impedance input of the instrumentation amplifier there is no need to change values as there will be little if any change in results and it would also have no effect on the loading of the transformer as this is buffered by the amplifier. The input however, would have an effect although as many tend to be in the region of 10-20k Ω or more, the 100k Ω option was chosen.

In each FFT test, Prism-7 windowing is used which offers the best compromise with respect to dynamic range and spectral leakage and frequency domain averaging is also used across 16 buffers which helps provide a clear plot (window function plot). Noise measurements are integrated across the range of FFT bins. When taking the FFT plots at lower frequencies the number of points were increased to provide better resolution however the higher the FFT points the longer the averaging process takes therefore a compromise was made between the number of points and the plotting speed. The FFT

detectors used in the dScope perform the calculations such as the integration of noise, account for bins of spectral leakage, implementation of analysis filters, THD+N, nth harmonic with over 40 of these detectors can be used simultaneously.

Before testing of all the devices, the dScope analyser was tested to provide an understanding showing how the analyser performs with no DUT connected. In this setup both channel A and B input were connected to the respective channel outputs then measured using a similar testing script intended for the device tests the only difference was the inclusion of more signal levels. This was decided so as to provide a control test for testing the individual transformers without the test circuit, across a wide dynamic range and compare with the other device responses.

The dScope script consisted of individual FFT plots at the frequencies and levels: 20Hz, 50Hz, 200Hz, 1kHz, 5kHz, 10kHz & 20kHz and input levels as shown in section 2.6 table 2. Individual THD+N versus frequency and THD+N versus amplitude, combined THD+N versus frequency versus amplitude and THD+N versus amplitude versus frequency. The script allows the tests to be run automatically and produce a test report providing the measurements and the setup conditions of the analyser. All these measures were taken using a sample rate of 48kHz but to maintain a higher resolution graph across the frequency range and to reduce the speed of testing it was decided to change the number depending on the frequency starting with 128k at 20Hz through to 4k at 20kHz.

The self-measurement results of the analyser presented a completely flat frequency and phase response with a relatively flat THD+N response which does not exceed 0.001% at a level of +4dBu (fig.39) however the level rises as the input signal level is decreased

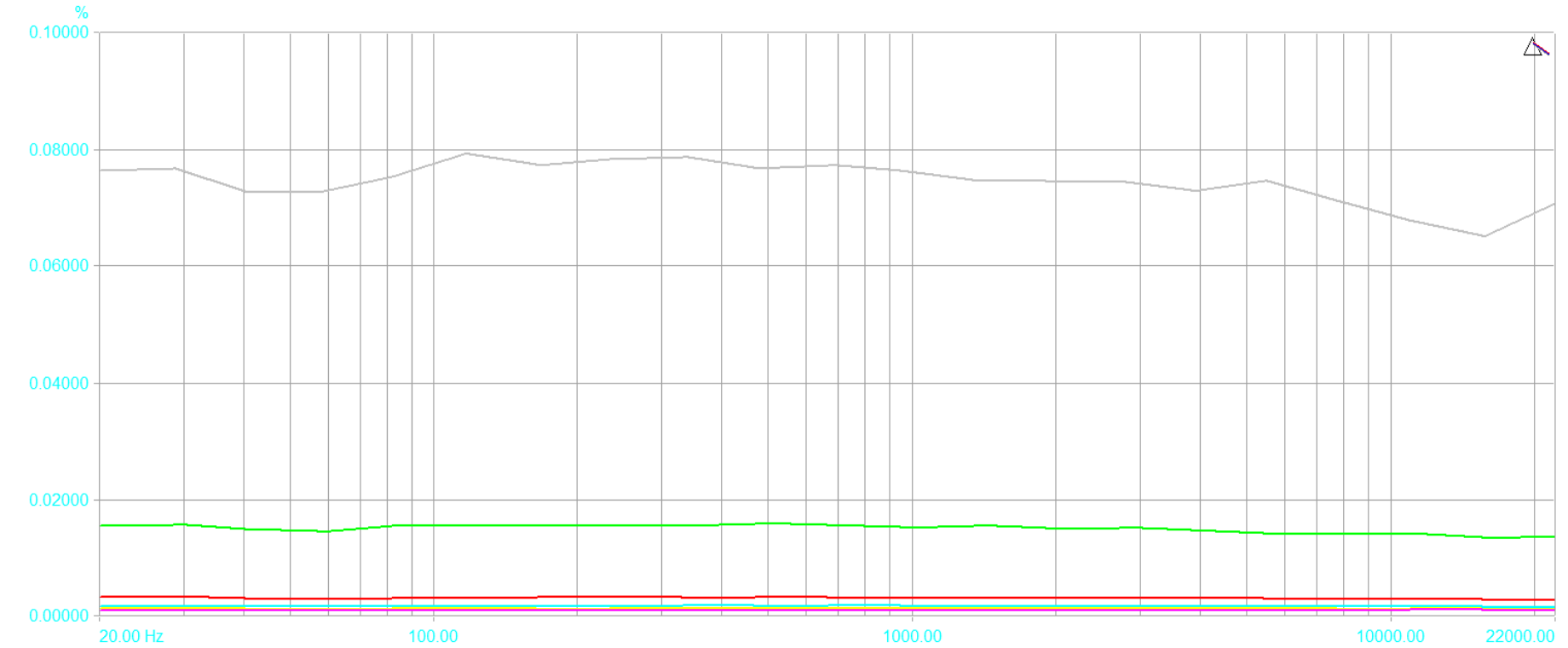
reporting approximately 0.017% at -40dBu (fig.40). The FFT results show some distortion products however all of these are below -100dBu across the test frequencies at +4dBu such as that in figure 41 and IMD of less than -96dB both of which were considered to not pose a problem. Using the Jensen multi-tone test the distortion products were extremely low, mostly below -140dBu this was considered to be transparent. Concluding that the dScope analyser was sufficient enough to measure the low-level nonlinearities of the test circuit and transformers. All further results are presented in appendix A.

The spectrograms were made using the samples created for the listening test and Sonic Visualiser analysis software. The files were used to create the graphics offline which provides a tool to visually show any differences between having the transformer in and out the test circuit. The samples as detailed in section 4.1 were carefully chosen and recorded individually through the instrumentation amplifier and then together with each transformer.

The test circuit was tested in isolation as the control experiment; providing the reference with which the processed signals are compared to. As the instrumentation amplifier accepts a balanced input but only provides a single-ended output, the dScope signal generator was used in balanced mode and the analyser input was unbalanced. Using the test script, the tests were automatically executed and saved to report files. The frequency and phase response of the test circuit (fig.42 & 43) shows a flat response with no visible deviation from 0dB and 0 degrees phase shift respectively across all gains. Using a THD+N versus frequency plot it is clear to see that the distortion is relatively uniform across the frequency range not rising above 0.08% at -38dBu (0dB gain) decreasing to an average of 0.0012% at +4dBu (fig.15). When viewing the THD+N with relation to

amplitude (fig.16) it is also clear to see the uniformity across the levels. At +6dB and +16dB gain the trend across frequency and amplitude stays relatively similar with the exception that the overall THD+N level drops further the higher the highest level of THD+N being approximately 0.014% at an input signal level of -38dBu. This was expected due to the improved CMRR of the instrumentation amplifier with higher gains. IMD levels present close to the dScope self-measurements not exceeding -96dB across the frequency range at +4dBu input level.

THD+N vs Frequency



Line	Name	Points	Log X	Log Y		Cursor X	Cursor Y
1	Ch A Sweep of CT Det : THD+N - relative : Ch A (Ampl[A]=38.00 dBu)	21	<input checked="" type="checkbox"/>	<input type="checkbox"/>	<input type="checkbox"/>	<input type="checkbox"/>	<input type="checkbox"/>
2	Ch A Sweep of CT Det : THD+N - relative : Ch A (Ampl[A]=-24.00 dBu)	21	<input checked="" type="checkbox"/>	<input type="checkbox"/>	<input type="checkbox"/>	<input type="checkbox"/>	<input type="checkbox"/>
3	Ch A Sweep of CT Det : THD+N - relative : Ch A (Ampl[A]=-10.00 dBu)	21	<input checked="" type="checkbox"/>	<input type="checkbox"/>	<input type="checkbox"/>	<input type="checkbox"/>	<input type="checkbox"/>
4	Ch A Sweep of CT Det : THD+N - relative : Ch A (Ampl[A]=-4.00 dBu)	21	<input checked="" type="checkbox"/>	<input type="checkbox"/>	<input type="checkbox"/>	<input type="checkbox"/>	<input type="checkbox"/>
5	Ch A Sweep of CT Det : THD+N - relative : Ch A (Ampl[A]=0.00 dBu)	21	<input checked="" type="checkbox"/>	<input type="checkbox"/>	<input type="checkbox"/>	<input type="checkbox"/>	<input type="checkbox"/>
6	Ch A Sweep of CT Det : THD+N - relative : Ch A (Ampl[A]=4.00 dBu)	21	<input checked="" type="checkbox"/>	<input type="checkbox"/>	<input type="checkbox"/>	<input type="checkbox"/>	<input type="checkbox"/>

Figure 15. Test Circuit- THD+N vs Frequency- 0dB Gain

THD+N vs Amplitude

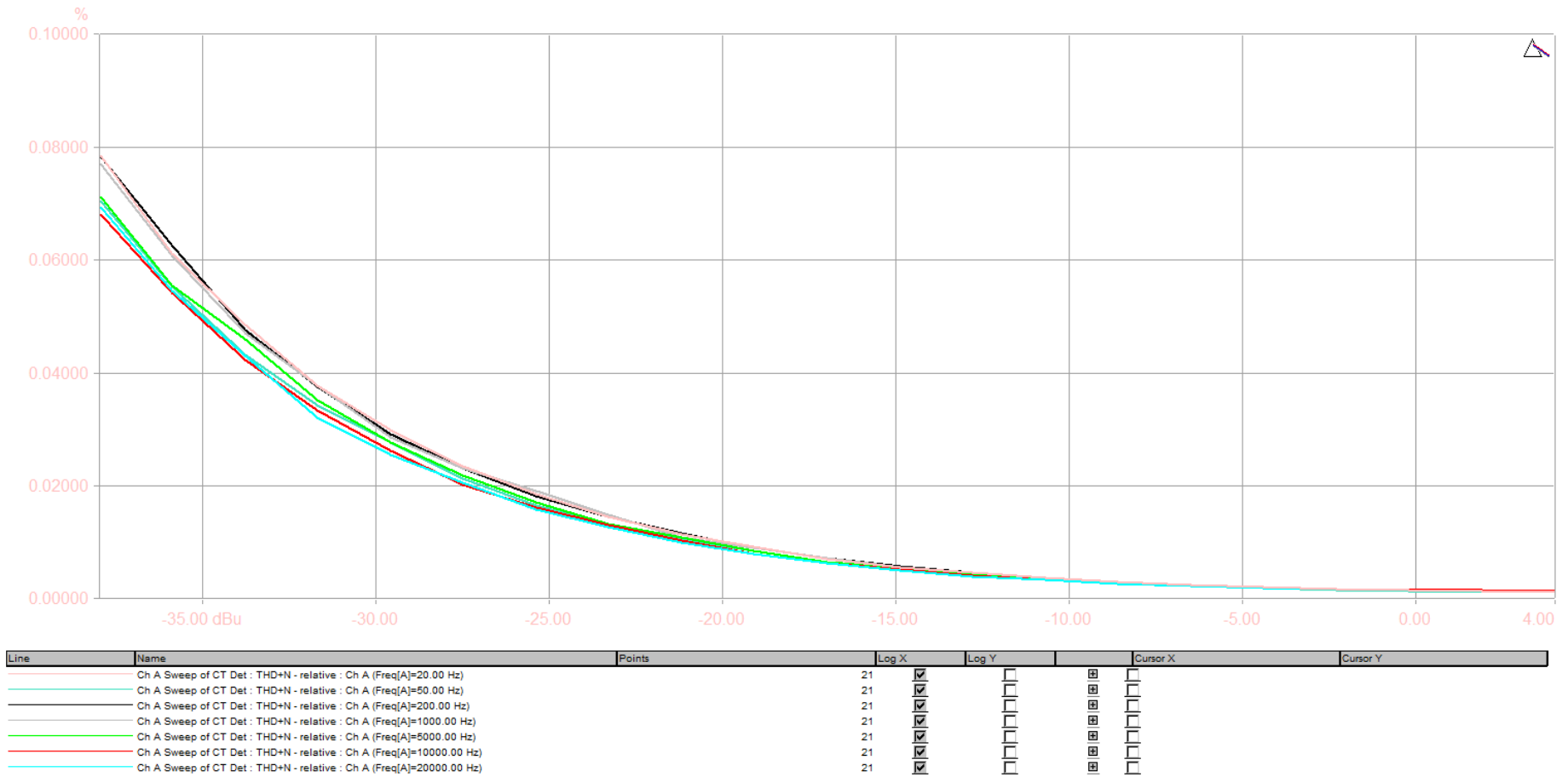


Figure 16. Test Circuit- THD+N vs Amplitude- 0dB Gain

The FFT plots show a visible 50Hz component with related products decreasing in amplitude, consistent with mains power interference, that do not exceed -100dBu shown at an input level of -38dBu at 1kHz with a gain of 0dB (fig.44) which only slightly changes with gain. The multi-tone testing in figure 45 shows few modulated products however indicates the induced 50Hz mains components all not exceeding -100dBu. Overall the test circuit performs within the tolerances expected providing a low distortion and low noise foundation whilst providing appropriate loading and gain for the testing of the devices. The spectrograms recorded across all samples and for each gain setting showed no visible difference.

To achieve these configurations both primary and secondary windings were wired in series. The primary was then driven by the test circuit at the in-phase side whilst the out-of-phase side was connected to ground. This is a common application of an output transformer although another well-used design is to connect either side to the high and low side of a push-pull output stage and using a centre-tap to cancel the DC. One configuration that is suggested in the device datasheet is to use a 2:1 ratio as this reduces the level and requires the use of a mixed feedback system this would introduce more noise and distortion to the circuit.

The transformers were tested both with the instrumentation amplifier and without during the distortion testing to give a clearer view of the device's effects using the same setup and technique as with the instrumentation amplifier in section 2.6 and 2.7. The measures taken of the individual devices contain slight differences such as an increase in distortion across most amplitudes however overall the measures are similar, and focus is drawn to the performance with a fixed test circuit. All inductance, capacitance, impedance and

reactance measures were taken using the Rohde & Schwarz HM8118 LCR bridge. These were measured by connecting the transformer winding in five different configurations.

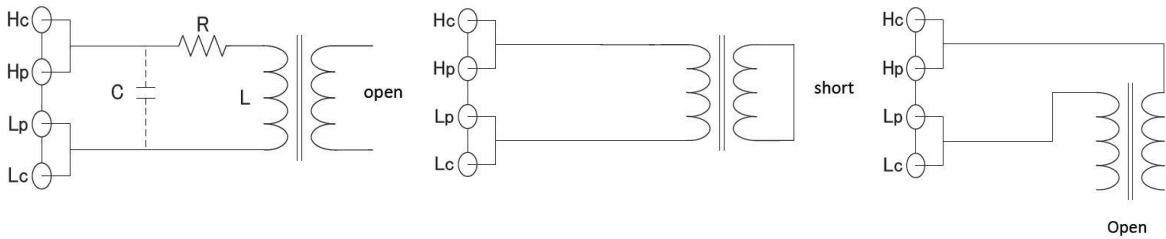


Figure 17. Measurement methods for Primary and Secondary Inductance (a. left), Leakage Inductance (b. centre) and Winding Capacitance (c. right) (Hioki, 2017)

For the primary inductance the primary winding was measured with the secondary open-circuit and the opposite was done for the secondary inductance (fig.17a). The leakage inductance measurement then involved shorting the secondary winding (fig.17b). For the inter-winding capacitance only one side of each winding is connected to the bridge (fig.17c) and the other open-circuit. The mutual inductance comprised of two series of measurements with both windings connected to each other in series: the first configuration connects the in-phase side (denoted by the dot convention) to the out-of-phase side of each transformer known as ‘aiding’ (fig.18a) and the second connects the two out-of-phase connections also known as ‘opposing’ (fig.18b). These two measurements are calculated using the formulae in equation (15 & 16) using both primary and secondary winding inductance and respective aiding and opposing inductance. This is then rearranged giving equations (17 & 18) to calculate the mutual inductance.

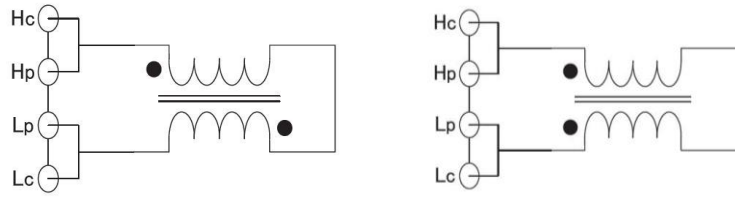


Figure 18. Mutual Inductance Measurement Methods: Aiding (left) and Opposing (right) (Hioki, 2017)

$$L_a = L_1 + 2M + L_2 \quad (15)$$

$$L_o = L_1 - 2M + L_2 \quad (16)$$

$$L_a - L_o = 4M \quad (17)$$

$$\therefore M = \frac{(L_a + L_o)}{4} \quad (18)$$

where:

M is Mutual Inductance

L_a is Inductance (Aiding)

L_o is Inductance (Opposing)

L_1 is Primary Inductance

L_2 is Secondary Inductance

As stated in section 2.3 and 2.4, Hysteresis curves show the relationship between the flux density and the magnetising force (B-H) of a magnetic material this can be found by measuring the primary winding current with relation to the secondary winding voltage. Each measure is taken using a two-channel oscilloscope each channel is then used to displace the plot on an X-Y plane, this integration using the two values provides a rudimentary hysteresis or B-H graph of each device. This is a similar method used to

measure the hysteresis of a magnetic material samples as stated in the IEC 60404-6 standard (CENELEC, 2018).

For the microphone transformer testing the devices were tested individually without the test circuit present. As both devices have two primary windings it was decided like that for the output transformers to use the same primary winding configuration for both devices however the secondary winding of the LL1538 consists of a single winding whereas the VTB9045 consists of two secondary windings that were connected in series.

3.3 Results

Testing of the test circuit with the Lundahl LL1582 produced a relatively flat frequency response with a slight reduction of level approximately -0.5dB at 20Hz (fig.19) and a -10° phase shift at a gain of 0dB (fig.20) that stayed constant across all gains. As gain is increased the frequency response gradually flattens back to 0dB (fig.47 & 49). It can be clearly seen that the THD+N level rises significantly at low signal levels reaching 1.4% at 20Hz when the input signal level is -38dBu (fig.21) it is also clear to see the gradual increase in distortion as the input level drops (fig.22). This shows an increase of over 1.3% from that of the test circuit measurement.

Figure 23 at a signal level of -38dBu at 20Hz with 0dB gain shows the increased level of 2nd harmonic to -82dBu and 3rd harmonic distortion to -78dBu and the following even and odd order components relative to the fundamental; the cause of the increased THD+N. At this level the amount of intermodulation distortion increases dramatically to around -34dB compared to that of around -75dB at the same input level at 1kHz. The level of IMD then improves with increased frequency and signal level. The overall increase in distortion at low signal level is evidence of the effect of the core coercivity and the energy needed for the formation of an electromagnetic field. Another reasoning for the increased level of THD+N is also due to the low CMRR of the instrumentation amplifier at lower voltage gain.

Frequency Response and Inter-channel Phase

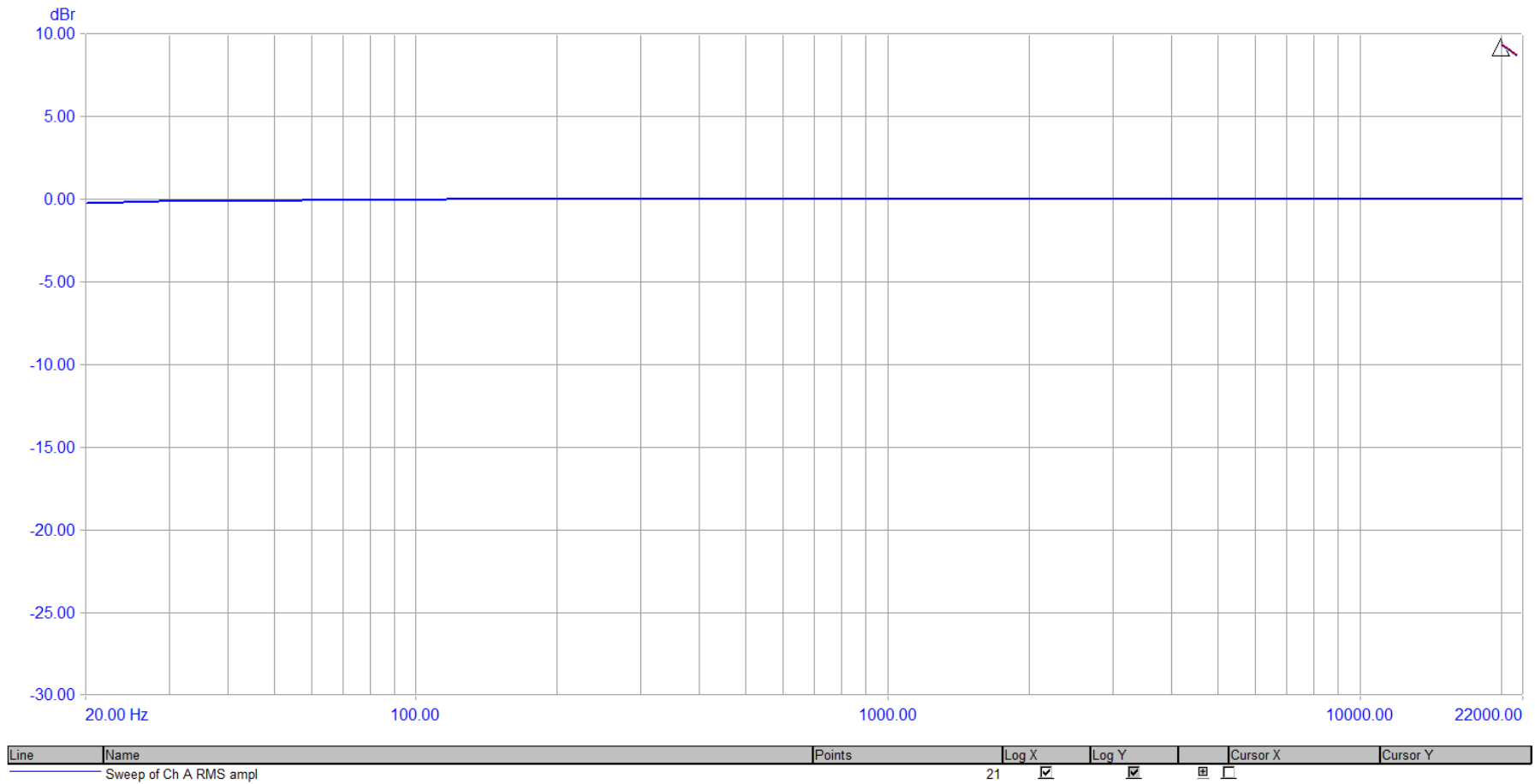


Figure 19. Test Circuit and Lundahl LL1582- Frequency Response- 0dB Gain

Frequency Response and Inter-channel Phase

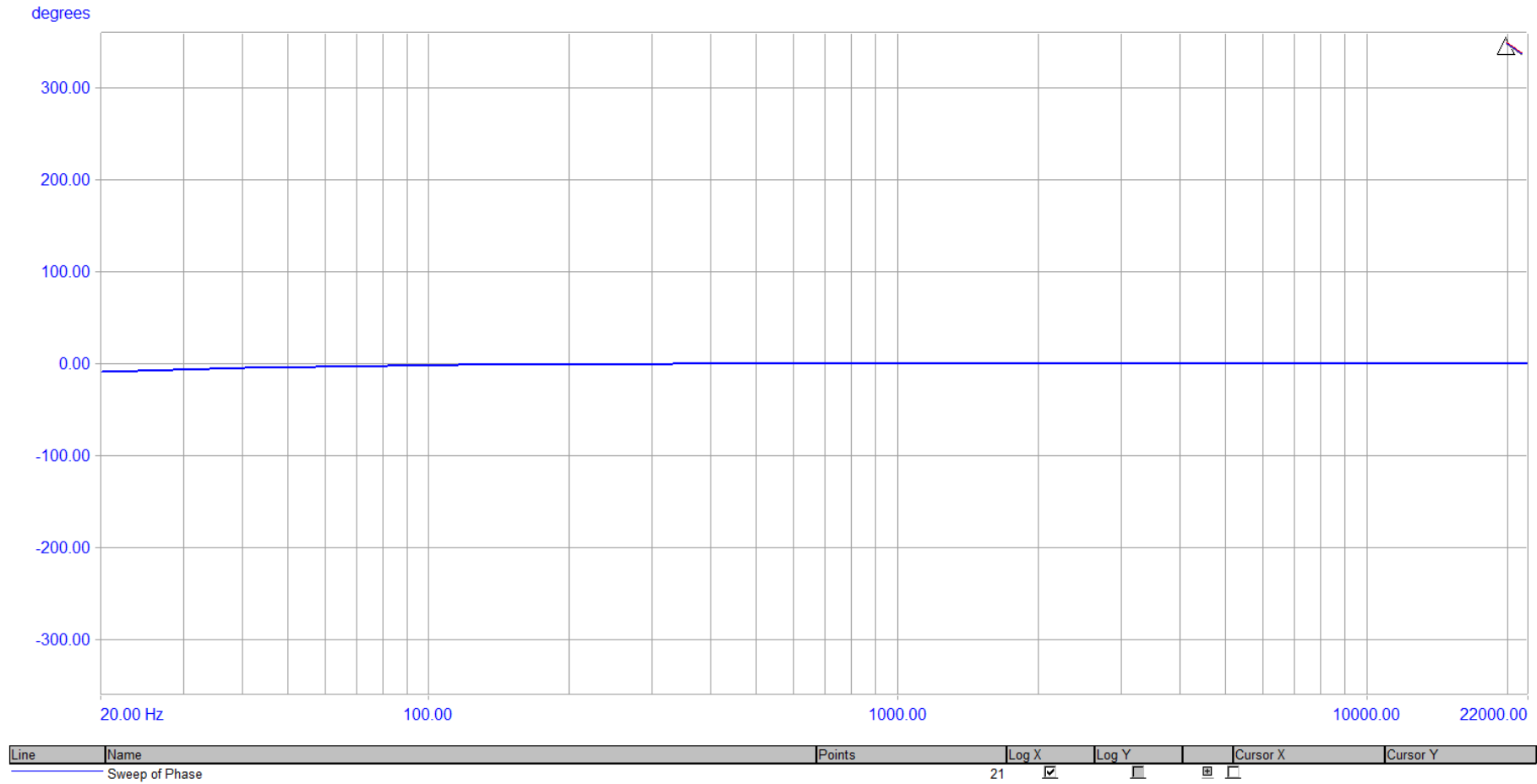


Figure 20. Test Circuit and Lundahl LL1582- Phase Response- 0dB Gain

THD+N vs Frequency

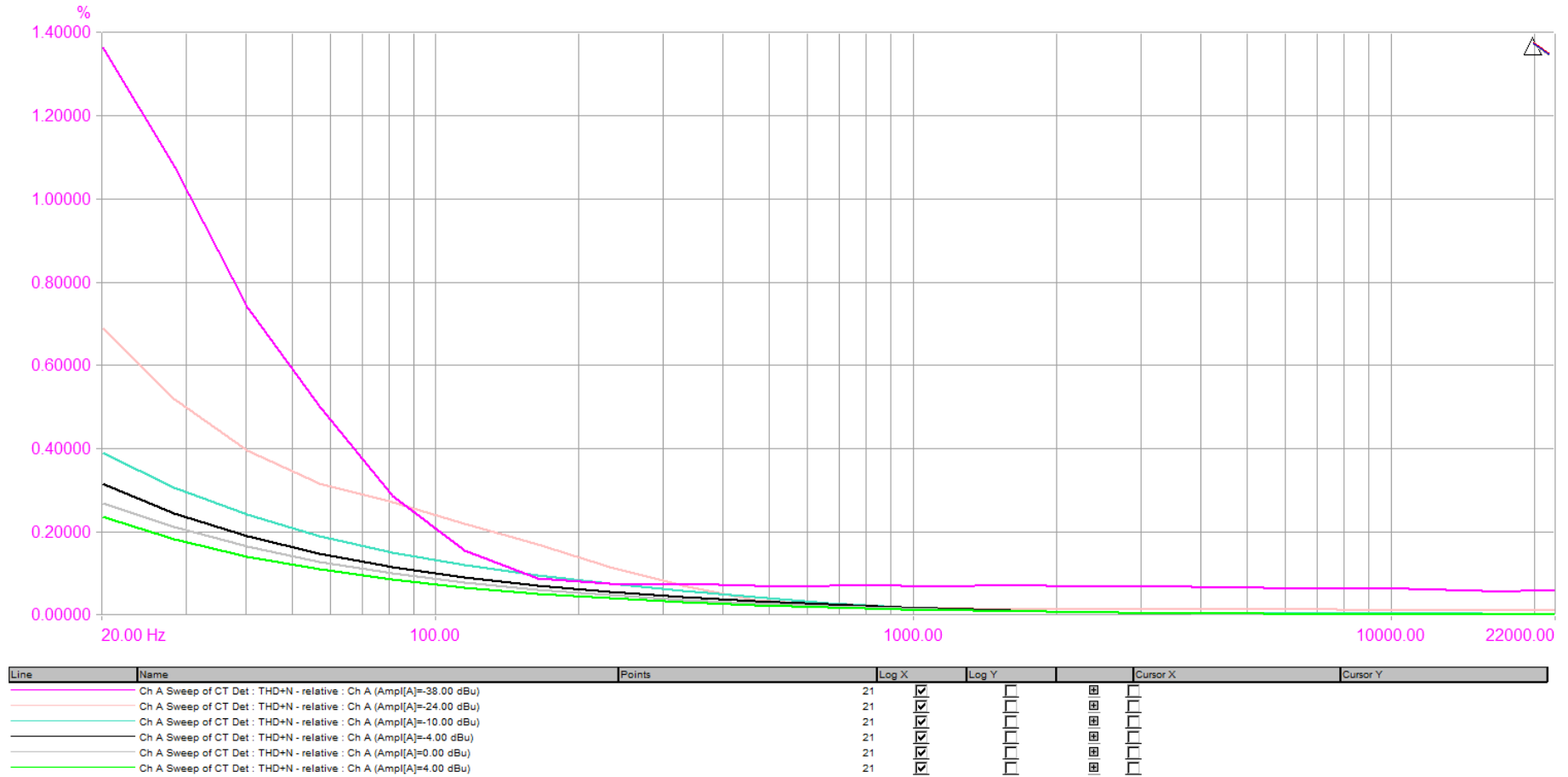


Figure 21. Test Circuit and Lundahl LL1582- THD+N vs Frequency- 0dB Gain

THD+N vs Amplitude

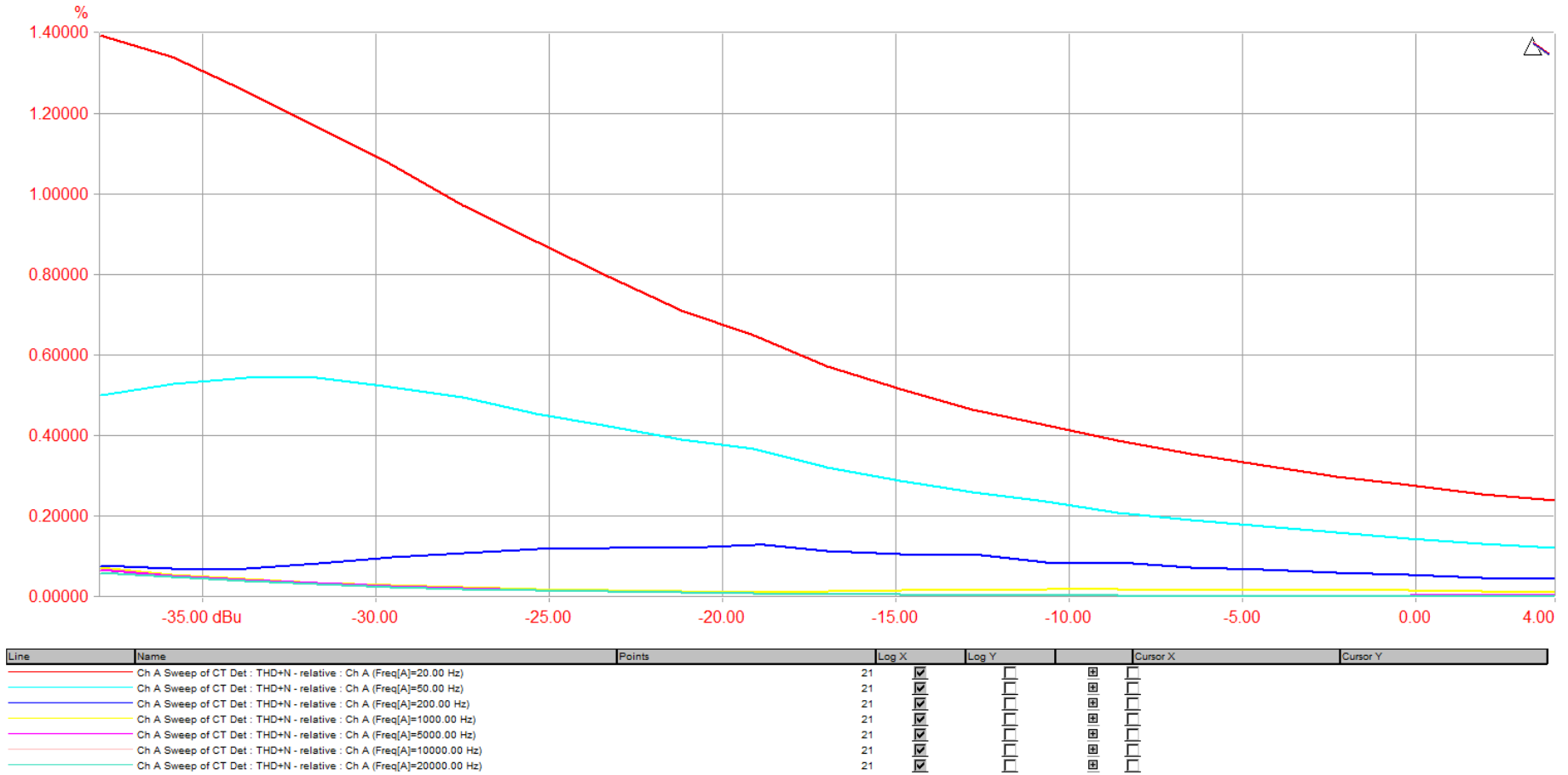


Figure 22. Test Circuit and Lundahl LL1582- THD+N vs Amplitude- 0dB Gain

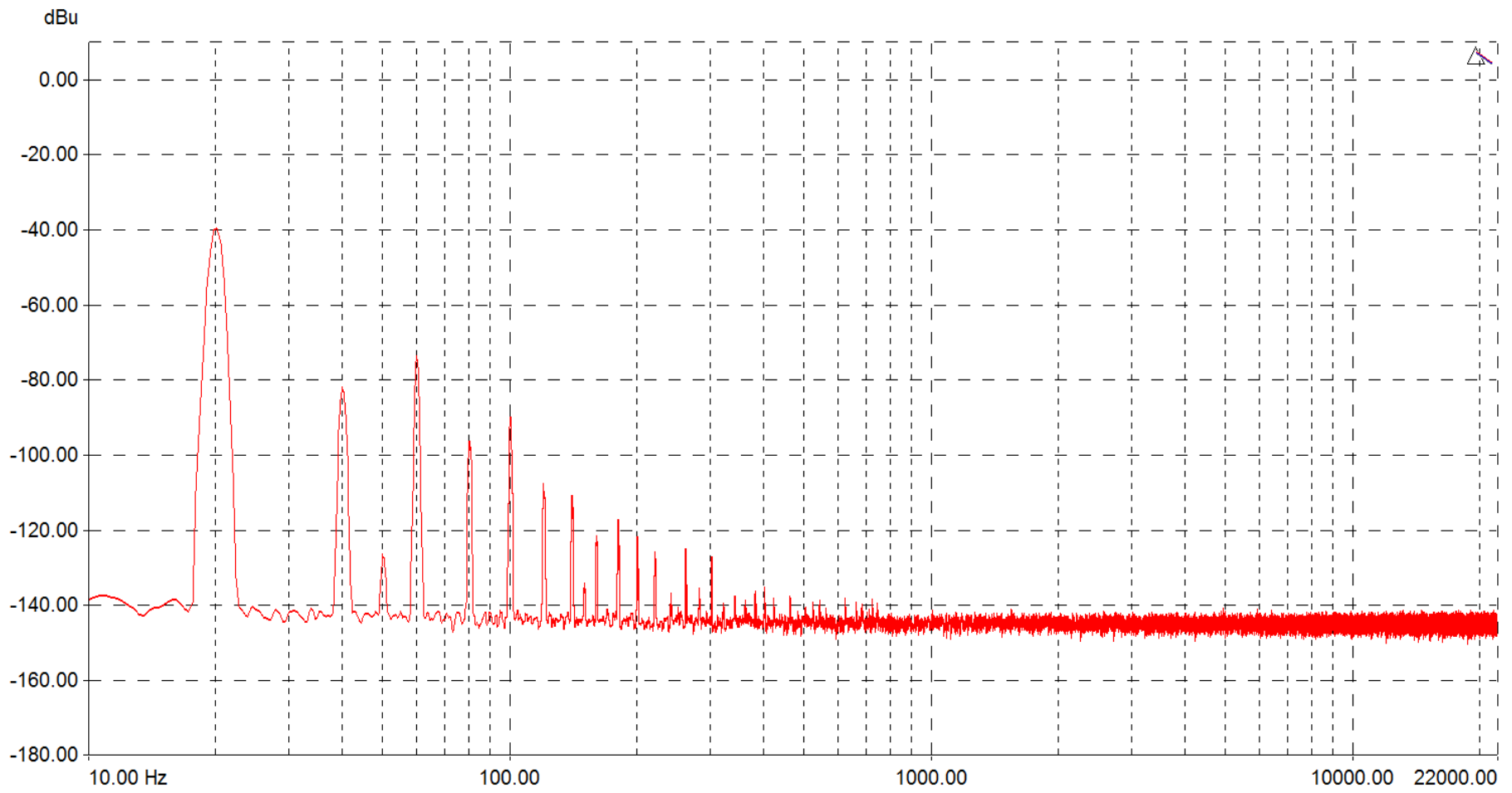


Figure 23. Test Circuit and Lundahl LL1582- FFT at 20Hz -38dBu Input- 0dB Gain

At an input level of +4dBu the THD+N is low across the first two gain settings, but lowest at +6dB gain (fig.48) however at +16dB gain the LL1582 shows an increase in THD+N (fig.25) above most other input levels, which is a result of the core moving closer towards saturation. In the frequency domain it is clear to see the increased 3rd harmonic distortion reaching -30dBu at an input level of +4dBu at 20Hz with (fig.26) and -60dBu at 1kHz (fig.27). Figure 25 clearly shows the curved response increasing at both extremes of the input level on the 20Hz trace. Although the level produced is approximately 0.4% at 20Hz with a level of +20dBu across the primary winding compared to 1.4% at -38dBu. If testing continued up to a level above +20dBu output the 20Hz response curve is expected to increase gradually to the point of full core saturation. Figure 24 shows the reasoning for this through the approximate B-H relationship produced by the transformer when driven with a 20Vp-p (approximately +22dBu) sine wave at 20Hz, which shows the increase in core coercivity which then flattens back to a linear function with an increase in frequency.

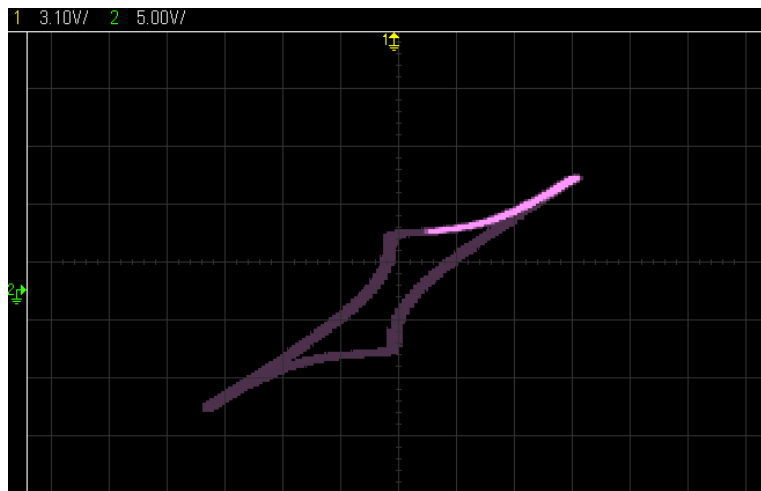


Figure 24. Approximate hysteresis measurement of LL1582- 20Vp-p input at 20Hz

THD+N vs Amplitude

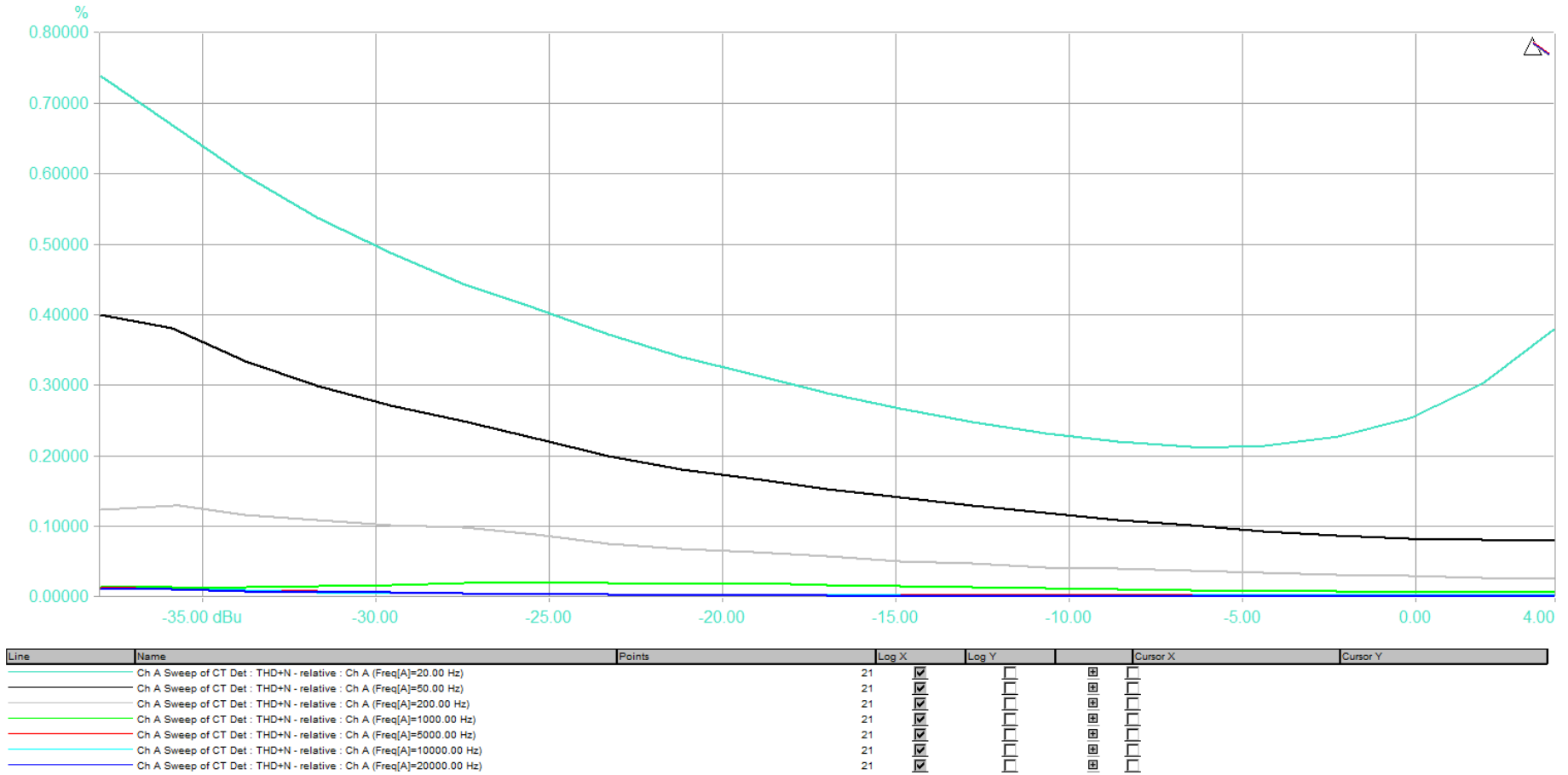


Figure 25. Test Circuit and Lundahl LL1582- THD+N vs Amplitude- +16dB Gain

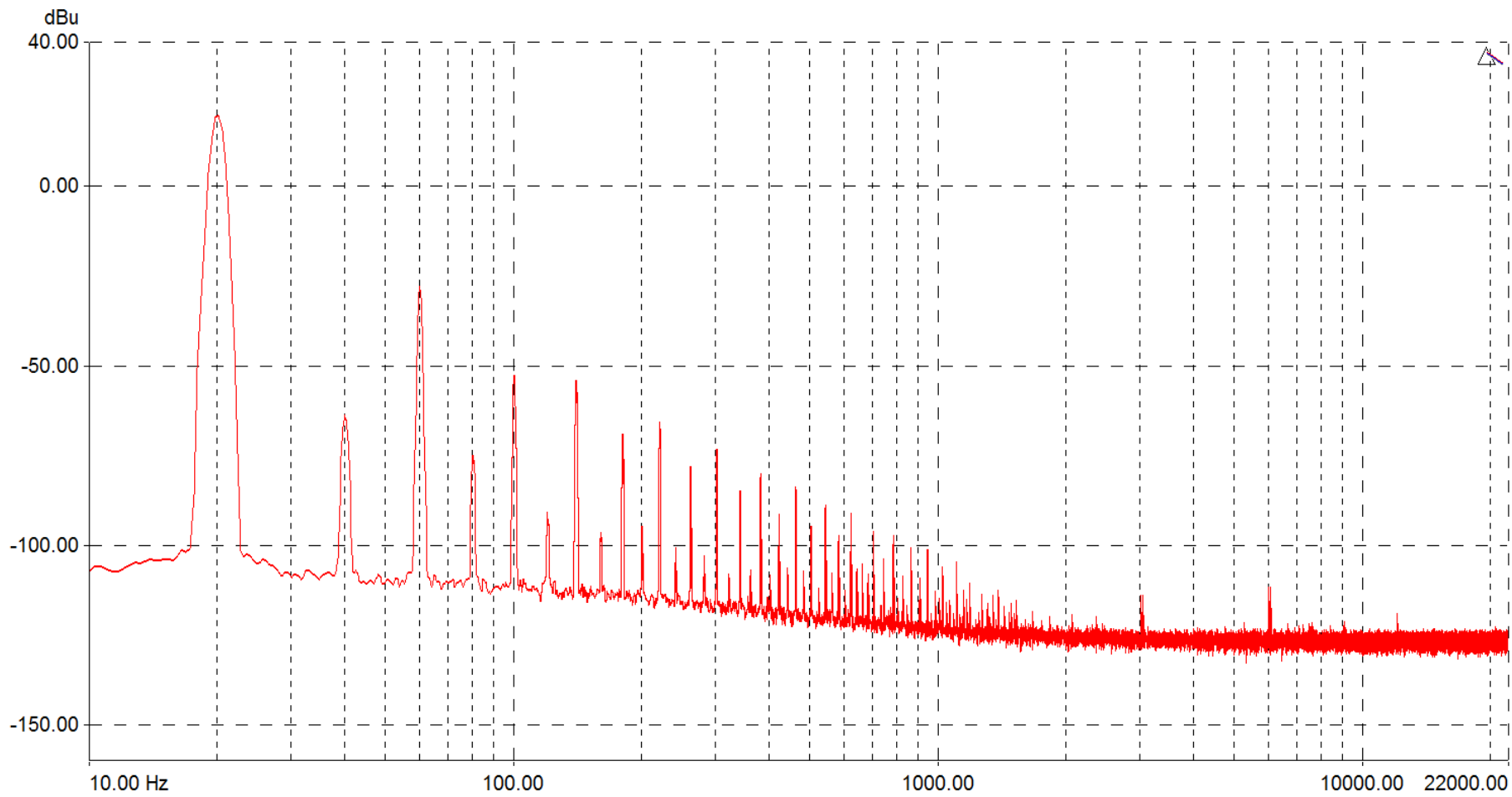


Figure 26. Test Circuit and Lundahl LL1582- FFT at 20Hz +4dBu Input- +16dB Gain

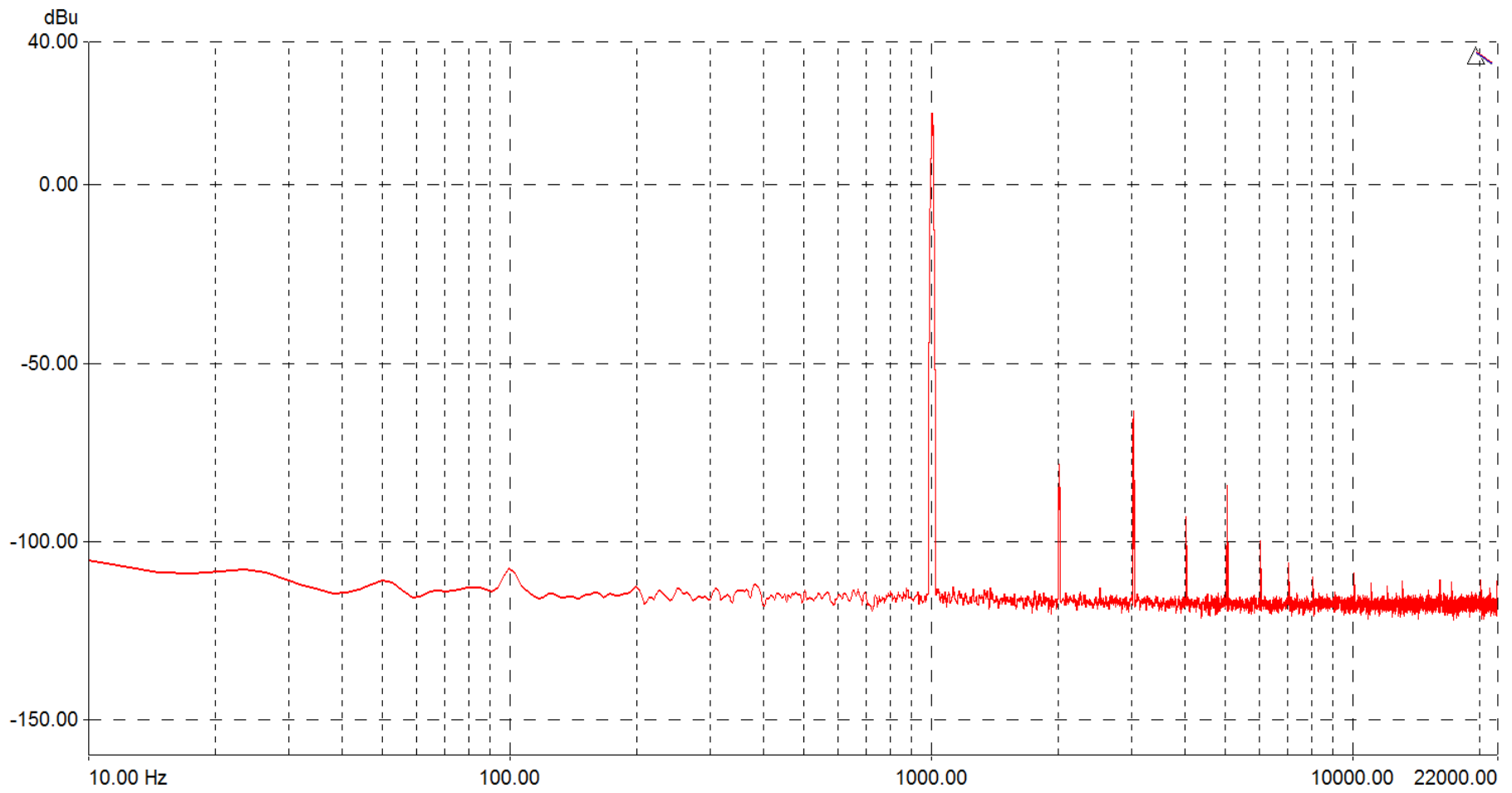


Figure 27. Test Circuit and Lundahl LL1582- FFT at 1kHz +4dBu Input- +16dB Gain

When viewing the responses in the frequency domain many harmonic components are visible at low frequencies both odd-order and even-order such as that shown in figure (23), the amplitudes of which decrease the higher the order. The amplitude of the odd-order products is at a higher level than that of the even and the number of harmonics decrease as the fundamental frequency increases. This is explained by Sowter (1987) as frequency rises, the flux density (B) reduces and so does the generation of harmonic content. The 50Hz mains component has also been greatly reduced from the test circuit measurement which is attributed to the improved EMI susceptibility provided by the CM rejection of the device, the balanced output at the secondary winding and the electromagnetic shield encasing the transformer. The change of the mains products can be seen in the multi-tone test with components barely rising above -120dBu (fig.46).

When viewing the spectrograms, only very minor differences are visible with the bass and double bass sample with all other samples showing no obvious changes. The bass sample shows the reduction of harmonic components around 500-600Hz at progressively higher gain (fig.56-59). The double bass sample shows the introduction of components in the periods of silence at the beginning and end of the excerpt (fig.60-63) however this seems to be consistent with extraneous noise. The bass sample shows the reduction of harmonic components around 500-600Hz at progressively higher gain (fig.57-59). The double bass sample shows the introduction of components in the periods of silence at the beginning and end of the excerpt (fig.61-63) however this seems to be consistent with extraneous noise.

During the testing of the Carnhill VTB1148 with the test circuit gain set to +16dB a problem arose where the instrumentation amplifier began to draw a large amount of current

(approximately +20mA) and produced an irregular output signal with an input signal below 50Hz at levels above -10dBu. The increase in current then caused the IC to rapidly heat up and ultimately destroyed the first device when left for an extended period. It is thought that the increase in current was caused by the low static DC resistance of the primary winding (as the AC impedance was considered adequately matched) however due to time constraints, the problem could not be resolved in time for testing although the measurements at lower levels still exhibit the performance without issues. It is thought that the issue could have been rectified with a discrete emitter follower that could act as a buffer however this would have also increased the overall noise and distortion level if not designed properly. Figures (53) & (54) show the frequencies and amplitudes during the THD+N measurements at which the testing fails due to the high current. Using the FFT analysis at a level of +4dBu at 20Hz with +16dB gain (fig.55) the response contains an extensive number of odd and even harmonic components with the odd order products having the overall highest amplitudes.

The measures showed a frequency response like that of the Lundahl LL1582 showing a level drop in the low frequencies although the drop is less than -0.5dB at 0dB gain (fig.28) with no obvious change at +6dB. The phase response as shown in figure 29 is also similar showing approximately -10° shift at 20Hz across 0db and +6dB gain although this change starts gradually around 80Hz. Figure 30 shows a response like that of the LL1582 but shows decreased distortion at 50Hz due to the presence of mains interference. The THD+N versus amplitude graphs (fig.31 & 52) show in better detail the decreasing levels at higher gains and higher input signal level as expected however overall the measures are significantly lower than that of the LL1582. In the frequency domain it can be seen that the harmonic content consists of odd and even order components whose amplitude decreases

with frequency as with the LL1582 including the reduction in the number of components,
the higher the fundamental frequency.

Frequency Response and Inter-channel Phase

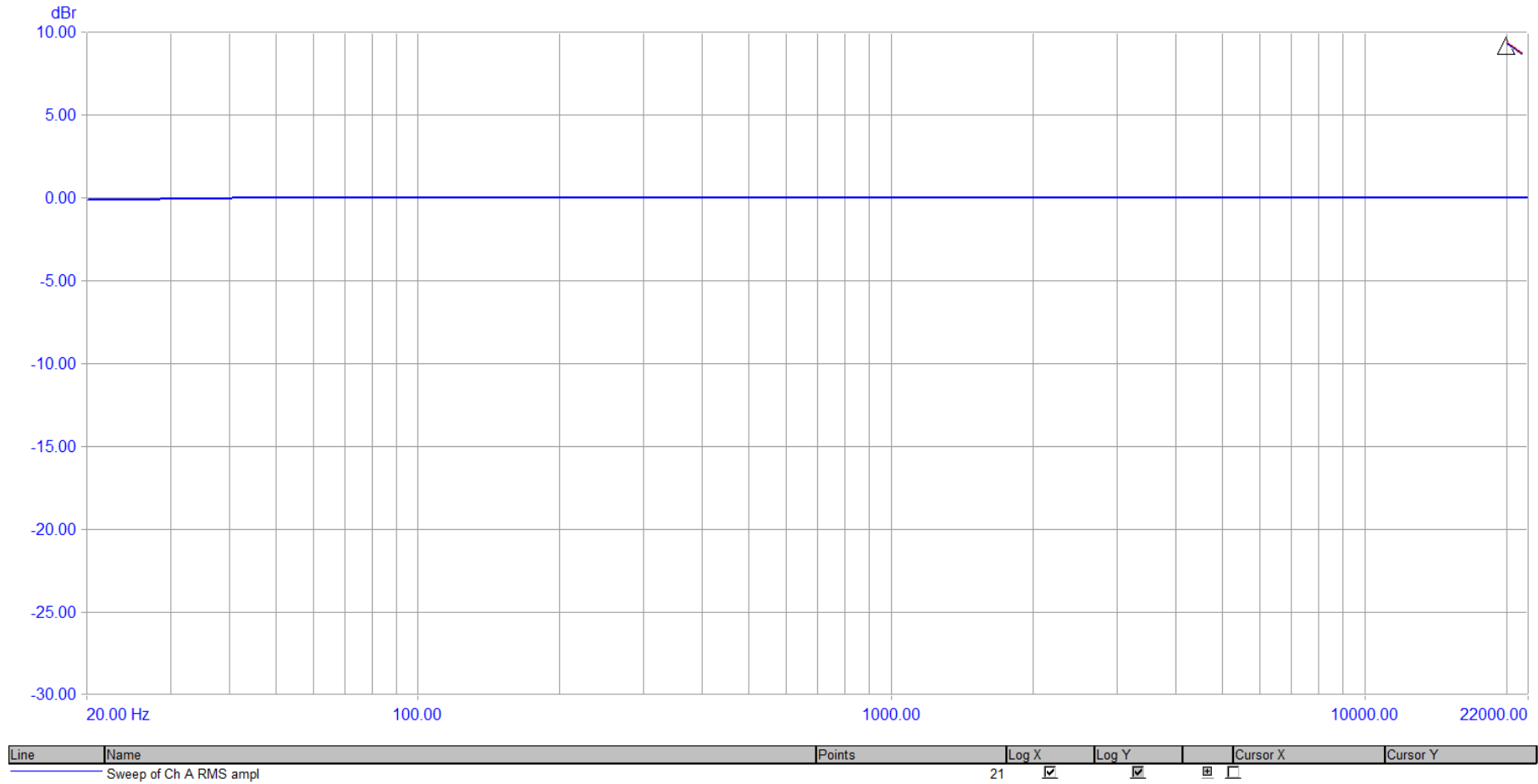


Figure 28. Test Circuit and Carnhill VTBI148- Frequency Response- 0dB Gain

Frequency Response and Inter-channel Phase

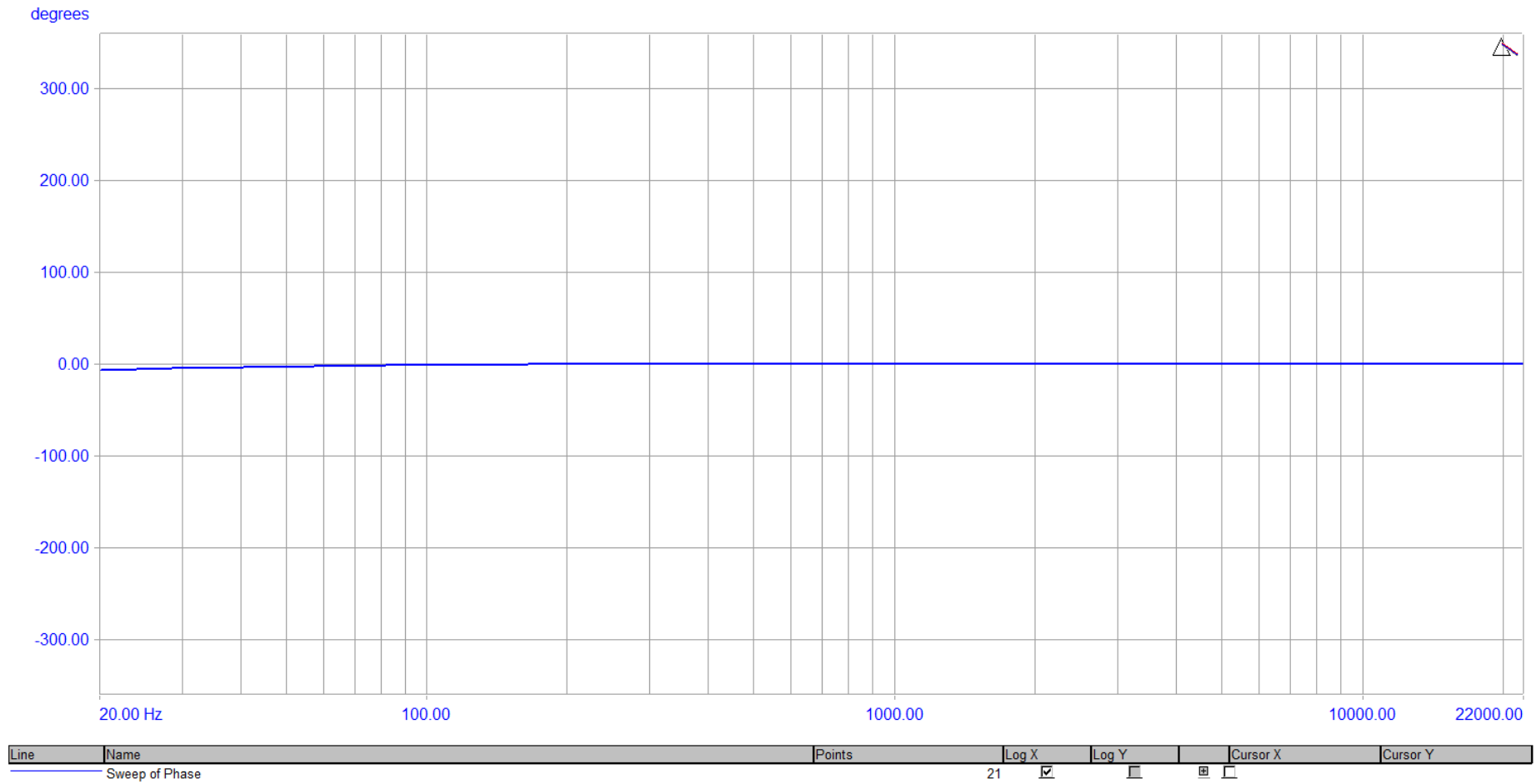


Figure 29. Test Circuit and Carnhill VTBI148- Phase Response- 0dB Gain

THD+N vs Frequency

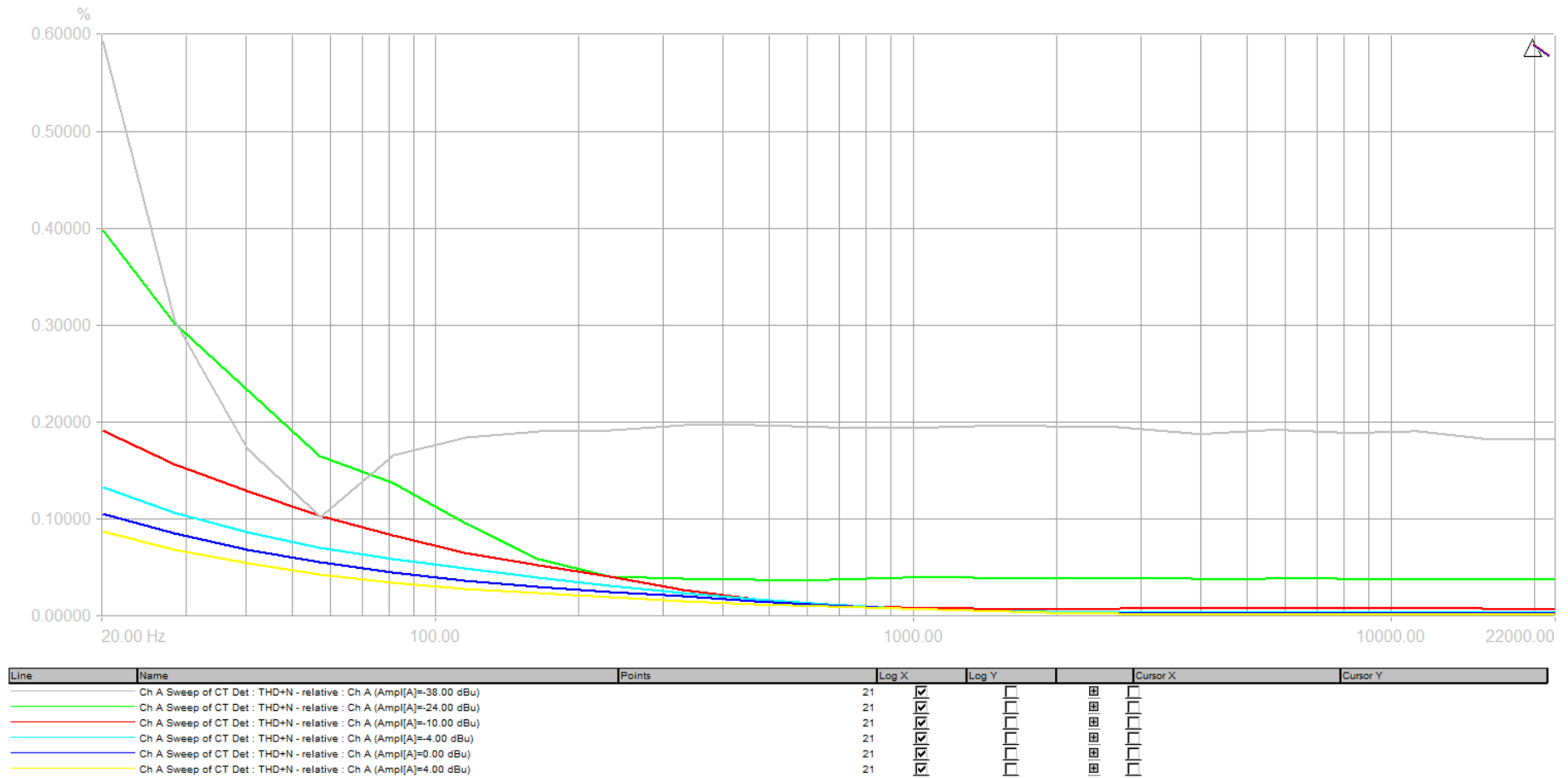


Figure 30. Test Circuit and Carnhill VTB1148- THD+N vs Frequency- 0dB Gain

THD+N vs Amplitude

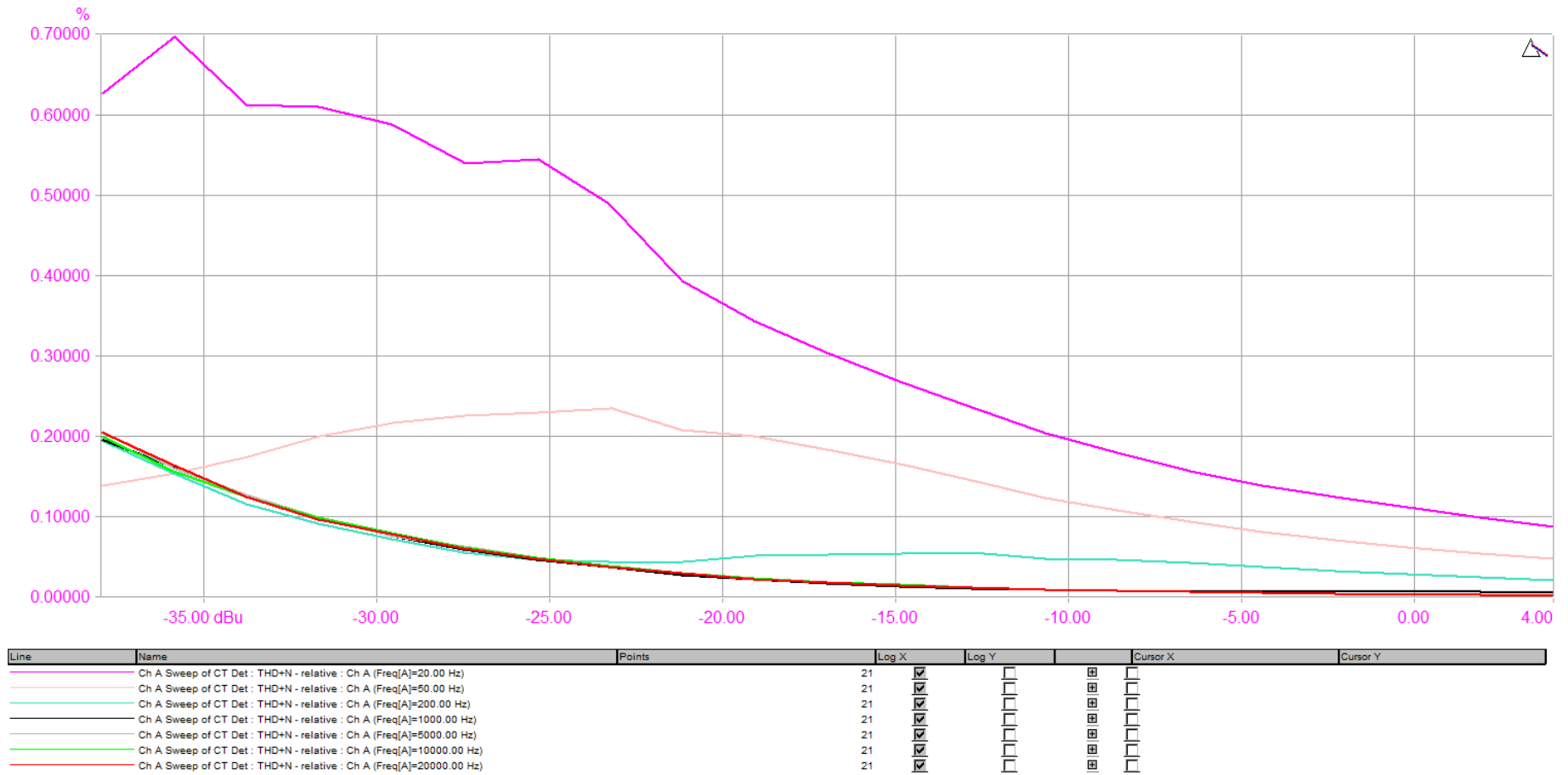


Figure 31. Test Circuit and Carnhill VTB1148- THD+N vs Amplitude- 0dB Gain

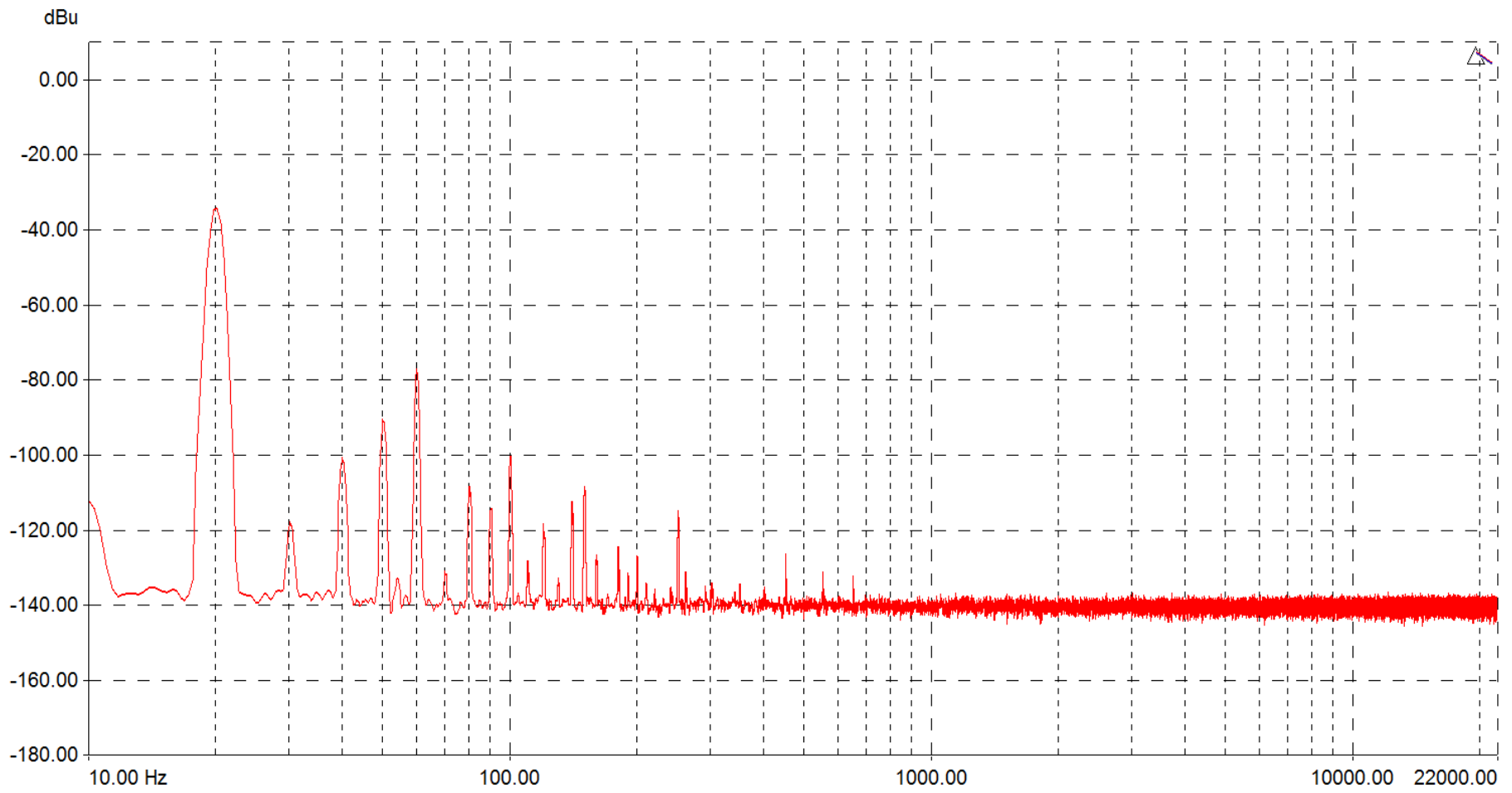


Figure 32. Test Circuit and Carnhill VTB1148- FFT at 20Hz -38dBu Input- 0dB Gain

Figure 32 shows that at a level of -38dBu at 20Hz with a gain of 0dB a 30Hz component, a high 3rd harmonic around -80dBu and a high 50Hz component around -90dBu which all seem to interact to produce intermodulation distortion. The level of IMD measurement is also close to that of the LL1582 at -43dB and like that of the LL1582 the level improves with increased frequency and signal level. When comparing both the LL1582 and VTB1148 THD+N responses across the gains whilst at an input level of +4dBu at 20Hz it can be seen that the LL1582 has a level between 0.2-0.4% compared to the lower 0.08-0.09% of the VTB1148.

It is clear to see that the VTB1148 has a higher susceptibility to mains power interference shown presenting a 50Hz component at approximately -90dBu with an input level of +4dBu at 1kHz and a gain of 0dB (fig.50). This can also be seen in figure 51 the multi-tone test, at the same gain and input level. Ultimately, this issue is attributed to the lack of electromagnetic shielding around the transformer to protect from induced mains interference.

On assessment of the electronic measures of winding, leakage, mutual inductance and capacitance across the frequency range show an inverse relationship as expected: an increase in frequency causes a decrease in inductance and capacitance. It was found that the measured level of leakage inductance of the VTB1148, 14mH at 20Hz, was considerably lower than the 128mH of the LL1582. This is possible evidence towards an improved coupling provided by the shell-type E-I core surrounding the windings.

The spectrograms, overall show no significant difference with the exception of a minute change on the snare sample in the low frequency region around 20-200Hz (fig.66-68). The

double bass sample shows a similar response to that of the LL1582 by presenting components in the sections of silence at the beginning and the end of the samples (fig.64-65) which are consistent with that of mains power interference.

The microphone transformer measurements show similar responses albeit at overall lower levels. THD increases at lower signal levels presenting approximately 0.022% at -50dBu at 20Hz and approximately 0.042% for the VTB9045. Both show susceptibility to mains as expected for a low-level signal transformer however the LL1538 shows increased levels at approximately -90dBu. One difference between the transformer types is the frequency response shows a boost at high frequency around 0.5dBr at 22kHz for the LL1538 and approximately 2dBr at 22kHz for the VTB9045.

It has been shown that the devices produce an increased level of THD+N at both extremes of level and at low frequencies, caused by an increasing amount of odd and even order harmonic components. This is attributed to the limiting factor of core permeability: particularly the effects of the core coercivity and saturation at low and high signal levels respectively. The effect of transformer construction on the overall permeability of the device is also highlighted as a pivotal element in the devices performance.

Chapter 4: Subjective Analysis

The subjective analysis begins with the consideration of suitable stimuli, listening subjects, listening environment and playback system. Each of these aspects are incorporated into the method section which discusses the listening test method and statistical analysis method. Finally, the results of the statistical analysis are presented and discussed.

4.1 Stimuli

It is stated in the ITU-R BS.1116-3 recommendation (2015) that for small impairment tests critical listening material, such as the EBU ‘Sound Quality Assessment Material’ (SQAM) (European Broadcasting Union, 2008). However, it was decided that it would be more beneficial if the samples were chosen to be representative of real-life signals that would be encountered by a microphone/ line-level preamplifier such as an electric bass, snare drum, vocal and guitar. A double bass sample was also included as it is already known that transformers have a higher flux density at low frequencies therefore begin to saturate first so this excerpt was used to excite the low frequency response to provoke a slightly more extreme effect than that of the other stimuli that lack lower frequency content. It could be argued that a bias could be introduced through the use of a vocal track in the English language as all participants in the test were English speakers, the lyrics could create a distraction in a similar way to how a melodic excerpt could distract the listener from the task by focusing on the words or melody.

The five samples used in the tests were comprised of instruments from sample libraries and from the European Broadcasting Union (EBU) Sound Quality Assessment Material

(SQAM) CD (European Broadcasting Union, 2008). What was considered as high-quality samples were used all at 24-bit 96kHz. The signals were considered relatively ‘dry’ or having little if any reverberation as this was decided would cause distraction. The levels of the samples were reduced in the DAW to correspond to an average level of approximately -20dBFS (approximately +4dBu at the output) to replicate a line level signal at the input of the test circuit.

The samples were then recorded through a MOTU 16A using an Apple Mac Pro and the Pro Tools DAW with and without the transformer present in the test circuit to eliminate a difference between recordings that could be caused by artefacts from the signal chain. All samples were recorded in the Wave file format at 96kHz sampling rate, 24 bit providing better resolution and avoiding any possible effects caused by recording quality. All the samples that had been recorded through the transformer (the processed samples) had the level adjusted to the corresponding level of the recording that had not been recorded through the transformer (the reference sample) using the LUFS (also known as LKFS) algorithm to measure the loudness. By analysing the reference and the processed samples individually using a MATLAB script this provided a level difference. This removed the ambiguities that would otherwise be caused by measuring the difference using a level meter in a DAW. The second script was then used to adjust the level using the value produced by the first script, which once again eliminates the inaccuracy of the faders in the DAW.

4.2 Listening Subjects

In the recommendation for small impairment testing (International Telecommunication Union, 2015) it is important that the listening subjects are all considered ‘trained’ or ‘expert’ listeners as opposed to ‘naïve’ or untrained subjects. By using untrained listening subjects this would introduce a bias towards a random result as the subjects are not likely to detect small differences between stimuli.

All listening subjects who took part in the test were university students, researchers and lecturing staff of different ages, who were considered trained or expert listeners who all have a level of critical listening experience.

4.3 Listening Environment and Playback System

The listening environment and playback equipment were principal factors in the test as every part of the playback signal chain could introduce distortion or noise therefore all were carefully chosen to limit the introduction of any bias. The choice was made to run the test using headphones to reduce any room effects or noise which could mask any content or distract the subject if the test was done using loudspeakers instead. The headphones used were the Sennheiser HD650, which are open-backed and circumaural, that provide an extended frequency range from 10Hz to 41kHz and a THD figure of less than 0.05% (Sennheiser, 2019). As the headphones are open-backed and do not isolate sound from around the listener this had an influence on the choice of listening environment leading to the choice of the Applied Psychoacoustic Laboratory (APL) at the University of Huddersfield (fig.33): an ITU-R BS.1116 compliant reference listening room.



Figure 33. The Applied Psychoacoustic Laboratory at The University of Huddersfield (University of Huddersfield, 2019)

The interface used was the Merging Horus which was chosen for its high-quality digital to analogue converters which offers a flat frequency response of up to +0/-3dB from 6Hz to 88kHz, a THD figure of less than -100dB (0.001%) and a dynamic range of 109dB (A-weighted) contributing to the interface's overall transparency (Merging Technologies, 2019). The output level was set using the sensitivity value of the headphones and the desired playback level using equation (19). By measuring the r.m.s. voltage output from the interface and adjusting the output level until the voltage matched that above.

$$V_{rms} = 78dB \left(\frac{1V}{103dB} \right) \approx 0.76V_{rms} \quad (19)$$

where:

V_{rms} is the rms output voltage

4.4 Method

For this study the alternative and null hypothesis were defined as follows:

- Alternative hypothesis: There is an audible difference with the transformer
- Null hypothesis: There is not an audible difference with the transformer

By using the hypothesis, the level of difference produced by the device was assumed to be small or non-existent therefore demanding a listening test that will test if a subject is guessing or making the correct choices producing a binomial result. It was therefore decided that the double-blind triple-stimulus with hidden reference method or ABX test was the most appropriate testing method. The first implementation of the test was done using the Web Audio Evaluation Tool (WAET) (Jillings et al., 2016) due to the simplicity of the graphical user interface, comment box facility and the diagnostics however, the HTML setup interface was not easy to understand and implement. Ultimately when the design was checked it did not execute and due to time constraints, the issue could not be fixed ready for testing therefore HULTI-GEN (Gribben & Lee, 2015) was used in its place.

The HULTI-GEN interface (fig.34) offered an easy setup, randomisation of samples and simple user interface however the ABX test did not implement buttons for the selection of the A sample or B sample instead a customised slider was used to select between ‘same as reference’ and ‘different to reference’ which produced a binary result of 1 and 0 respectively. It was imperative that the samples in each trial and the trial order were randomised to eliminate any bias caused by the repetitions or patterns however when the

results files were produced information about the order of the stimuli and the test order were also included along with the binary test results.

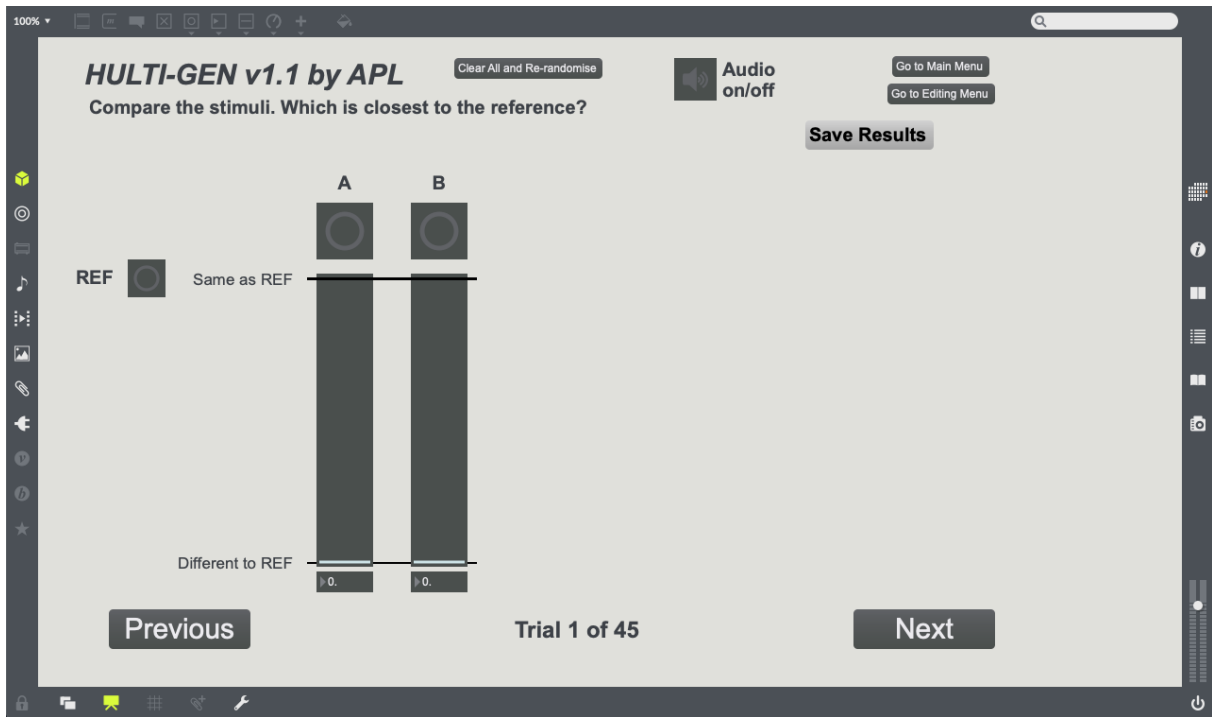


Figure 34. The Listening Test User Interface Implemented on HULTI-GEN (Gribben & Lee, 2015)

At the beginning of the test setup playback level was set at a peak level of +78dBA as specified by the ITU-R BS.1116-3 recommendation (International Telecommunication Union, 2015) as opposed to allowing the listener to select the level. Using a pink noise alignment signal and the files used in the testing, the r.m.s. voltage was taken using a DMM and the level of the headphones adjusted using the headphone gain on the Horus interface.

Before the start of the subjects' testing, a training session was introduced preceding the first test to allow them to familiarise themselves with the stimuli with the aim that there would be less distraction caused by any melodies or rhythms during the actual testing.

Each subject was also given a comments sheet, so they could write down informal notes about what they thought sounded different if they heard a difference. It was also decided that to eliminate any issues with the design before starting the main testing a short pilot test was conducted using 2 subjects to check for any errors in the test design and audio files and to gauge how long the test could take to complete.

Although 10-15 trials are specified by the ITU-R BS.1116-3 recommendation (International Telecommunication Union, 2015), it was decided that the more repetitions of a given condition would provide better statistics resolution with only 11 subjects taking part in the test therefore each test contained 12 repetitions of each condition (15 samples/ conditions) per subject split into 4 sub sessions (table 4). Thus, resulting in 45 trials per session providing a total of 180 trials per subject. Each session taking approximately 20-30 minutes to complete with each subject receiving a minimum of 15-minutes break between sessions. It was important that the tests did not run for longer than 30 minutes to avoid the fatigue of the subjects whilst concentrating on the repeated samples for prolonged periods of time.

	No. of Conditions (Audio Samples)	No. of Repetitions	Total trials per session	Time
Session 1	15	3	45	30-40 mins
Session 2	15	3	45	30-40 mins
Session 3	15	3	45	30-40 mins
Session 4	15	3	45	30-40 mins
Total		12	180	120-160 mins

Table 4. Listening Test Structure Per Subject

Due to time constraints and listening subject availability the Carnhill VTB1148 was only tested using 4 subjects. The smaller ‘pilot’ test used the same test setup as with the

LL1582 however due to the obvious level of distortion caused by the increased current draw of the instrumentation amplifier only the 0dB and +6dB gain samples were used during testing. This resulted in only 10 samples therefore 10 trials that were repeated 12 times in total (30 trials per session).

To interpret the binary data produced by the testing software the IBM SPSS software package was used to execute a binomial one-tailed test. Two confidence intervals were used in the analysis, the first being the psychological/ social sciences standard of 95% and a stricter level of 99% commonly used for medical applications which shows that less than 5% or 1% of results are a guess respectively. The LL1582 and VTB1148 p-values produced by the binomial test were arranged into a table to produce a heatmap of any significant values. The resulting p-values from a binomial were arranged in a table and shaded according to the size of the value and another table could be shaded to only show significant values. This helps to visualise any trends presented by the results even if none of the results are significant. This was done for a confidence interval of 95% and 99%.

4.5 Results

By analysing the amount of correct identifications (fig.35): the distribution produced is not completely random, with a concentrated amount of correct results around the three bass samples at a frequency of over 80%. A selection of other samples such as the double bass and snare are also shown to be correctly identified over 80% albeit by fewer subjects. This trend is also shown somewhat when examining the mean correct identifications of each sample for all subjects (fig.36): the bass sample has the largest concentration of mean correct answers with most of the other responses closer to 50%. Using 95% CI error bars, varying amounts of overlap are presented which would suggest that the results are not conclusive although, this alone is not a reliable method to determine statistical significance.

Using a binomial test and p-value heatmap the results for the LL1582 showed that the 0dB bass samples were correctly identified the most by 4 subjects producing a low p-value (table 5). Across the 3 different gain settings 2 subjects produced a significant result using a 95% CI this is also visible across all subjects for each gain with 95% and 99% CI (table 6 & 7). However, with the 99% CI there is a reduced amount of significant values as expected. Overall the bass sample indicated that the amount of correct identifications was higher than the expected .50, $p = .00$ at 0dB and +16dB gain and $p = .001$ at +6dB gain (1-tailed). The comment sheets produced by the subjects also described how many of them thought the bass was “brighter”, “has more presence” and “has more low-end”. With all other samples there is no obvious pattern presented with the p-values although there are some significant result values presented (table 5 & 6). It is thought that this is due to a possible bias caused by the limited amount of repetitions per sample only being 12 for each subject.

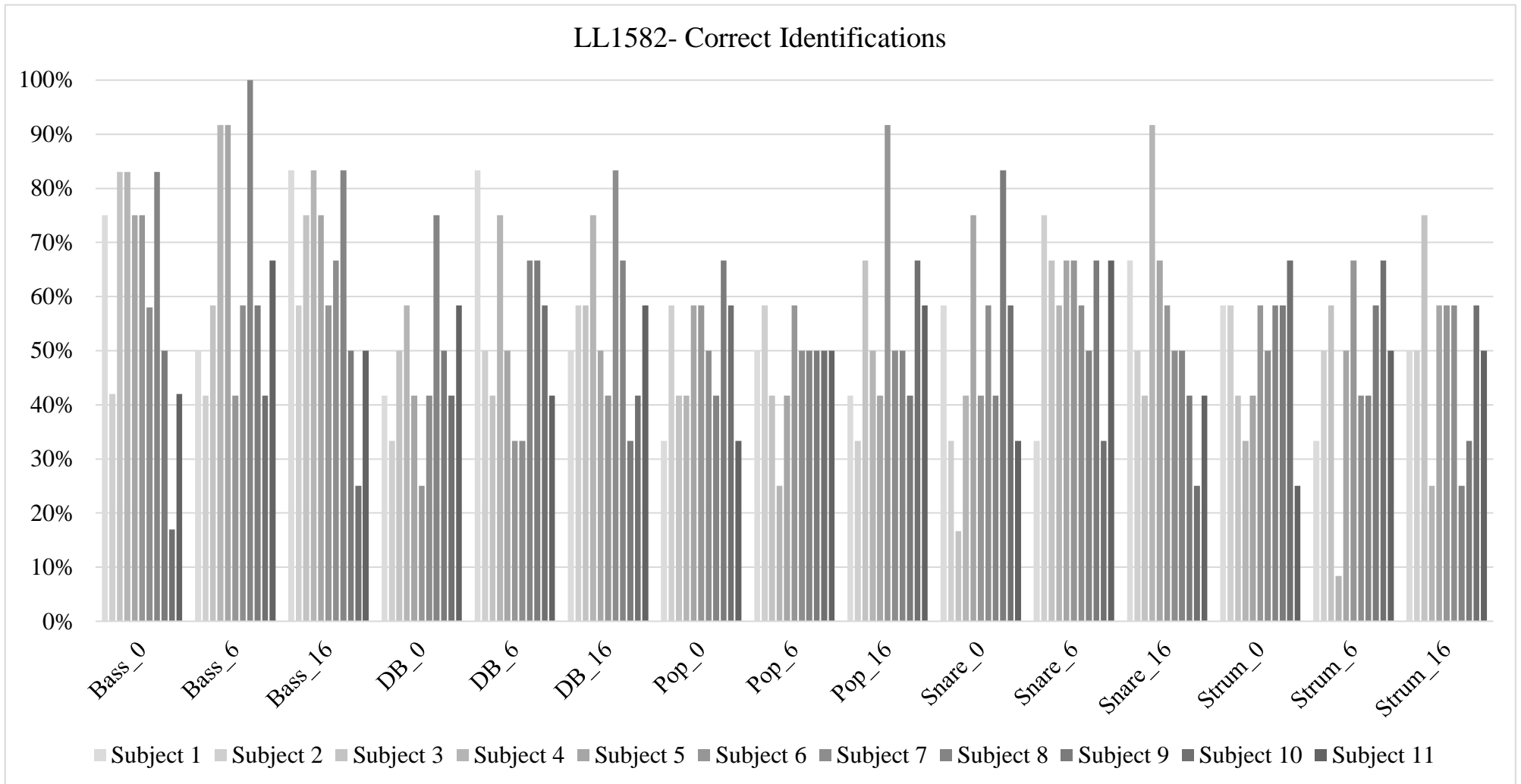


Figure 35. Correct Identifications of Each Sample Per Subject- LL1582 Tests

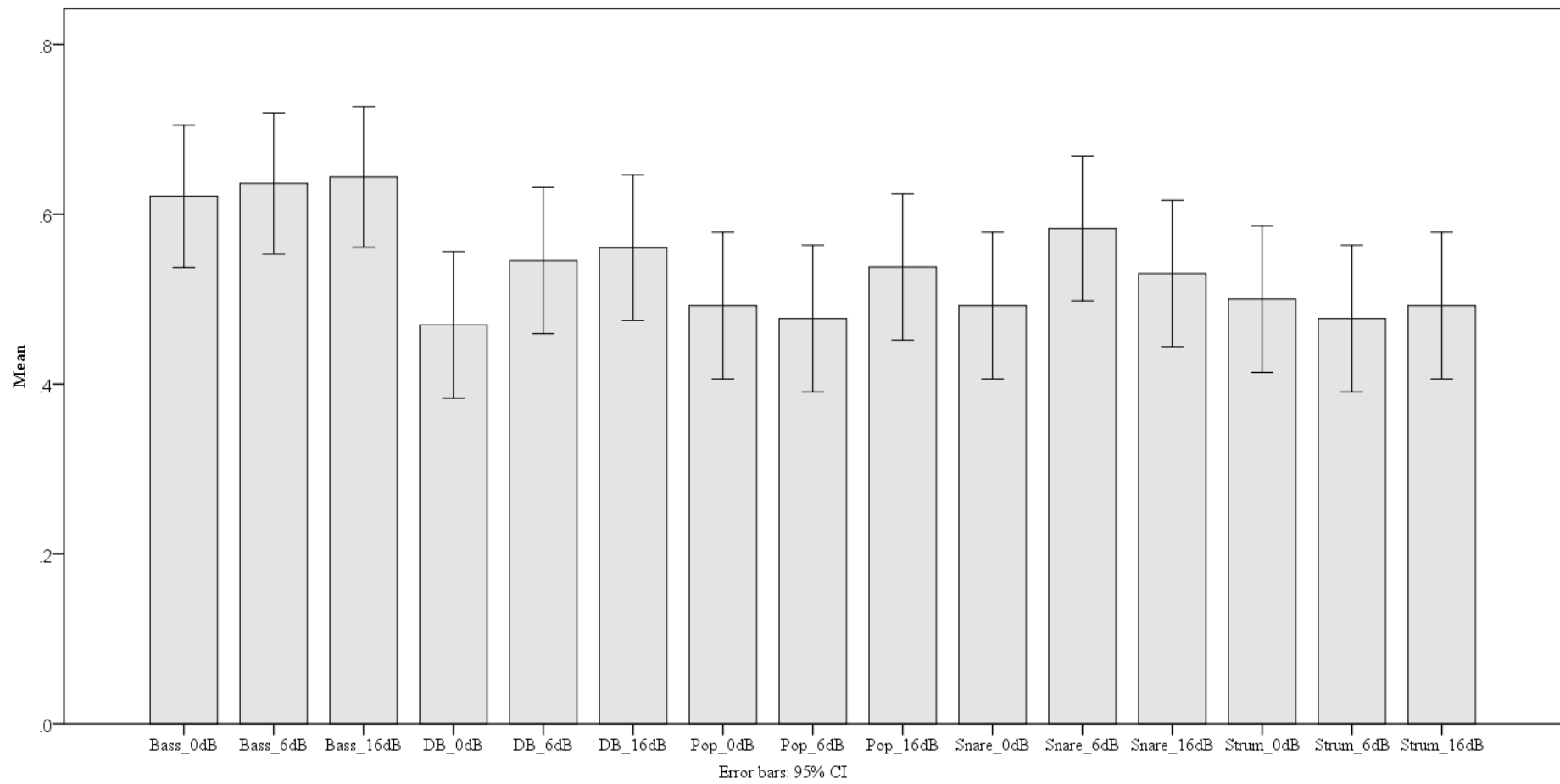


Figure 36. Mean Correct Identifications with 95% CI Error Bars for All Subjects- LL1582 Tests

Subject ID	Bass_0	Bass_6	Bass_16	DB_0	DB_6	DB_16	Pop_0	Pop_6	Pop_16	Snare_0	Snare_6	Snare_16	Strum_0	Strum_6	Strum_16
1	0.064	0.585	0.016	0.415	0.016	0.585	0.214	0.585	0.36	0.36	0.175	0.214	0.415	0.214	0.585
2	0.36	0.36	0.415	0.175	0.585	0.415	0.415	0.36	0.175	0.214	0.064	0.585	0.36	0.585	0.585
3	0.016	0.36	0.064	0.585	0.415	0.415	0.36	0.415	0.175	0.016	0.214	0.36	0.36	0.415	0.064
4	0.016	0.003	0.016	0.36	0.083	0.064	0.415	0.064	0.585	0.36	0.415	0.003	0.214	0.003	0.064
5	0.083	0.003	0.083	0.36	0.585	0.585	0.36	0.36	0.36	0.064	0.175	0.175	0.36	0.585	0.36
6	0.064	0.36	0.415	0.064	0.175	0.415	0.415	0.415	0.003	0.36	0.175	0.36	0.36	0.175	0.415
7	0.415	0.36	0.214	0.415	0.214	0.016	0.585	0.585	0.585	0.415	0.415	0.585	0.585	0.415	0.415
8	0.023	0.000	0.023	0.083	0.214	0.175	0.415	0.585	0.585	0.415	0.585	0.585	0.415	0.36	0.064
9	0.585	0.36	0.585	0.585	0.175	0.175	0.175	0.585	0.415	0.016	0.175	0.415	0.415	0.415	0.175
10	0.016	0.36	0.064	0.36	0.36	0.36	0.415	0.585	0.175	0.36	0.214	0.064	0.214	0.214	0.36
11	0.415	0.214	0.585	0.415	0.36	0.36	0.175	0.585	0.36	0.175	0.175	0.36	0.064	0.585	0.585
ALL	0.002	0.002	0	0.352	0.118	0.141	0.5	0.253	0.29	0.5	0.055	0.352	0.443	0.419	0.376
Post	0	0.001	0	0.392	0.072	0.197	0.456	0.189	0.197	0.245	0.197	0.255	0.468	0.392	0.381

Table 5. Lundahl LL1582 Subjective Statistical Analysis Results- Heatmap (95% & 99% CI)

Where:

Sample names are presented with the voltage gain of the test circuit (0, 6 and 16)

DB is Double Bass

Subject ID	Bass_0	Bass_6	Bass_16	DB_0	DB_6	DB_16	Pop_0	Pop_6	Pop_16	Snare_0	Snare_6	Snare_16	Strum_0	Strum_6	Strum_16
1	0.064	0.585	0.016	0.415	0.016	0.585	0.214	0.585	0.36	0.36	0.175	0.214	0.415	0.214	0.585
2	0.36	0.36	0.415	0.175	0.585	0.415	0.415	0.36	0.175	0.214	0.064	0.585	0.36	0.585	0.585
3	0.016	0.36	0.064	0.585	0.415	0.415	0.36	0.415	0.175	0.016	0.214	0.36	0.36	0.415	0.083
4	0.016	0.003	0.016	0.36	0.083	0.064	0.415	0.064	0.585	0.36	0.415	0.003	0.214	0.003	0.064
5	0.083	0.003	0.083	0.36	0.585	0.585	0.36	0.36	0.36	0.064	0.175	0.175	0.36	0.585	0.36
6	0.064	0.36	0.415	0.064	0.175	0.415	0.415	0.415	0.003	0.36	0.175	0.36	0.36	0.175	0.415
7	0.415	0.36	0.214	0.415	0.214	0.016	0.585	0.585	0.585	0.415	0.415	0.585	0.585	0.415	0.415
8	0.023	0.000	0.023	0.083	0.214	0.175	0.415	0.585	0.585	0.415	0.585	0.585	0.415	0.36	0.064
9	0.585	0.36	0.585	0.585	0.175	0.175	0.175	0.585	0.415	0.016	0.175	0.415	0.415	0.415	0.175
10	0.016	0.36	0.064	0.36	0.36	0.36	0.415	0.585	0.175	0.36	0.214	0.064	0.214	0.214	0.36
11	0.415	0.214	0.585	0.415	0.36	0.36	0.175	0.585	0.36	0.175	0.175	0.36	0.064	0.585	0.585
ALL	0.002	0.002	0	0.352	0.118	0.141	0.5	0.253	0.29	0.5	0.055	0.352	0.443	0.419	0.376
Post	0	0.001	0	0.392	0.072	0.197	0.456	0.189	0.197	0.245	0.197	0.255	0.468	0.392	0.381

Table 6. Lundahl LL1582 Subjective Statistical Analysis Results- Significant p-values (95% CI)

Subject ID	Bass_0	Bass_6	Bass_16	DB_0	DB_6	DB_16	Pop_0	Pop_6	Pop_16	Snare_0	Snare_6	Snare_16	Strum_0	Strum_6	Strum_16
1	0.064	0.585	0.016	0.415	0.016	0.585	0.214	0.585	0.36	0.36	0.175	0.214	0.415	0.214	0.585
2	0.36	0.36	0.415	0.175	0.585	0.415	0.415	0.36	0.175	0.214	0.064	0.585	0.36	0.585	0.585
3	0.016	0.36	0.064	0.585	0.415	0.415	0.36	0.415	0.175	0.016	0.214	0.36	0.36	0.415	0.083
4	0.016	0.003	0.016	0.36	0.083	0.064	0.415	0.064	0.585	0.36	0.415	0.003	0.214	0.003	0.064
5	0.083	0.003	0.083	0.36	0.585	0.585	0.36	0.36	0.36	0.064	0.175	0.175	0.36	0.585	0.36
6	0.064	0.36	0.415	0.064	0.175	0.415	0.415	0.415	0.003	0.36	0.175	0.36	0.36	0.175	0.415
7	0.415	0.36	0.214	0.415	0.214	0.016	0.585	0.585	0.585	0.415	0.415	0.585	0.585	0.415	0.415
8	0.023	0.000	0.023	0.083	0.214	0.175	0.415	0.585	0.585	0.415	0.585	0.585	0.415	0.36	0.064
9	0.585	0.36	0.585	0.585	0.175	0.175	0.175	0.585	0.415	0.016	0.175	0.415	0.415	0.415	0.175
10	0.016	0.36	0.064	0.36	0.36	0.36	0.415	0.585	0.175	0.36	0.214	0.064	0.214	0.214	0.36
11	0.415	0.214	0.585	0.415	0.36	0.36	0.175	0.585	0.36	0.175	0.175	0.36	0.064	0.585	0.585
ALL	0.002	0.002	0	0.352	0.118	0.141	0.5	0.253	0.29	0.5	0.055	0.352	0.443	0.419	0.376
Post	0	0.001	0	0.392	0.072	0.197	0.456	0.189	0.197	0.245	0.197	0.255	0.468	0.392	0.381

Table 7. Lundahl LL1582 Subjective Statistical Analysis Results- Significant p-values (99% CI)

One method of reviewing results of a binomial test when a bias is suggested is through the use of signal detection theory as recommended by Boley and Lester (2009). However, as the test implemented free user switching between samples, the method of signal detection theory was no longer valid to further analyse the results. This is due to the presentation of A, B and X to the subject: with the original design of the ABX test providing a single presentation of the samples, including a short interval between each after which the subject is prompted to give a response thus avoiding a bias towards A or B.

Many of the subjects described how they heard little or no difference with most of the samples presented. When analysing the results across all subjects a post-selection result was also included in the heatmap table, removing the data of two subjects who did not produce a p-value lower than 0.05. This presented little difference although showed that it is highly likely that a difference could be heard with all three bass samples.

The Carnhill VTB1148 pilot study results show a close to random response when presented as the amount of correct identifications (fig.37) with few results exceeding 70%. By examining the mean values, an increased amount of correct identifications is produced for the double bass at 6dB (fig.38). When compared to that of the LL1582 bass sample means the amount is relatively close however the 95% error bars show a large degree of error spanning a range of greater than 20%. Due to the limited number of subjects and trials in the test the bias introduced greatly reduces the resolution of all analysis compared to that of the LL1582 tests.

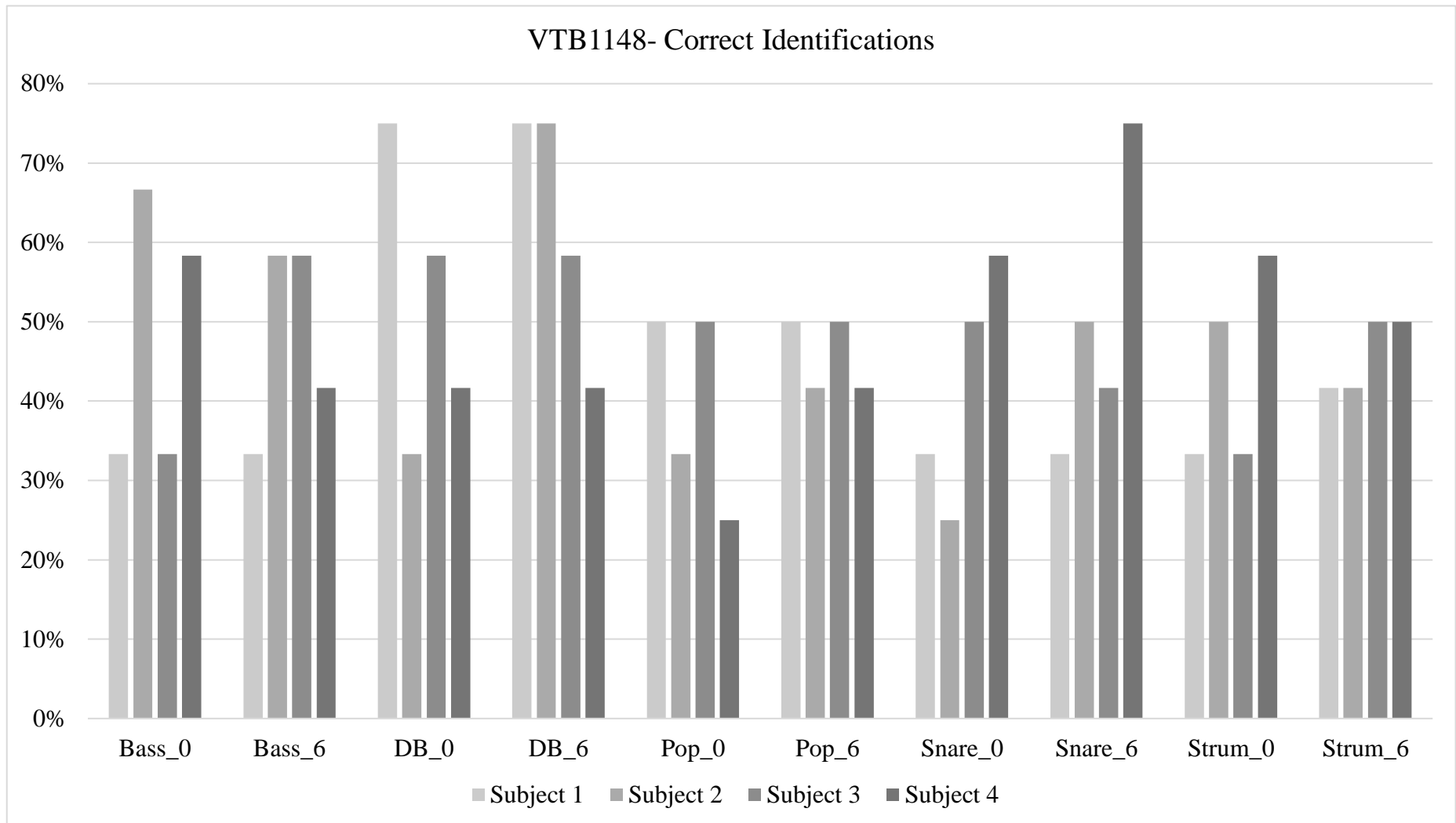


Figure 37. Correct Identifications of Each Sample Per Subject- VTB1148 Tests

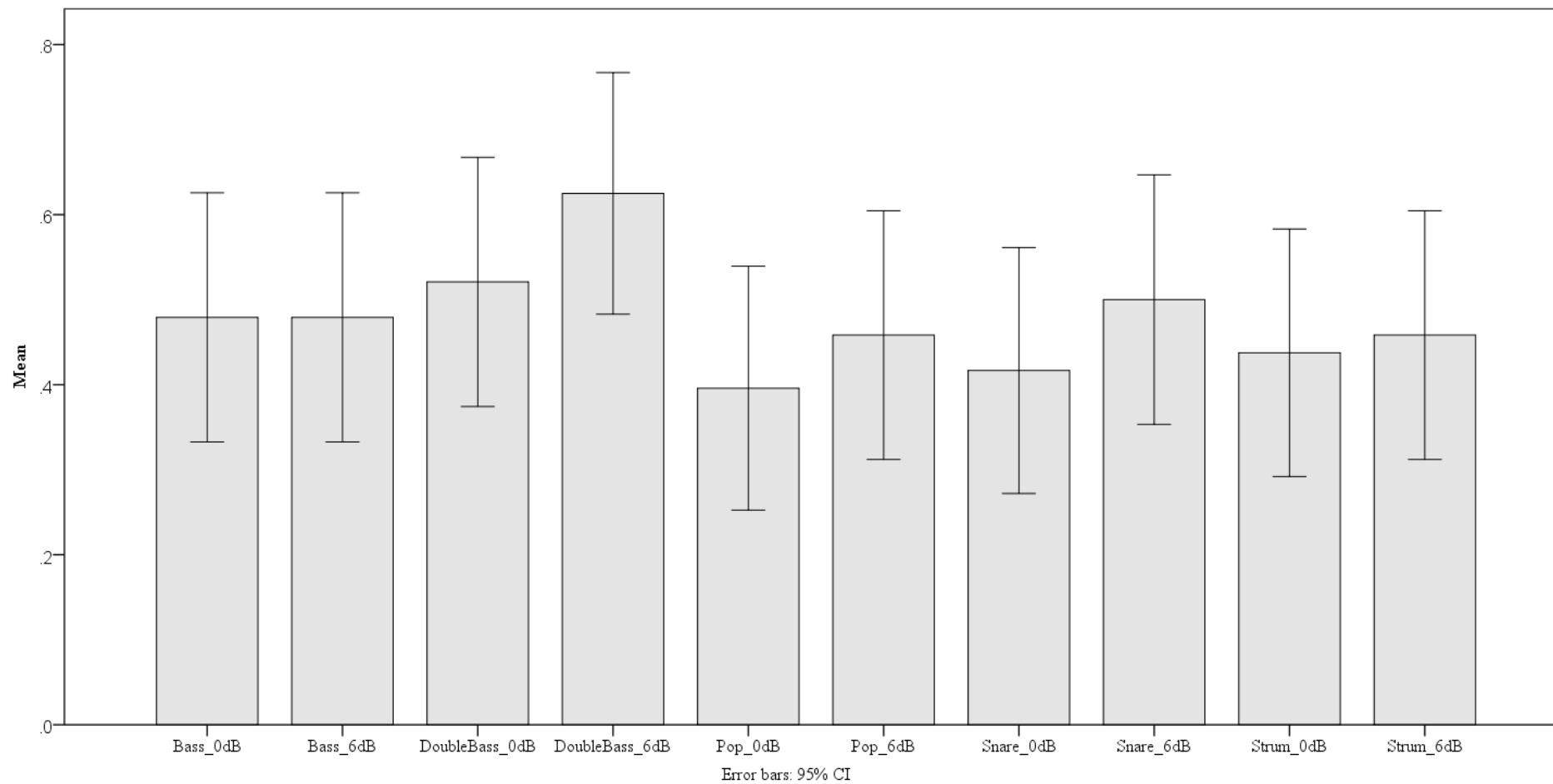


Figure 38. Mean Correct Identifications with 95% CI Error Bars for All Subjects- VTB1148 Tests

Subject ID	Bass 0	Bass 6	DB 0	DB 6	Pop 0	Pop 6	Snare 0	Snare 6	Strum 0	Strum 6
1	0.175	0.36	0.415	0.36	0.585	0.585	0.585	0.36	0.175	0.585
2	0.36	0.36	0.360	0.360	0.064	0.36	0.415	0.064	0.36	0.585
3	0.175	0.36	0.175	0.064	0.175	0.415	0.064	0.585	0.585	0.36
4	0.175	0.175	0.064	0.083	0.585	0.585	0.175	0.175	0.175	0.415
ALL	0.389	0.389	0.389	0.074	0.123	0.384	0.125	0.5	0.195	0.384

Table 8. Carnhill VTB1148 Subjective Statistical Analysis Results- Heatmap (95% & 99% CI)

Subject ID	Bass 0	Bass 6	DB 0	DB 6	Pop 0	Pop 6	Snare 0	Snare 6	Strum 0	Strum 6
1	0.175	0.36	0.415	0.36	0.585	0.585	0.585	0.36	0.175	0.585
2	0.36	0.36	0.360	0.360	0.064	0.36	0.415	0.064	0.36	0.585
3	0.175	0.36	0.175	0.064	0.175	0.415	0.064	0.585	0.585	0.36
4	0.175	0.175	0.064	0.083	0.585	0.585	0.175	0.175	0.175	0.415
ALL	0.389	0.389	0.389	0.074	0.123	0.384	0.125	0.5	0.195	0.384

Table 9. Carnhill VTB1148 Subjective Statistical Analysis Results- Significant p-values (95% & 99% CI)

By analysing the data further using the binomial test and heatmaps, produced no significant p-values (table 9). The heatmap (table 8) shows how both the double bass (DB) samples show a concentration of low values suggesting a larger number of correct observations compared to incorrect. Using the spectrograms for the double bass there are low-level changes in the silent periods at the beginning and end of the double bass excerpt where the more harmonic products are present when compared with the reference signal. When comparing the other spectrograms there is no obvious change with most of the signals which seems to be reflected in the statistical results. With such a limited number of subjects for this test no substantial conclusion can be made however when considering the spectrogram images there is no visible differences between most stimuli.

Through the use of frequency bar charts and binomial tests a significant outcome for all bass samples has been found for the LL1582 across all subjects, whereas testing using the VTB1148 has shown no significant differences (although these tests consisted of less results overall). This would suggest a perceptual difference that is programme dependant and by analysis of both objective and subjective this will provide further insight into the cause.

Chapter 5: Discussion

The statistical analysis has revealed that some subjects produced significant results with various samples with no obvious trend. This could be due to a bias error however the analysis of all subjects at each gain of the bass sample presents a significant result, with $p = 0.001$ or less, rejecting the null hypothesis, showing that it is likely that these subjects could hear a difference. This is supported by a visible difference that is shown in the corresponding spectrograms presenting an increased number of harmonics visible in the low to mid frequency range and is described by most subjects as being “brighter” and as having “...more low-end” and “...more presence”.

Comparing both the spectrograms and subjective data it is probable that spectral and temporal masking impacted upon the detectability of distortion as most of the samples contain content across a wide frequency range which is likely to mask the relatively low-level harmonics. This is even more plausible when considering that not all of the samples used were single instrument notes with an extended envelope but a combination of notes and durations. The snare drum is an example of both as it contains a broad range of frequencies and has a short envelope with many subjects commenting how difficult it was to detect any difference due to its transient nature. Considering the bass sample, that contains a high signal level attack with the extended envelope as the signal level decreases over time, would be most likely to produce an audible response at 0dB and +16dB gain as the THD+N versus level data for the transformers are non-linear at both the high and low extremes of operating levels. The high-level attack and the gradual drop in level results in an increase of harmonic content, relative to the original signal. However, the THD+N with a gain of +6dB should be around the lowest level at approximately 0.2% at 20Hz but the statistical results are still significant. Although the p-value of the sample at +6dB after

post-processing is slightly higher than that of the other gains, suggesting that this level of distortion is audible, it also provides some support of the idea that there is a level of correlation between THD+N and the audibility. This is also evidence of the programme dependence of the device on level, spectral content and time.

FFT analysis has shown that there is a large number of harmonic products produced by the transformer non-linearities especially at lower frequencies and lower levels which are more likely to be masked by the higher amplitude low frequency content of the stimuli. The frequency domain responses have shown high-order harmonics which are less likely to be masked and relatively high-levels of 3rd harmonic distortion across both transformers. It is also a salient fact that the distortion is not static with complex signals such as the stimuli used therefore more susceptible to both spectral and temporal masking and may not produce the same levels of harmonic products as the sine waves used in the FFT analysis. Each subject's comments also explain how there was no perceivable difference with most of the samples.

It is clear to see that the LL1582 measures present a higher level of EMI compared to the VTB1148, although the objective measures for the VTB1148 show an increased amount of 50Hz mains components at low voltage gain, this is evident in the double bass spectrograms in the silent periods before and after the excerpt. This could be the possible cause of any audible difference between the samples concerned.

The objective measures have shown that there is a higher level of distortion, in particular 3rd harmonic, when the transformer is operated at low frequencies close to the extreme operating levels of the device and that this distortion is likely to be audible with a stimulus

containing substantial low frequency content even at line level (providing that the level of masking is limited). However, it is highly likely that the distortion encountered in the tests was programme dependent and the effects of spectral and temporal masking could have played a significant role in affecting the perception of any differences. As the tests were also completed under controlled conditions; within ITU-R recommended critical listening environment conditions using headphones, with many subjects commenting how difficult the task was of discerning a difference between stimuli, it is questionable whether the effects would be perceivable in a non-critical 'real-world' listening environment with a less transparent playback system.

As most professional microphone preamplifiers have a maximum output around +26dBu it is clear that there would be a greater increase in THD+N caused by the transformer. However, the distortion produced by the preceding circuitry will produce an amount of distortion particularly with varied gain and level which would inevitably sum together with the distortion from the transformer to a certain degree. Other effects such as clipping distortion caused by the output being driven close to the power supply rails is also a factor when driving the transformer to create 'colour' which could affect the perception of difference.

It is also suggested that the perceived difference is affected by all the components in the signal path and their interaction which will contribute to the overall level of distortion such as that created in preamplifier circuits, subsequently adding to the overall colour. An example of this is discussed in a paper by Li (2011) on the effect of the nonlinear transformer inductance along with thermionic valve nonlinearity and impedance showed that the interaction of these attributes cause nonlinear feedback therefore nonlinear

distortion which is frequency dependant. This is likely to be the condition in professional preamplifier designs such as those mentioned in section 2.2 which use discrete transistor operational amplifiers that often produce different levels of distortion or ‘colouration’ than that of an IC op-amp or thermionic valve which are shown by Gaskell et al. (2011) and Hamm (1973) to produce varying amounts.

It is also possible that transformers offer better interfacing for example improved impedance matching and CMRR when compared to circuits that contain capacitors such as a standard high-pass RC input or output filter. As concluded by Gaskell (2011) most compositions of capacitors produce increased levels of distortion when presented with both low and high-level signals at the extremes of the device operating range.

Chapter 6: Conclusion

Through the review of current knowledge about the theory of transformer operation, the causes of the device distortion have been presented. Relating this to the principles of the perception of distortion has provided a foundation for analysing objective measurements and subjective responses allowing reasonable assessments to be made about the audibility of colouration.

Using objective measurements such as THD+N and FFT analysis along with the appropriate listening test procedure and statistical analysis, it has been concluded that it is likely that a transformer can cause an audible difference. It has also been shown that a level of programme dependence is likely as distortion becomes evident with content containing low-frequency energy and a long sustain. Overall, the information collected would support the idea of driving a transformer at high signal levels and at low frequencies ‘creatively’ to produce distortion, giving the signal a level of colouration and it has also shown that driving the transformer at an average line output signal level of +4dBu is also likely to produce an effect too.

The key points are as follows:

- The distortion produced is mostly at low frequencies below 200Hz
- Distortion is level dependent: THD+N increases at low and high signal levels
- 3rd harmonic distortion is a large component of the produced distortion
- Increased distortion due to the effects of core coercivity and saturation
- Select listeners could statistically identify the difference with the bass sample
- Across all subjects it was likely that the bass samples were statistically audible

It is important to note that this is not a complete study of transformer colouration. As there are many different designs and applications of transformers available, more study into the operation and measurement of other devices and parameters must be done to increase the amount of information known.

6.1 Future Work

Continuing from this study, it would be beneficial to use a wider range of stimuli covering a wider selection of frequency content and envelopes for subjective testing to assess the level of programme dependence on device distortion. Using other tools such as wavelet analysis could prove useful when trying to analyse distortion products which could otherwise be masked therefore providing more information about the types of distortion and ultimately work towards a perceptual model.

Building upon this study and others such as the method presented by Sowter (1944) for the prediction of harmonic distortion, the eventual ambition of this research is the creation of a software tool that could utilise transformer design parameters such as materials, core shape, winding technique, etc. to produce estimated levels of distortion and the perceptual attributes relating to the presented values. For this, it is felt that a more comprehensive study of the relationship between the performance of audio electronics and the perception of colouration would be beneficial to audio electronics design as an aid to design engineers as well as providing more information for the end-user about the potential creative uses in the recording studio. This knowledge could also be used to better understand existing circuits and quantify the existing effects.

References

- AMS Neve. (2018). 1073 Mic Preamp & Equaliser. Retrieved January 13, 2019, from <https://ams-neve.com/1073-2/>
- Analog Devices. (2017). *AD8429 1 nV/ $\sqrt{\text{Hz}}$ Low Noise Instrumentation Amplifier*. Retrieved from <https://www.analog.com/media/en/technical-documentation/data-sheets/ad8429.pdf>
- API. (2018). 512c Discrete Mic/ Line Pre. Retrieved January 13, 2019, from <http://apiaudio.com/product.php?id=103>
- Bateman, C. (2002). Capacitor sound? *Electronics World*, (July).
- Bech, S., & Zacharov, N. (2007). *Perceptual Audio Evaluation*. John Wiley & Sons Ltd.
- Belcher, R. A. (1976). *Audio Non-Linearity a Comb Filter Method for Measuring Distortion*. London, UK.
- Blondel, C., & Wolff, B. (2013). Ampère Lays the Foundations of Electrodynamics (September 1820-January 1821). Retrieved January 10, 2019, from <http://www.ampere.cnrs.fr/histoire/parcours-historique/lois-courants/ampere-electrodynamique/eng>
- Boley, J., & Lester, M. (2009). Statistical Analysis of ABX Results Using Signal Detection Theory. In *Paper presented at the 127th AES Convention* (p. Convention Paper 7826). New York, USA. Retrieved from <http://www.aes.org/e-lib/browse.cfm?conv=127&papernum=7826>
- C Core. (2007). Retrieved January 5, 2019, from https://commons.wikimedia.org/wiki/File:C_core.png
- CENELEC. (2018). *BS EN IEC 60404-6:2018 Magnetic Materials- Part 6*. Brussels, Belgium.
- Dominios. (2004). Retrieved January 9, 2019, from <https://commons.wikimedia.org/wiki/File:Dominios.png>
- Duncan, P. J., Dodds, P. S., & Williams, N. (2008). Audio Capacitors. Myth or Reality? In *Paper presented at the 124th AES Convention*. Amsterdam, The Netherlands.
- Encyclopedia Britannica. (2019). Sir Alfred Ewing. Retrieved January 10, 2019, from <https://www.britannica.com/biography/Alfred-Ewing>
- European Broadcasting Union. (2008). *EBU Tech 3253 - SQAM: Sound Quality Assessment Material Recordings for Subjective Tests. EBU 3253*. Geneva. Retrieved

from

<https://tech.ebu.ch/docs/tech/tech3253.pdf><https://tech.ebu.ch/publications/sqamcd>

- Faraday, M. (1831). *Ring-Coil Apparatus*. London, UK. Retrieved from http://www.rigb.org/docs/faraday_notebooks__induction_0.pdf
- Farmelo, A. (2010, May). Neve Style Preamps: Imitation in the Sincerest Form. *Tape Op*. Retrieved from <https://tapeop.com/interviews/77/neve-style-preamps/>
- Farmelo, A., & Hampton, S. (2010, March). Using Transformers: To Transform Audio. *Tape Op*. Retrieved from <https://tapeop.com/articles/76/transformers/>
- Fastl, H., & Zwicker, E. (2007). *Psychoacoustics- Facts and Models. Journal of Experimental Psychology: General* (3rd ed., Vol. 136). Berlin, Germany: Springer.
- Fielding, R. E. (2018). Lee De Forest. Retrieved September 18, 2018, from <https://www.britannica.com/biography/Lee-de-Forest>
- Gaskell, R.-E. (2011). Capacitor “Sound” in Microphone Preamplifier DC Blocking and HPF Applications: Comparing Measurements to Listening Tests. In *Paper presented at the 130th AES Convention*. London, UK.
- Gaskell, R.-E., Gaskell, P. E., & Massenburg, G. (2011). Distortions in Audio Op-Amps and Their Effect on Listener Perception of Character and Quality. In *Paper presented at the 131st AES Convention*. New York, USA.
- Gribben, C., & Lee, H. (2015). Towards the Development of a Universal Listening Test Interface Generator in Max. *Proceedings of the 138th Convention of the Audio Engineering Society (2015)*, 2–5. Retrieved from <http://www.hud.ac.uk/research/researchcentres/mtprg/projects/apl/>
- Guarnieri, M. (2013). Who Invented the Transformer? *IEEE Industrial Electronics Magazine*, 7(4), 56–59. <https://doi.org/10.1109/MIE.2013.2283834>
- Hamm, R. O. (1973). Tube Versus Transistors- Is there an Audible Difference? *Journal of the Audio Engineering Society*, 21(4), 267–273.
- Harris, L. E., & Holland, K. R. (2009). Using Statistics To Analyse Listening Test Data: Some Sources and Advice for Non-Statisticians. *Proceedings of the Institute of Acoustics*, 31(4), 16.
- Herzog, S. (2009). Investigations of the Effects of Nonlinear Distortions on Psychoacoustical Measures. In *Paper presented at the 126th AES Convention*. Munich, Germany.
- Hioki. (2017). LCR Meters | Impedance Analyzers | Capacitance Meters How to Use.

- Retrieved January 14, 2019, from
<https://www.hioki.com/en/products/listUse/?category=10>
- Horowitz, P., & Hill, W. (2015). *The Art of Electronics*. New York, USA: Cambridge University Press.
- International Telecommunication Union. (2001). ITU-R Recommendation BS.1387-1 Method for Objective Measurements of Perceived Audio Quality.
- International Telecommunication Union. (2015). ITU-R Recommendation BS.1116-3: Methods for the Subjective Assessment of Small Impairments in Audio Systems. Geneva, Switzerland.
- Jensen, D., & Sokolich, G. (1988). Spectral Contamination Measurement. In *Paper presented at the 85th AES Convention*. Los Angeles, USA.
- Jillings, N., De Man, B., Moffat, D., Reiss, J. D., & Stables, R. (2016). Web Audio Evaluation Tool : A framework for subjective assessment of audio. *2nd Web Audio Conference*.
- Jordan, E. C., & Balmain, K. G. (1968). *Electromagnetic Waves and Radiating Systems*. Englewood Cliffs, N.J.: Prentice-Hall Inc.
- Jung, W. (2005). *Op Amp Applications Handbook*. Newnes, Elsevier.
- Lee, L. W., & Geddes, E. R. (2003). Auditory Perception of Nonlinear Distortion. In *Paper presented at the 115th AES Convention*. New York, USA. Retrieved from <http://www.aes.org/e-lib/browse.cfm?elib=12465>
- Leinonen, E., & Ojala, M. (1978). Correlation Audio Distortion Measurements. *Journal of the Audio Engineering Society*, 26(1/2), 12–19. Retrieved from <http://www.aes.org/e-lib/browse.cfm?elib=3296>
- Li, S. (2011). Why Do Tube Amplifiers Have Fat Sound While Solid State Amplifiers Don't. In *Paper presented at the 131st AES Convention*. New York, USA.
- Liebetrau, J., Sporer, T., Becker, M., Clauß, T., Duong, T. P., Ebert, A., ... Zierenner, M. (2015). Quantifying Auditory Perception: Underlying Dimensions of Pleasantness and Unpleasantness. In *Paper presented at the 138th AES Convention*. Warsaw, Poland.
- Lipshitz, S., & Vanderkooy, J. (1981). The Great Debate: Subjective Evaluation. *Journal of the Audio Engineering Society*, 29(7/8), 482–491. Retrieved from <http://www.aes.org/e-lib/browse.cfm?elib=3899>
- McLyman, C. W. T. (2004). *Transformer and Inductor Design Handbook* (3rd ed.). New York: Marcel Dekker, Inc. Retrieved from

- <http://www.crcnetbase.com/doi/book/10.1201/9780203913598>
- Merging Technologies. (2019). Specifications. Retrieved May 20, 2019, from <https://www.merging.com/products/interfaces/specifications>
- Minnick, P. (2012). Nonlinear Distortion Measurement in Audio Amplifiers: The Perceptual Nonlinear Distortion Response. In *Paper presented at the 132nd AES Convention*. San Francisco, USA.
- Nave, C. R. (2018). Ferromagnetism. Retrieved January 13, 2019, from <http://hyperphysics.phy-astr.gsu.edu/hbase/Solids/ferro.html>
- NDT Education Resource Center. (2018). The Hysteresis Loop and Magnetic Properties. Retrieved January 5, 2019, from <https://www.nde-ed.org/EducationResources/CommunityCollege/MagParticle/Physics/HysteresisLoop.htm>
- Partridge, N. (1942). An Introduction to the Study of Harmonic Distortion in Audio Frequency Transformers. *The British Institution of Radio Engineers*, 6–21.
- Permeability (electromagnetism). (n.d.). Retrieved November 17, 2018, from [https://en.wikipedia.org/wiki/Permeability_\(electromagnetism\)](https://en.wikipedia.org/wiki/Permeability_(electromagnetism))
- Reeder, R. (2005, April). Transformer-Coupled Front-End for Wideband A/D Converters. *Analog Dialogue*. Retrieved from <https://www.analog.com/en/analog-dialogue/articles/transformer-coupled-front-end-a-d-converters.html>
- Ronan, M., Ward, N., & Sazdov, R. (2016). Considerations When Calibrating Program Material Stimuli Using LUFFS. In *Paper presented at the 140th AES Convention*. Paris, France.
- Scace, R. I. (2017). Integrated Circuits. Retrieved January 10, 2019, from <https://www.britannica.com/technology/electronics#ref233776>
- Schumacher, C. (2005, November). Old School Audio: MP1-L3 mic preamp. *Tape Op*. Retrieved from <https://tapeop.com/reviews/gear/50/mp1-l3-mic-preamp/>
- Self, D. (2015). *Small Signal Audio Design* (Second). New York, USA: Focal Press.
- Sennheiser. (2019). HD650. Retrieved May 20, 2019, from <https://en-uk.sennheiser.com/high-quality-headphones-around-ear-audio-surround-hd-650>
- Sescom. (2019). Audio Transformers History. Retrieved January 10, 2019, from <http://www.sescom.com/audio-transformers-history.asp>
- Sowter, G. A. V. (1944). *Harmonic Distortion at Low Frequency in Circuits Containing Apparatus with Ferromagnetic Cores, Especially High Permeability Nickel Iron Cored Transformers and Chokes*. University of London.

- Sowter, G. A. V. (1987). Soft Magnetic Materials for Audio Transformers: History, Production, and Applications. *Journal of the Audio Engineering Society*, 35(10), 760–777.
- Suzuki, H., Morita, S., & Shindo, T. (1980). On The Perception of Phase Distortion. *Journal of the Audio Engineering Society*, 28(9), 570–574.
<https://doi.org/10.1177/089692057300300403>
- Tan, C.-T., Moore, B. C. J., & Zacharov, N. (2003). The Effect of Nonlinear Distortion on the Perceived Quality of Music and Speech Signals. *Journal of the Audio Engineering Society*, 51(11), 1012--1031. Retrieved from <http://www.aes.org/e-lib/browse.cfm?elib=12197>
- Tan, C.-T., Moore, B. C. J., Zacharov, N., & Mattila, V.-V. (2004). Predicting the perceived quality of nonlinearity distorted music and speech signals. *Journal of the Audio Engineering Society*, 52(7/8), 699–711.
- The Faraday Museum- The Royal Institution. (2014). Michael Faraday's induction ring. Retrieved January 5, 2019, from <http://www.bbc.co.uk/ahistoryoftheworld/objects/nSFvkPPCRdWQJ0hzSzrB4A>
- Transformer. (2006). Retrieved January 4, 2019, from https://commons.wikimedia.org/wiki/File:Transformer3d_col3.svg
- Transformer Core Interleaved. (2007). Retrieved January 5, 2019, from https://commons.wikimedia.org/wiki/File:EI-transformer_core_interleaved.svg
- Transformer Iron Core. (2006). Retrieved January 5, 2019, from https://commons.wikimedia.org/wiki/File:Transformer_Iron_Core.svg
- Tretkoff, E., Ramlagan, N., Chodos, A., & Ouellette, J. (2008). Oersted and Electromagnetism. *APS Physics- This Month in Physics History*, 17(7). Retrieved from <https://www.aps.org/publications/apsnews/200807/physicshistory.cfm>
- Turnbull, G. (2017). Maxwell's Equations. Retrieved January 10, 2019, from https://ethw.org/Maxwell%27s_Equations
- University of Huddersfield. (2019). Applied Psychoacoustics Laboratory (APL) - Facilities- APL Listening Room. Retrieved May 19, 2019, from <https://research.hud.ac.uk/institutes-centres/apl/facilities/>
- van der Veen, M. (2007). Low Level Audio Signal Transfer Through Transformers Conflicts with Permeability Behaviour Inside Their Cores. In *Paper presented at the 122nd AES Convention*. Vienna, Austria.
- van der Veen, M., & van Maanen, H. R. E. (2008). Non-Linear Distortions in Capacitors.

- In *Paper presented at the 124th AES Convention*. Amsterdam, The Netherlands.
- Voishvillo, A. (2007). Measurements and Perception of Nonlinear Distortion- Comparing Numbers and Sound Quality. In *Paper presented at the 123rd AES Convention*. New York, USA. Retrieved from <http://www.aes.org/e-lib/browse.cfm?elib=14232>
- Whelan, M., Rockwell, S., & Normandin, S. (2014). The History of the Transformer. Retrieved January 10, 2019, from <http://www.edisontechcenter.org/Transformers.html>
- Whitlock, B. (2002). Audio Transformers. In *Handbook for Sound Engineers* (Third Edit). Woburn, MA, USA: Focal Press. <https://doi.org/10.1016/B978-0-240-80969-4.50015-8>

Appendix A- dScope Signal Analyser Measures

THD+N vs Frequency

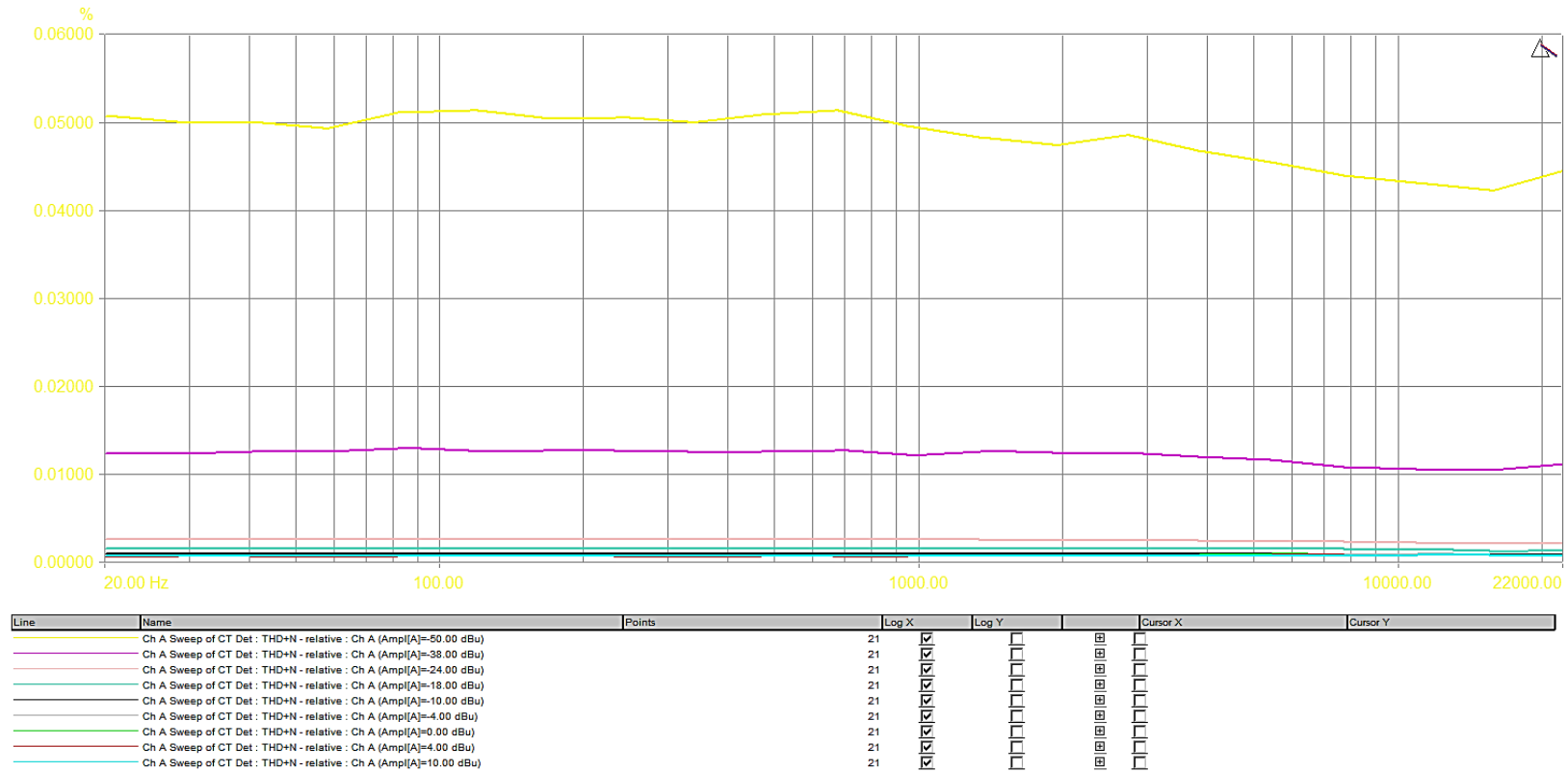
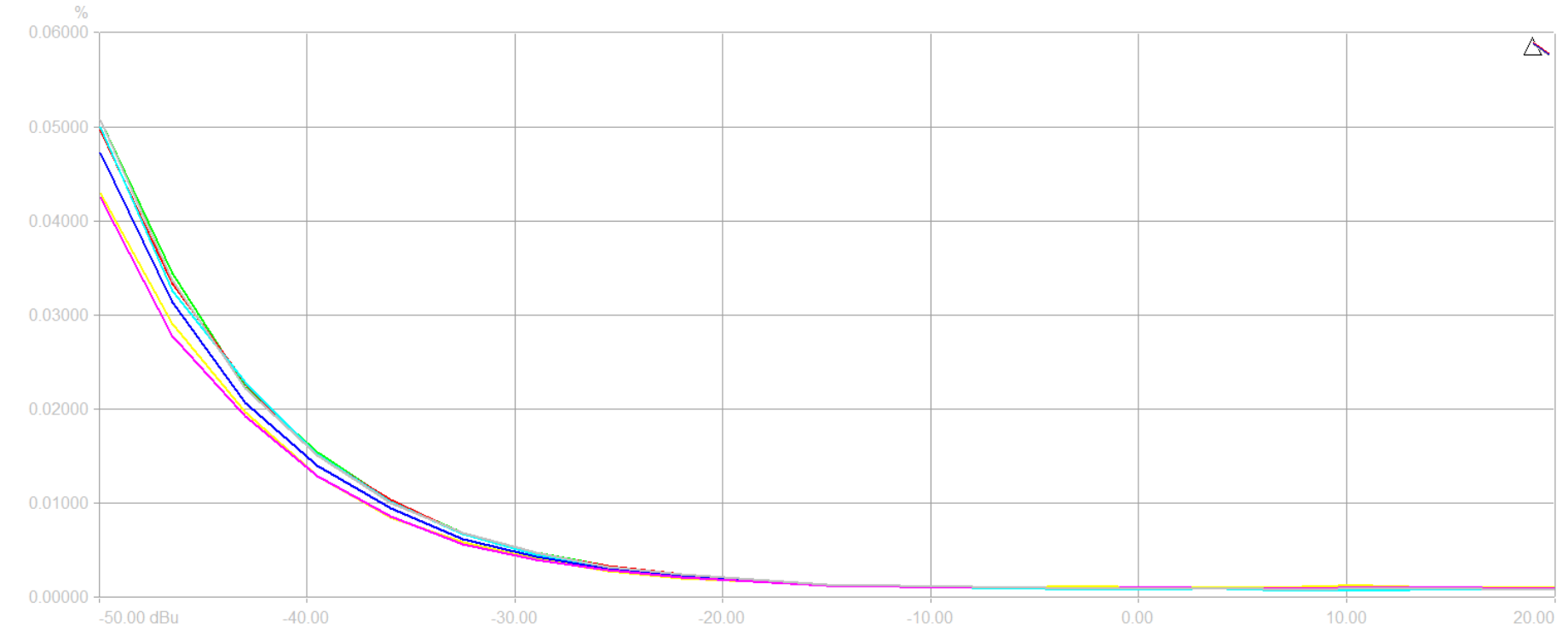


Figure 39. dScope Series III Self-Test THD+N vs Frequency

THD+N vs Amplitude



Line	Name	Points	Log X	Log Y	Cursor X	Cursor Y
1	Ch A Sweep of CT Det : THD+N - relative : Ch A (Freq[A]=20.00 Hz)	21	<input checked="" type="checkbox"/>	<input type="checkbox"/>	<input type="checkbox"/>	<input type="checkbox"/>
2	Ch A Sweep of CT Det : THD+N - relative : Ch A (Freq[A]=50.00 Hz)	21	<input checked="" type="checkbox"/>	<input type="checkbox"/>	<input type="checkbox"/>	<input type="checkbox"/>
3	Ch A Sweep of CT Det : THD+N - relative : Ch A (Freq[A]=200.00 Hz)	21	<input checked="" type="checkbox"/>	<input type="checkbox"/>	<input type="checkbox"/>	<input type="checkbox"/>
4	Ch A Sweep of CT Det : THD+N - relative : Ch A (Freq[A]=1000.00 Hz)	21	<input checked="" type="checkbox"/>	<input type="checkbox"/>	<input type="checkbox"/>	<input type="checkbox"/>
5	Ch A Sweep of CT Det : THD+N - relative : Ch A (Freq[A]=5000.00 Hz)	21	<input checked="" type="checkbox"/>	<input type="checkbox"/>	<input type="checkbox"/>	<input type="checkbox"/>
6	Ch A Sweep of CT Det : THD+N - relative : Ch A (Freq[A]=10000.00 Hz)	21	<input checked="" type="checkbox"/>	<input type="checkbox"/>	<input type="checkbox"/>	<input type="checkbox"/>
7	Ch A Sweep of CT Det : THD+N - relative : Ch A (Freq[A]=20000.00 Hz)	21	<input checked="" type="checkbox"/>	<input type="checkbox"/>	<input type="checkbox"/>	<input type="checkbox"/>

Figure 40. dScope Series III Self-Test THD+N vs Amplitude

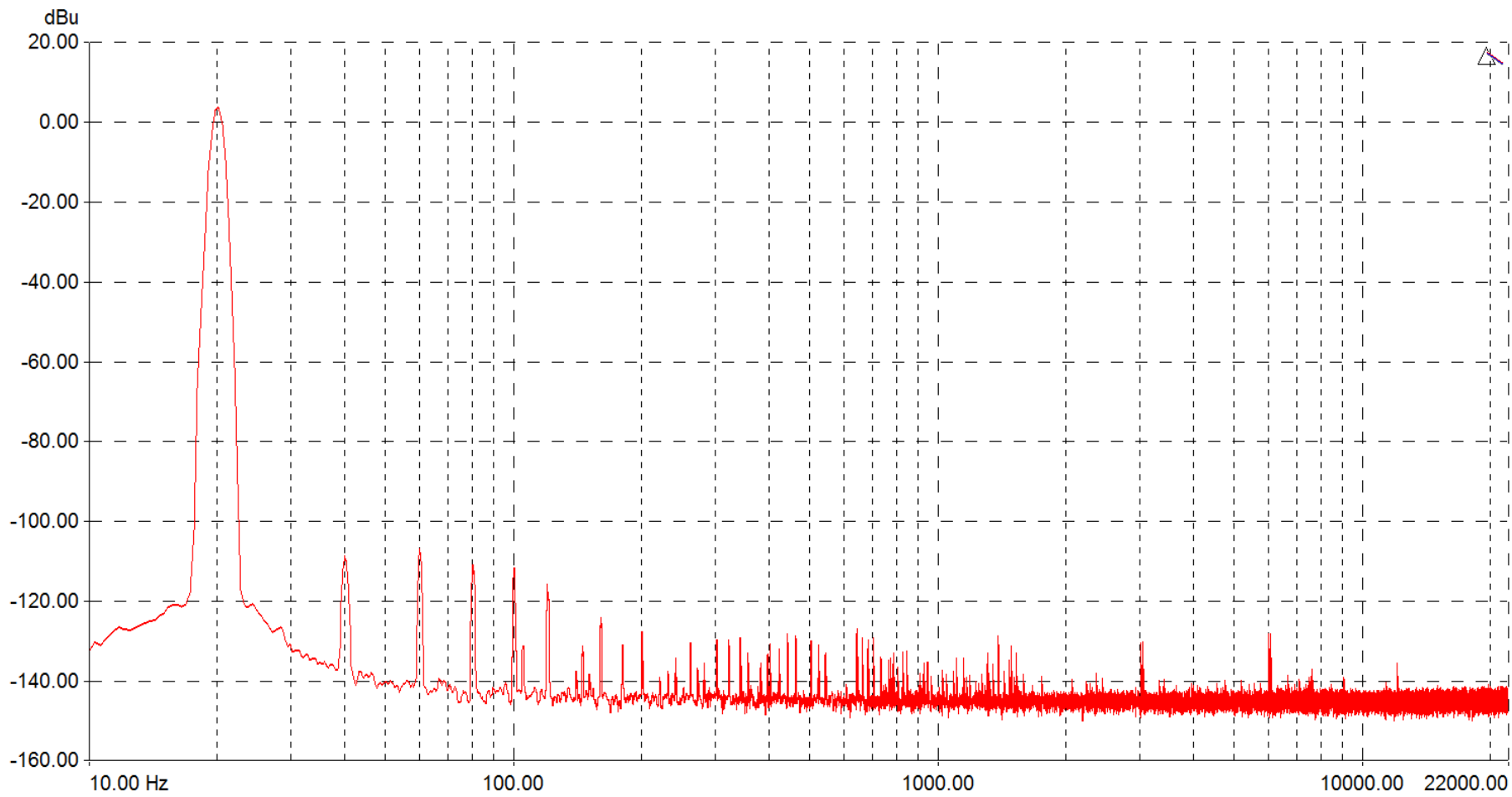


Figure 41. dScope Series III Self-Test- FFT at 20Hz +4dBu Input

Appendix B- Test Circuit Measures

Frequency Response and Inter-channel Phase

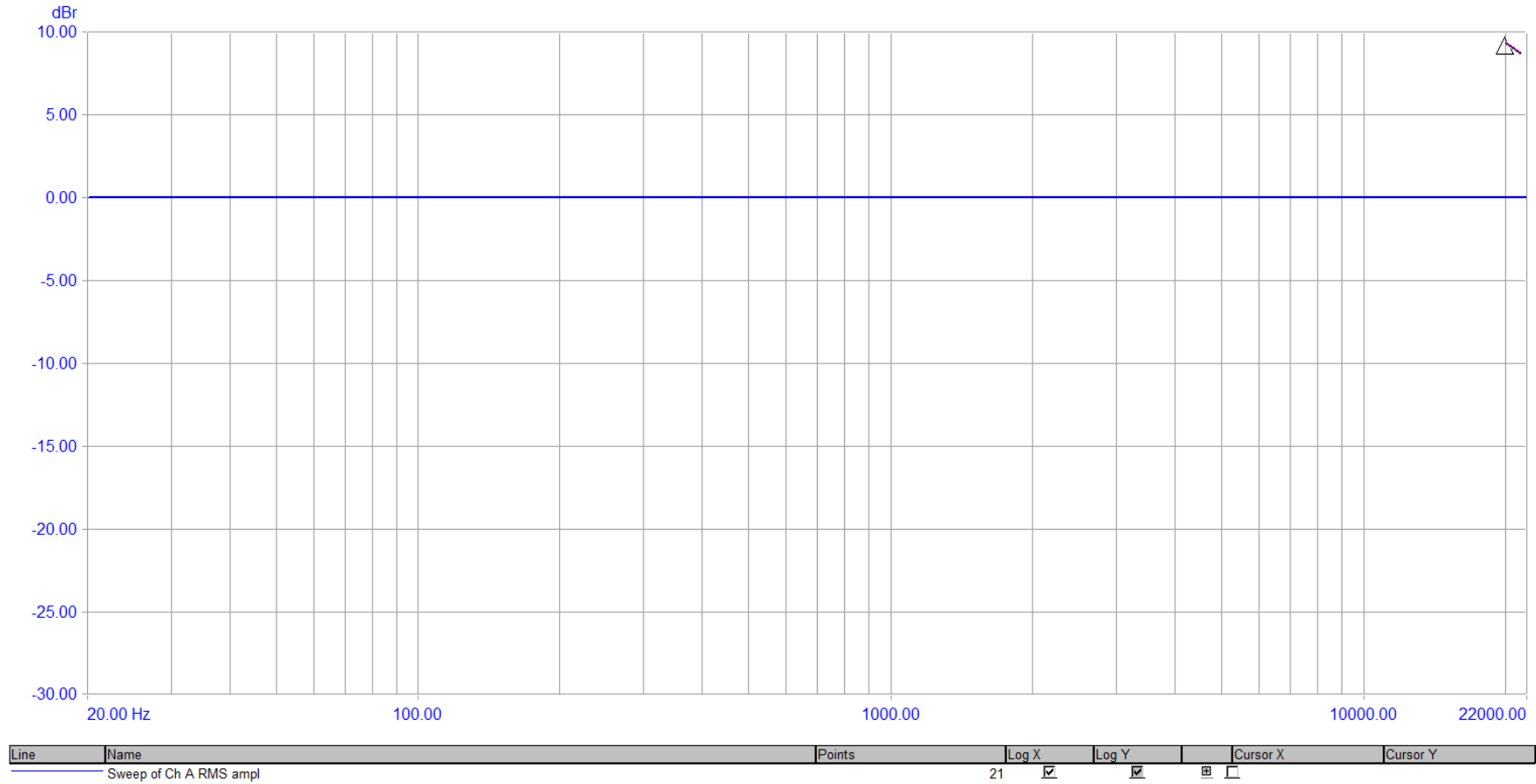


Figure 42. Test Circuit- Frequency Response- 0dB Gain

Frequency Response and Inter-channel Phase

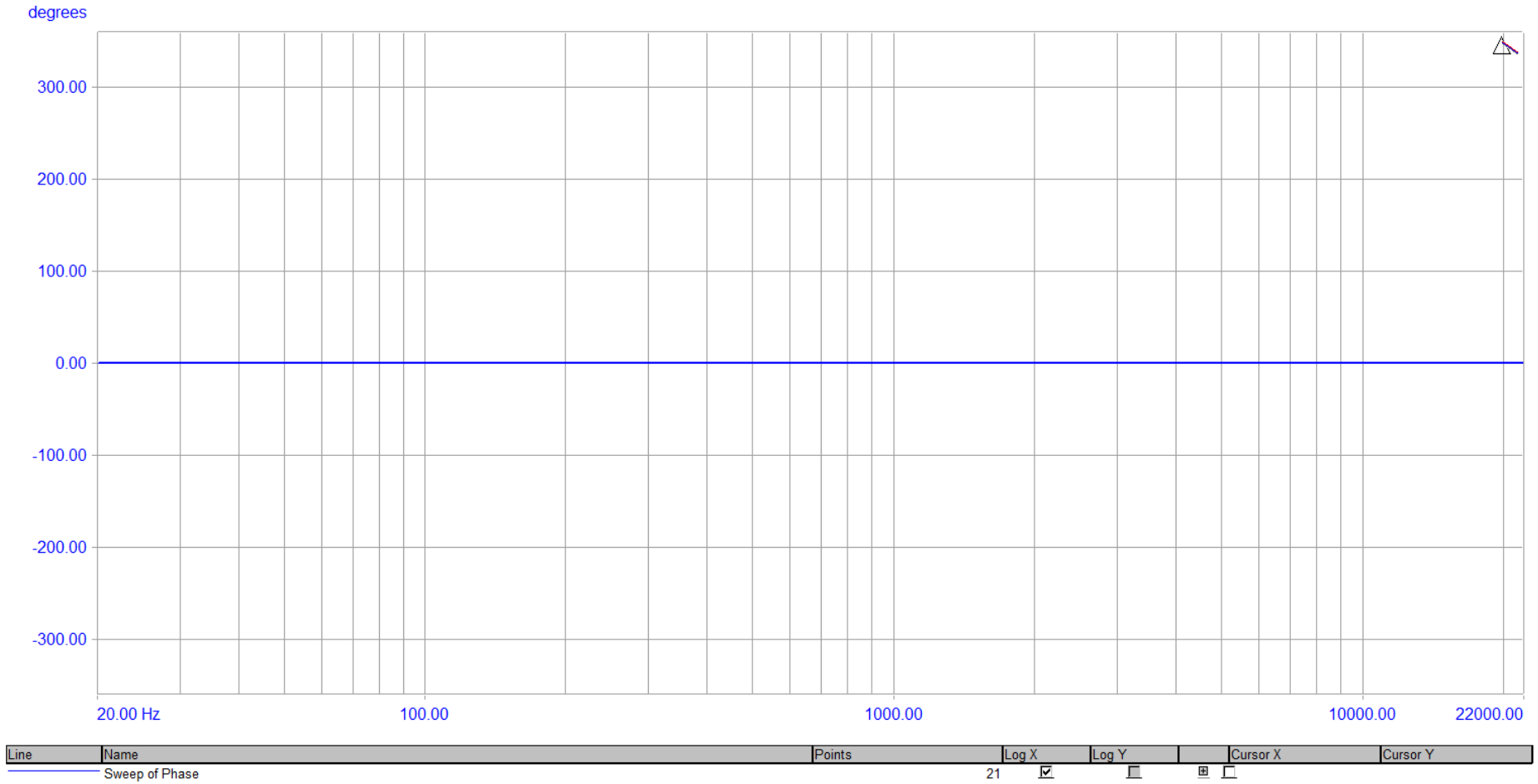


Figure 43. Test Circuit- Phase Response- 0dB Gain

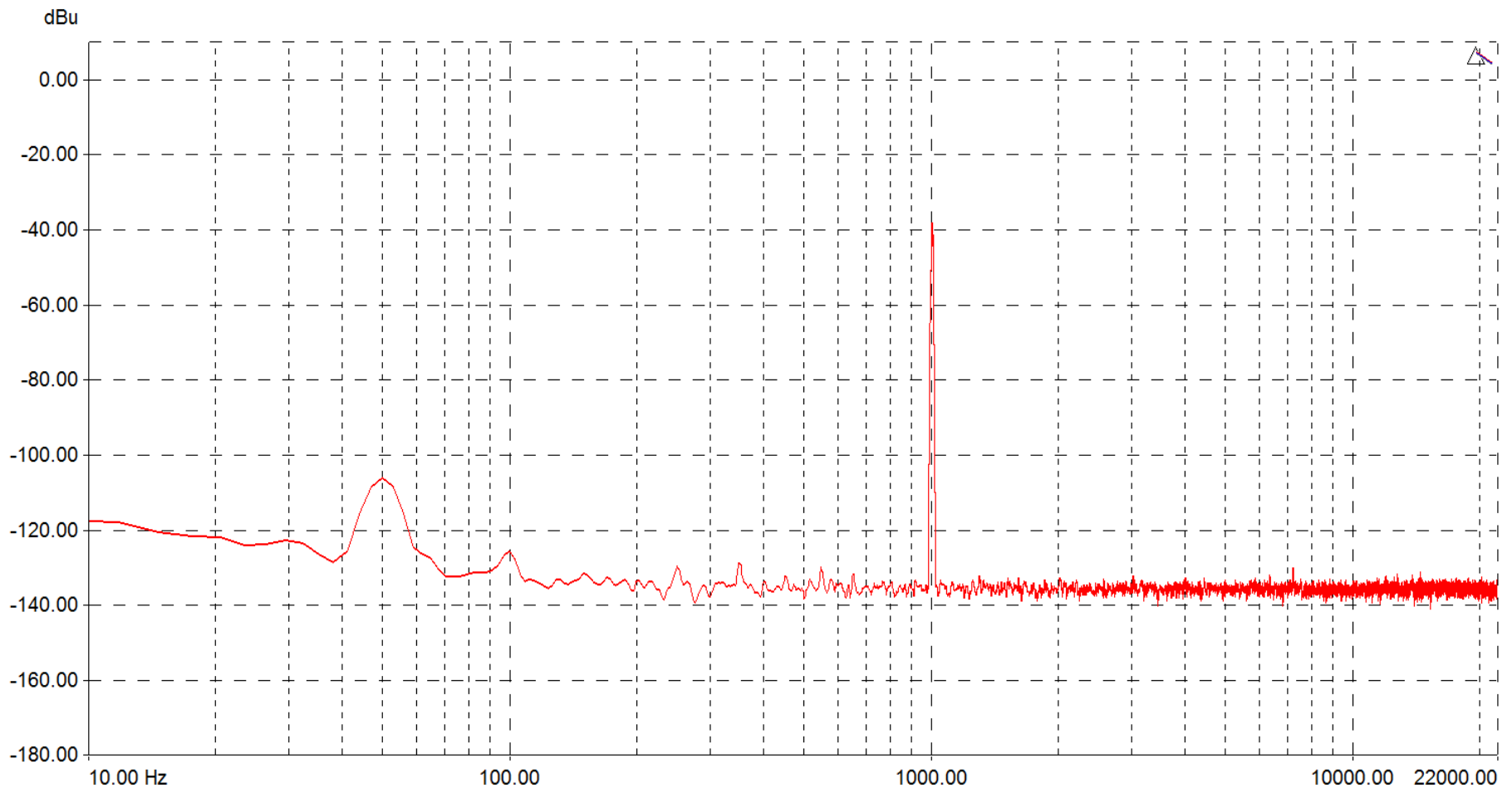


Figure 44. Test Circuit- FFT at 1kHz -38dBu Input- 0dB Gain

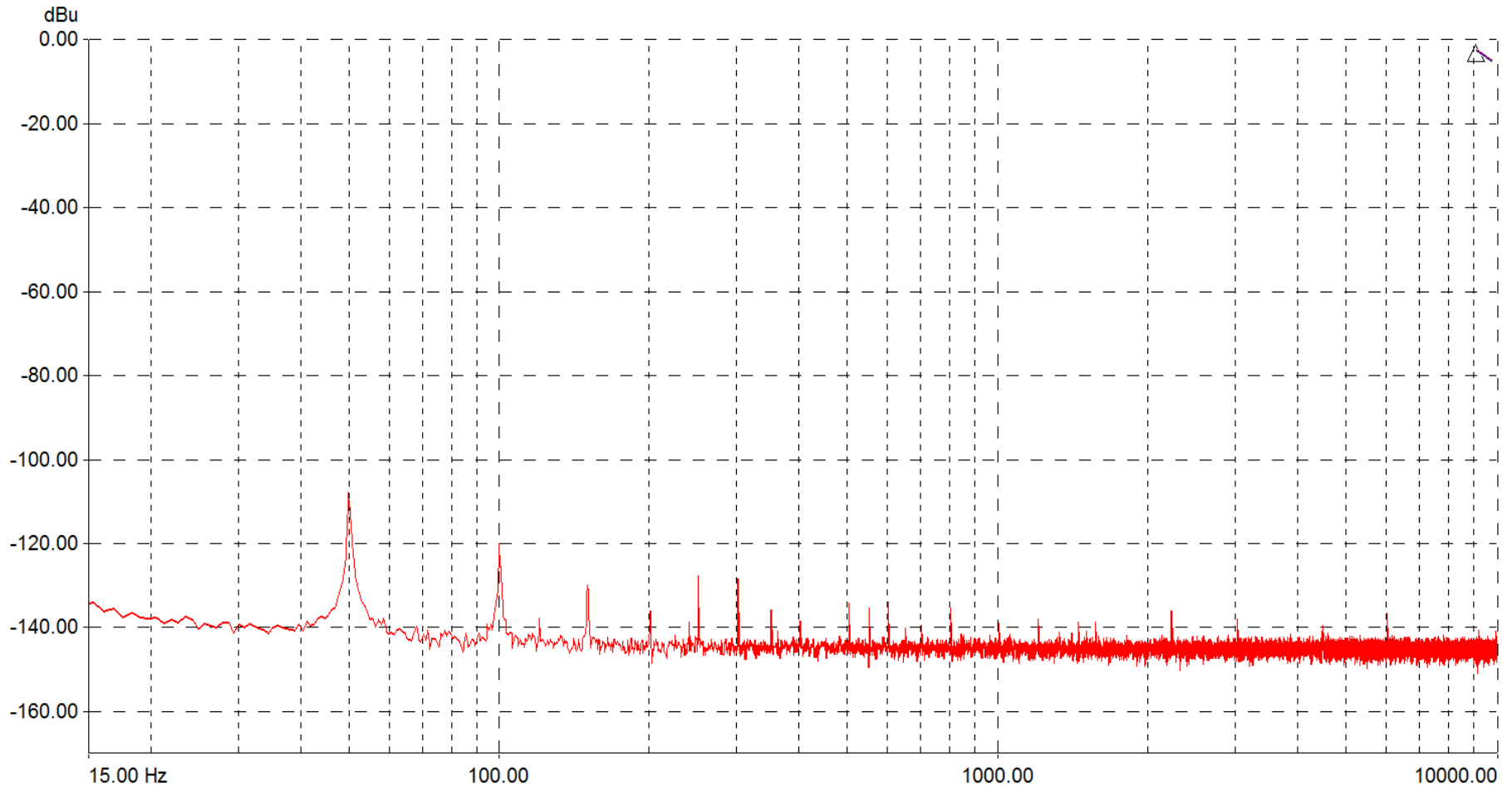


Figure 45. Test Circuit- Jensen MT Test- 0dB Gain

Appendix C- Lundahl LL1582 Measures

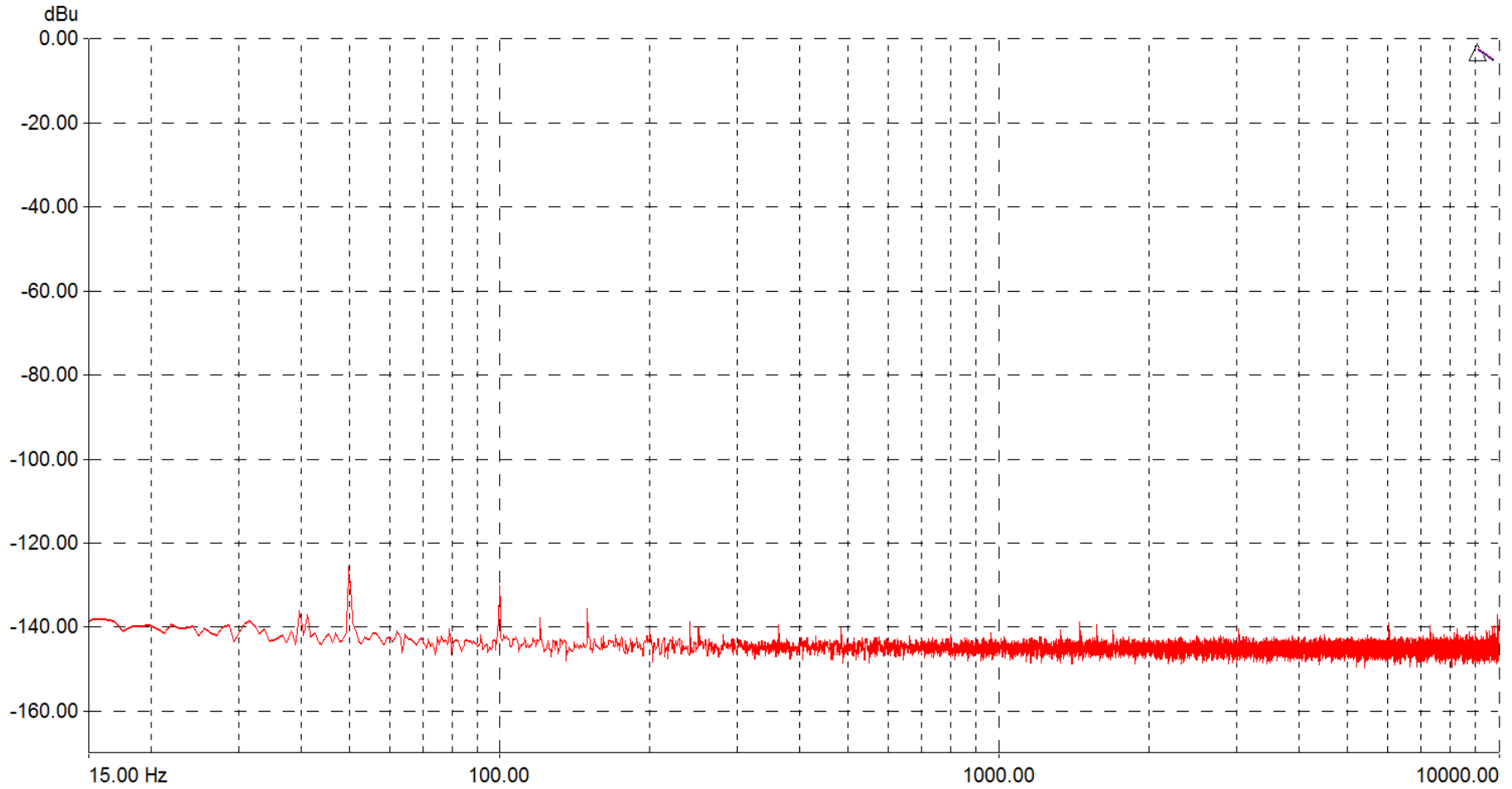


Figure 46. Test Circuit and Lundahl LL1582- Jensen MT Test- 0dB Gain

Frequency Response and Inter-channel Phase

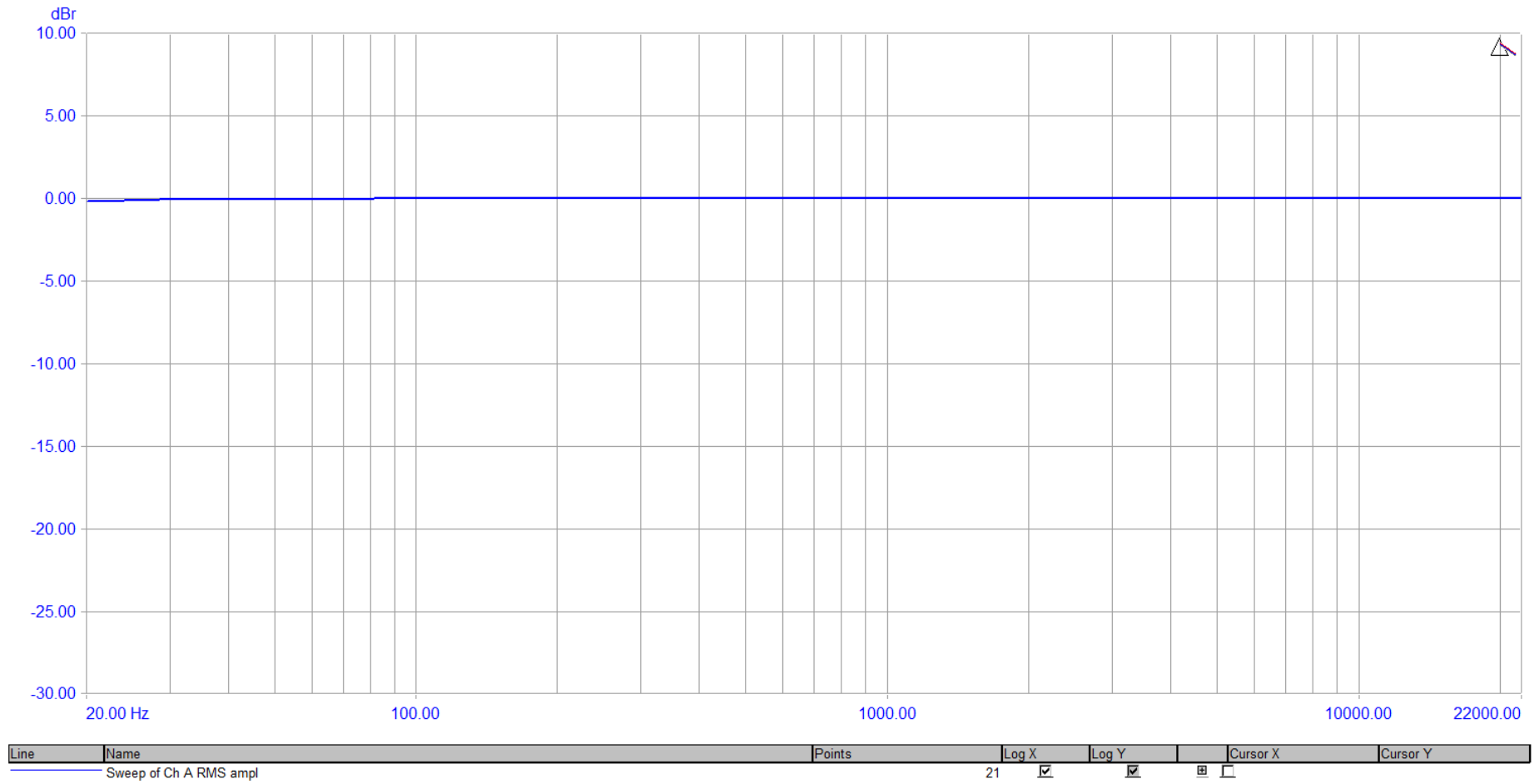
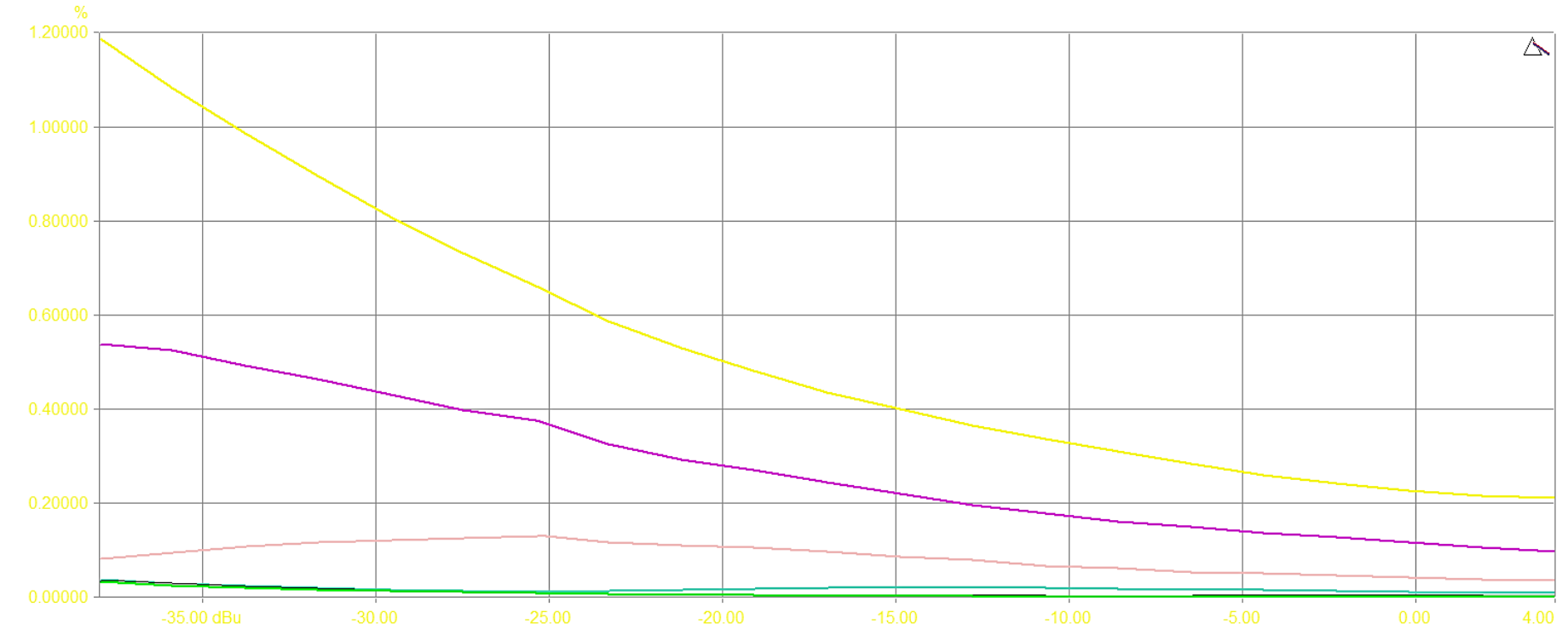


Figure 47. Test Circuit and Lundahl LL1582- Frequency Response- +6dB Gain

THD+N vs Amplitude



Line	Name	Points	Log X	Log Y	Cursor X	Cursor Y
1	Ch A Sweep of CT Det : THD+N - relative : Ch A (Freq[A]=20.00 Hz)	21	<input checked="" type="checkbox"/>	<input type="checkbox"/>	<input type="checkbox"/>	<input type="checkbox"/>
2	Ch A Sweep of CT Det : THD+N - relative : Ch A (Freq[A]=50.00 Hz)	21	<input checked="" type="checkbox"/>	<input type="checkbox"/>	<input type="checkbox"/>	<input type="checkbox"/>
3	Ch A Sweep of CT Det : THD+N - relative : Ch A (Freq[A]=200.00 Hz)	21	<input checked="" type="checkbox"/>	<input type="checkbox"/>	<input type="checkbox"/>	<input type="checkbox"/>
4	Ch A Sweep of CT Det : THD+N - relative : Ch A (Freq[A]=1000.00 Hz)	21	<input checked="" type="checkbox"/>	<input type="checkbox"/>	<input type="checkbox"/>	<input type="checkbox"/>
5	Ch A Sweep of CT Det : THD+N - relative : Ch A (Freq[A]=5000.00 Hz)	21	<input checked="" type="checkbox"/>	<input type="checkbox"/>	<input type="checkbox"/>	<input type="checkbox"/>
6	Ch A Sweep of CT Det : THD+N - relative : Ch A (Freq[A]=10000.00 Hz)	21	<input checked="" type="checkbox"/>	<input type="checkbox"/>	<input type="checkbox"/>	<input type="checkbox"/>
7	Ch A Sweep of CT Det : THD+N - relative : Ch A (Freq[A]=20000.00 Hz)	21	<input checked="" type="checkbox"/>	<input type="checkbox"/>	<input type="checkbox"/>	<input type="checkbox"/>

Figure 48. Test Circuit and Lundahl LL1582- THD+N vs Amplitude- +6dB Gain

Frequency Response and Inter-channel Phase

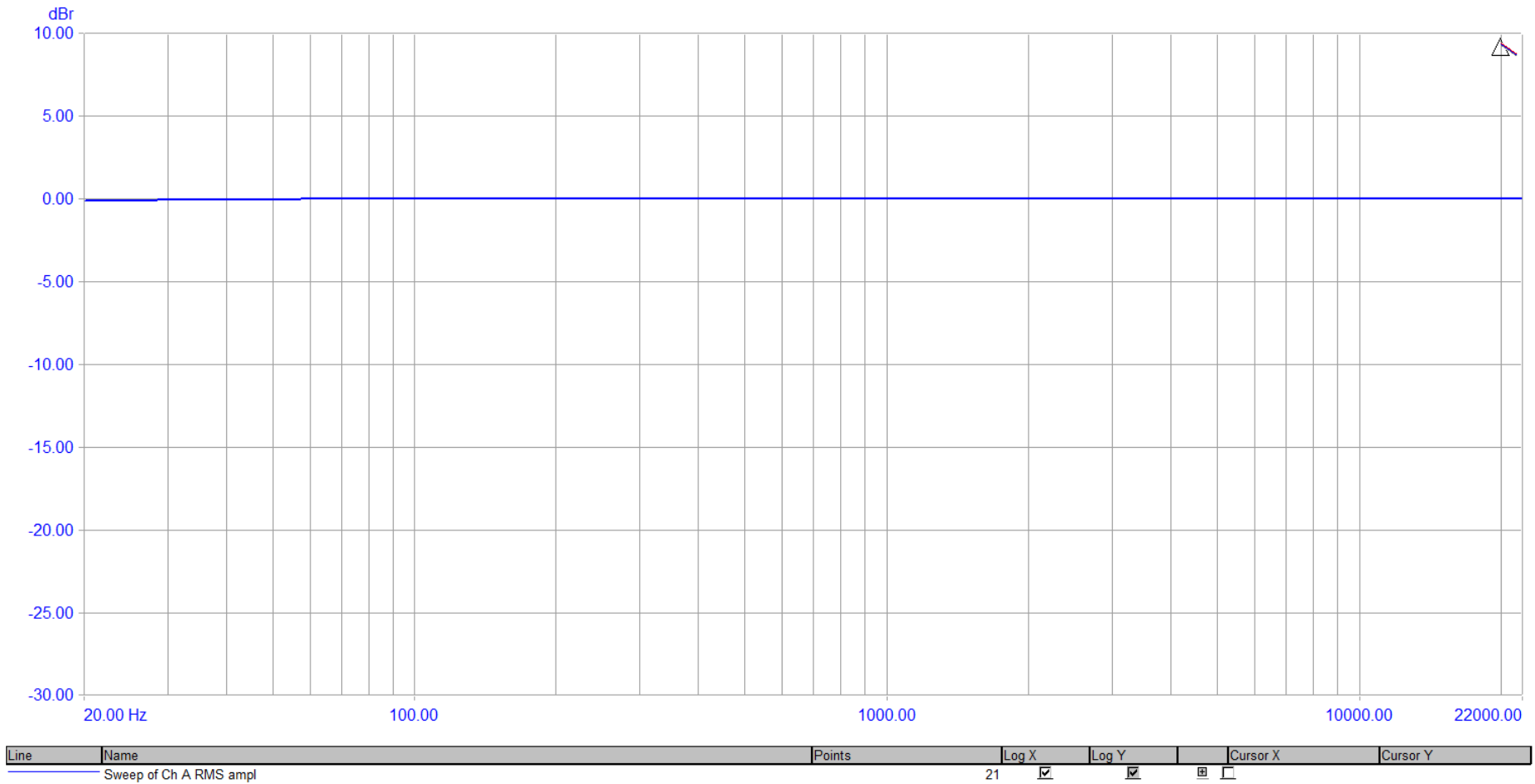


Figure 49. Test Circuit and Lundahl LL1582- Frequency Response- +16dB Gain

Appendix D- Carnhill VTB1148 Measures

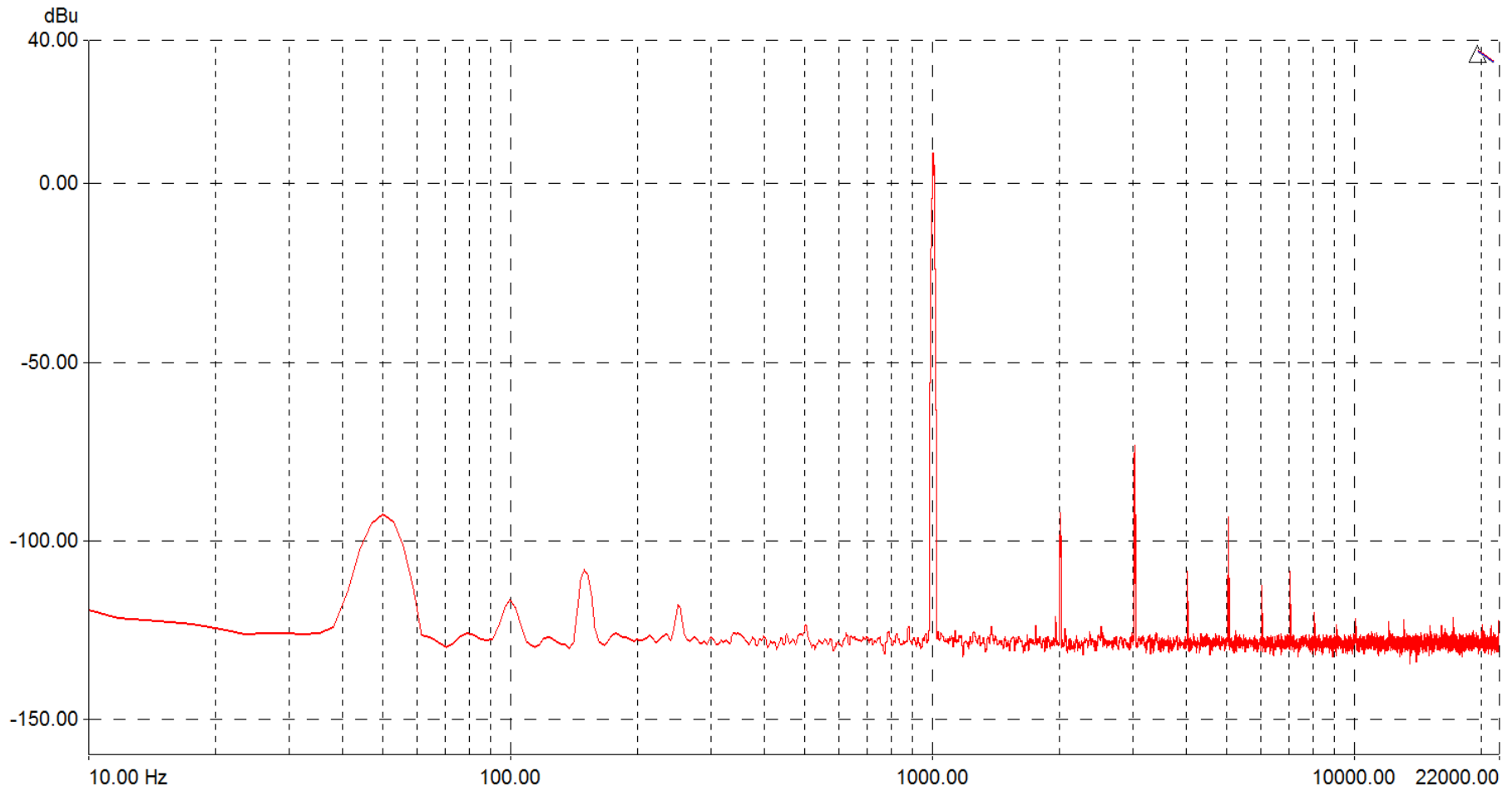


Figure 50. Test Circuit and Carnhill VTB1148- FFT at 1kHz +4dBu Input- 0dB Gain

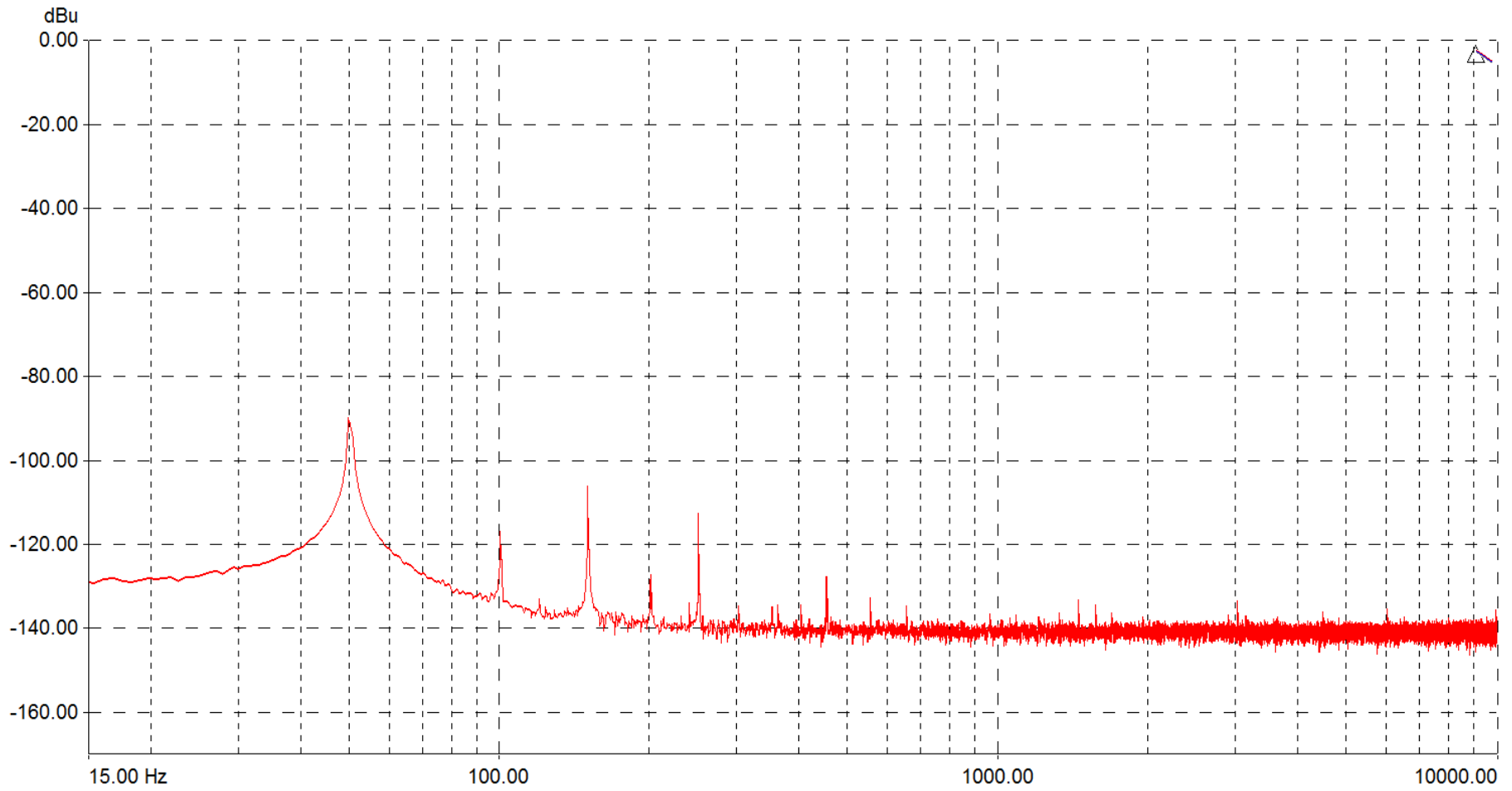
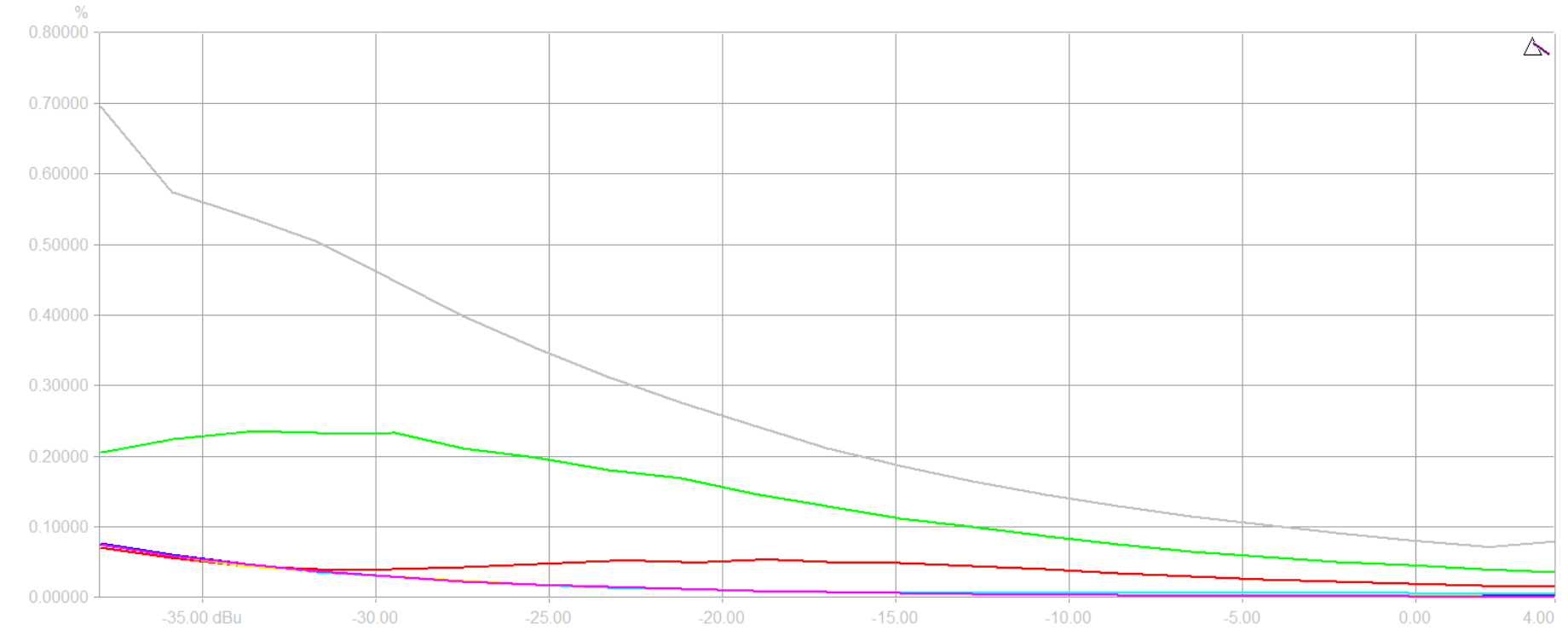


Figure 51. Test Circuit and Carnhill VTB1148- Jensen MT Test- 0dB Gain

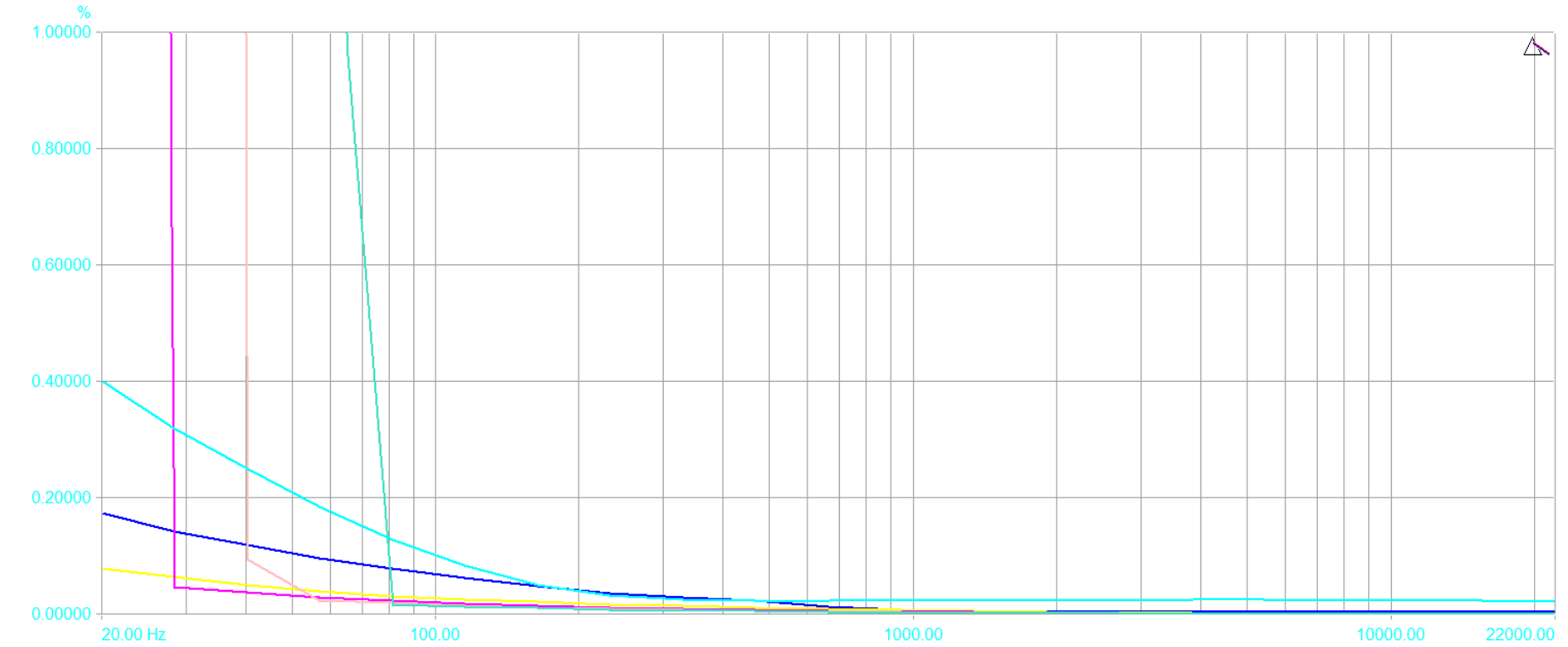
THD+N vs Amplitude



Line	Name	Points	Log X	Log Y	Cursor X	Cursor Y
1	Ch A Sweep of CT Det : THD+N - relative : Ch A (Freq[A]=20.00 Hz)	21	<input checked="" type="checkbox"/>	<input type="checkbox"/>	<input type="checkbox"/>	<input type="checkbox"/>
2	Ch A Sweep of CT Det : THD+N - relative : Ch A (Freq[A]=50.00 Hz)	21	<input checked="" type="checkbox"/>	<input type="checkbox"/>	<input type="checkbox"/>	<input type="checkbox"/>
3	Ch A Sweep of CT Det : THD+N - relative : Ch A (Freq[A]=200.00 Hz)	21	<input checked="" type="checkbox"/>	<input type="checkbox"/>	<input type="checkbox"/>	<input type="checkbox"/>
4	Ch A Sweep of CT Det : THD+N - relative : Ch A (Freq[A]=1000.00 Hz)	21	<input checked="" type="checkbox"/>	<input type="checkbox"/>	<input type="checkbox"/>	<input type="checkbox"/>
5	Ch A Sweep of CT Det : THD+N - relative : Ch A (Freq[A]=5000.00 Hz)	21	<input checked="" type="checkbox"/>	<input type="checkbox"/>	<input type="checkbox"/>	<input type="checkbox"/>
6	Ch A Sweep of CT Det : THD+N - relative : Ch A (Freq[A]=10000.00 Hz)	21	<input checked="" type="checkbox"/>	<input type="checkbox"/>	<input type="checkbox"/>	<input type="checkbox"/>
7	Ch A Sweep of CT Det : THD+N - relative : Ch A (Freq[A]=20000.00 Hz)	21	<input checked="" type="checkbox"/>	<input type="checkbox"/>	<input type="checkbox"/>	<input type="checkbox"/>

Figure 52. Test Circuit and Carnhill VTB1148- THD+N vs Amplitude- +6dB Gain

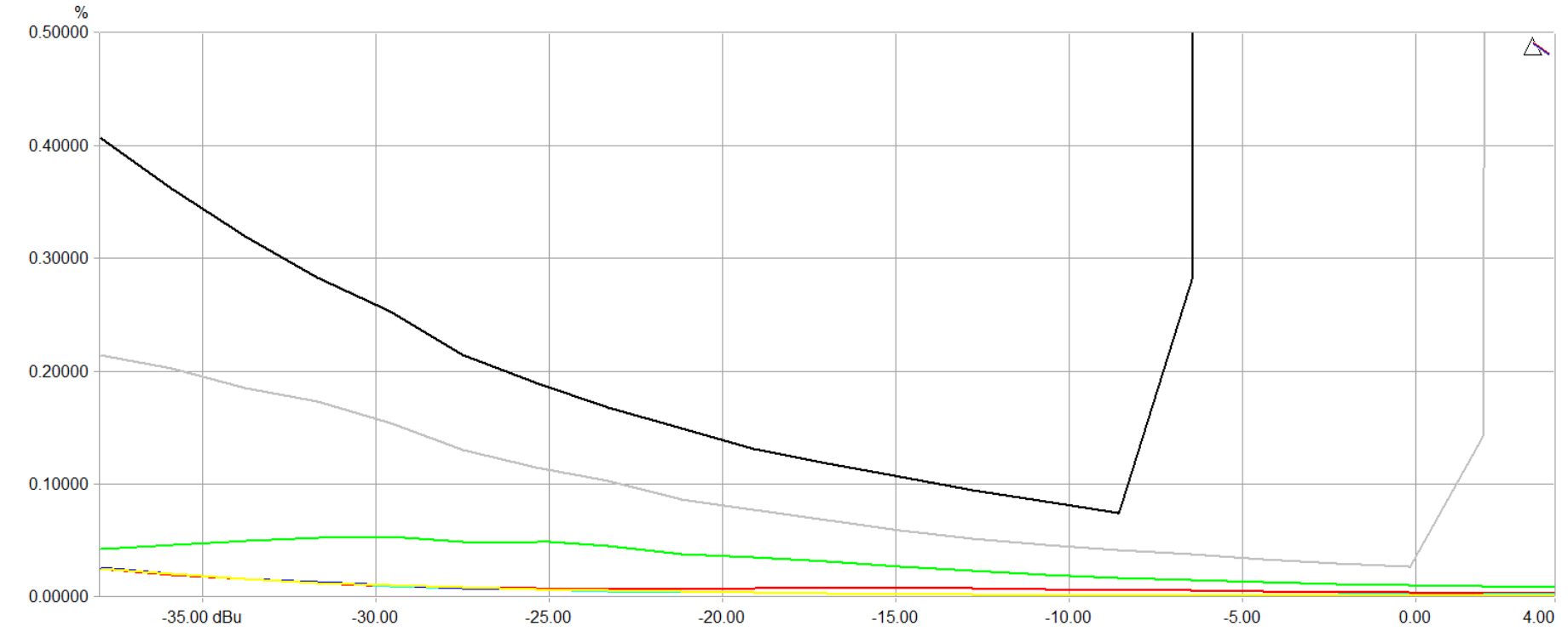
THD+N vs Frequency



Line	Name	Points	Log X	Log Y		Cursor X	Cursor Y
1	Ch A Sweep of CT Det : THD+N - relative : Ch A (Ampl[A]=-38.00 dBu)	21	<input checked="" type="checkbox"/>	<input type="checkbox"/>	<input type="checkbox"/>	<input type="checkbox"/>	<input type="checkbox"/>
2	Ch A Sweep of CT Det : THD+N - relative : Ch A (Ampl[A]=-24.00 dBu)	21	<input checked="" type="checkbox"/>	<input type="checkbox"/>	<input type="checkbox"/>	<input type="checkbox"/>	<input type="checkbox"/>
3	Ch A Sweep of CT Det : THD+N - relative : Ch A (Ampl[A]=-10.00 dBu)	21	<input checked="" type="checkbox"/>	<input type="checkbox"/>	<input type="checkbox"/>	<input type="checkbox"/>	<input type="checkbox"/>
4	Ch A Sweep of CT Det : THD+N - relative : Ch A (Ampl[A]=-4.00 dBu)	21	<input checked="" type="checkbox"/>	<input type="checkbox"/>	<input type="checkbox"/>	<input type="checkbox"/>	<input type="checkbox"/>
5	Ch A Sweep of CT Det : THD+N - relative : Ch A (Ampl[A]=0.00 dBu)	21	<input checked="" type="checkbox"/>	<input type="checkbox"/>	<input type="checkbox"/>	<input type="checkbox"/>	<input type="checkbox"/>
6	Ch A Sweep of CT Det : THD+N - relative : Ch A (Ampl[A]=4.00 dBu)	21	<input checked="" type="checkbox"/>	<input type="checkbox"/>	<input type="checkbox"/>	<input type="checkbox"/>	<input type="checkbox"/>

Figure 53. Test Circuit and Carnhill VTB1148- THD+N vs Frequency- +16dB Gain

THD+N vs Amplitude



Line	Name	Points	Log X	Log Y	Cursor X	Cursor Y
1	Ch A Sweep of CT Det : THD+N - relative : Ch A (Freq[A]=20.00 Hz)	21	<input checked="" type="checkbox"/>	<input type="checkbox"/>	<input type="checkbox"/>	<input type="checkbox"/>
2	Ch A Sweep of CT Det : THD+N - relative : Ch A (Freq[A]=50.00 Hz)	21	<input checked="" type="checkbox"/>	<input type="checkbox"/>	<input type="checkbox"/>	<input type="checkbox"/>
3	Ch A Sweep of CT Det : THD+N - relative : Ch A (Freq[A]=200.00 Hz)	21	<input checked="" type="checkbox"/>	<input type="checkbox"/>	<input type="checkbox"/>	<input type="checkbox"/>
4	Ch A Sweep of CT Det : THD+N - relative : Ch A (Freq[A]=1000.00 Hz)	21	<input checked="" type="checkbox"/>	<input type="checkbox"/>	<input type="checkbox"/>	<input type="checkbox"/>
5	Ch A Sweep of CT Det : THD+N - relative : Ch A (Freq[A]=5000.00 Hz)	21	<input checked="" type="checkbox"/>	<input type="checkbox"/>	<input type="checkbox"/>	<input type="checkbox"/>
6	Ch A Sweep of CT Det : THD+N - relative : Ch A (Freq[A]=10000.00 Hz)	21	<input checked="" type="checkbox"/>	<input type="checkbox"/>	<input type="checkbox"/>	<input type="checkbox"/>
7	Ch A Sweep of CT Det : THD+N - relative : Ch A (Freq[A]=20000.00 Hz)	21	<input checked="" type="checkbox"/>	<input type="checkbox"/>	<input type="checkbox"/>	<input type="checkbox"/>

Figure 54. Test Circuit and Carnhill VTBI148- THD+N vs Amplitude- +16dB Gain

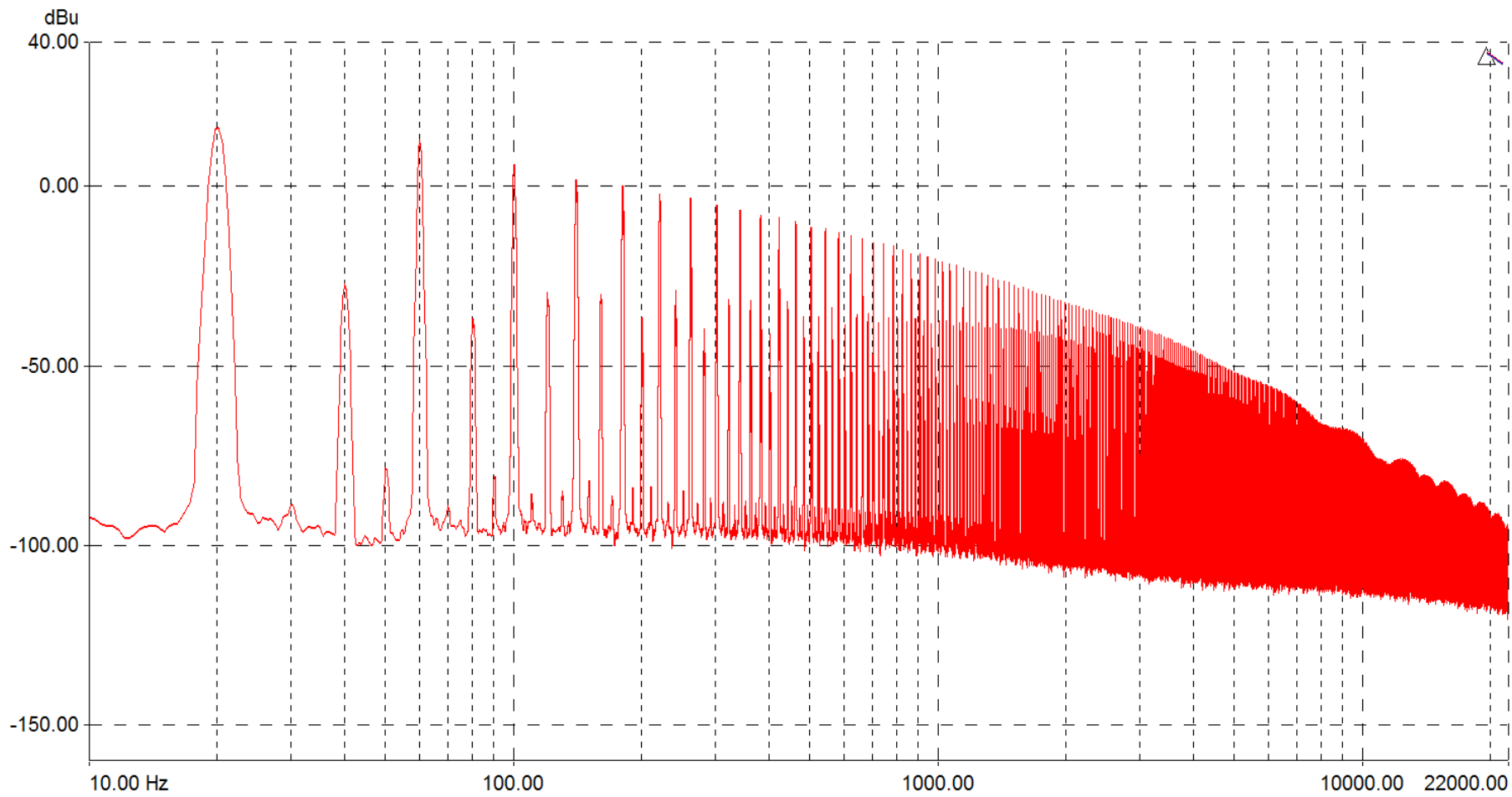


Figure 55. Test Circuit and Carnhill VTB1148- FFT at 20Hz +4dBu Input- +16dB Gain

Appendix E- Spectrogram Analysis

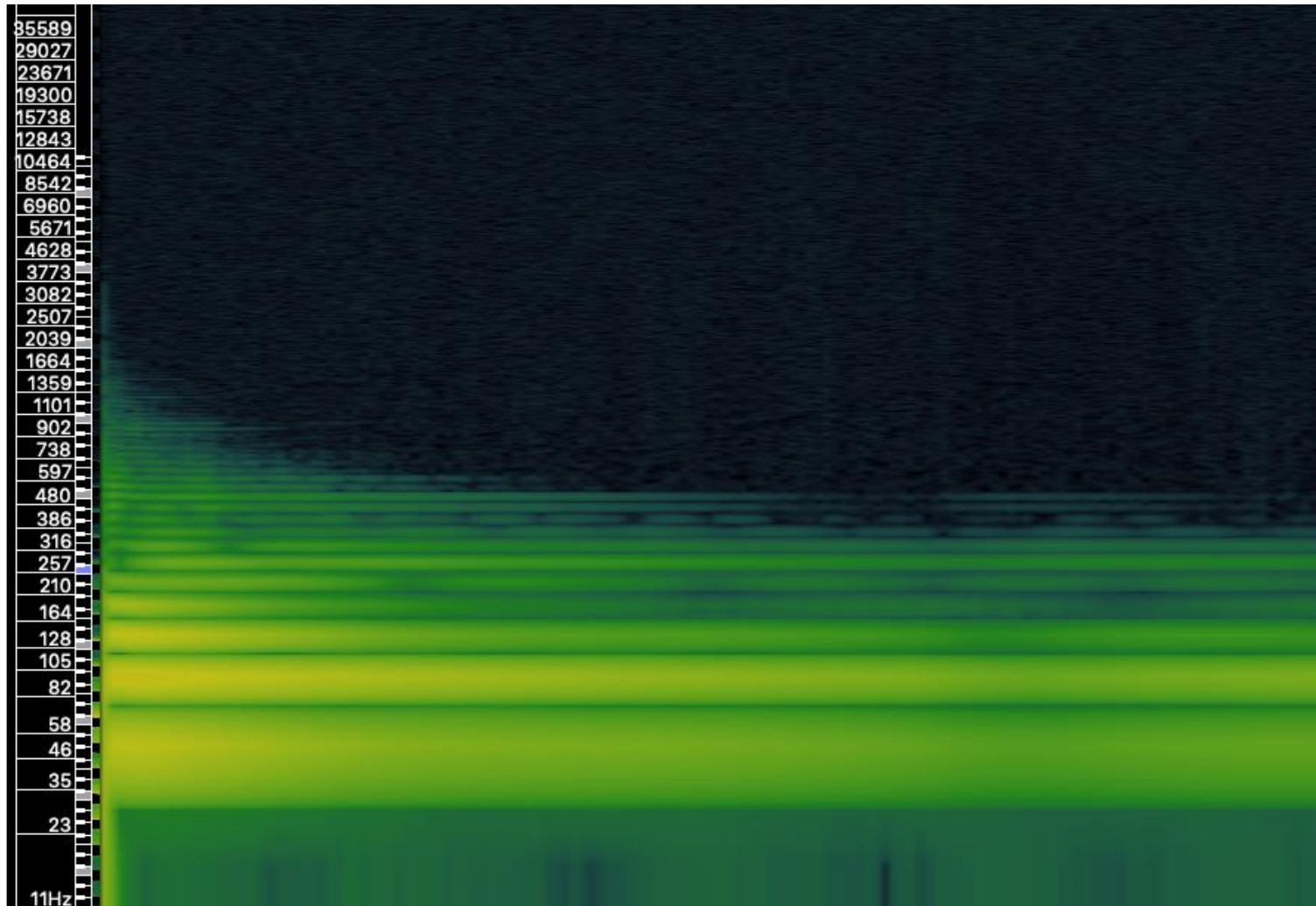


Figure 56. Test Circuit- Bass Sample- 0dB Gain

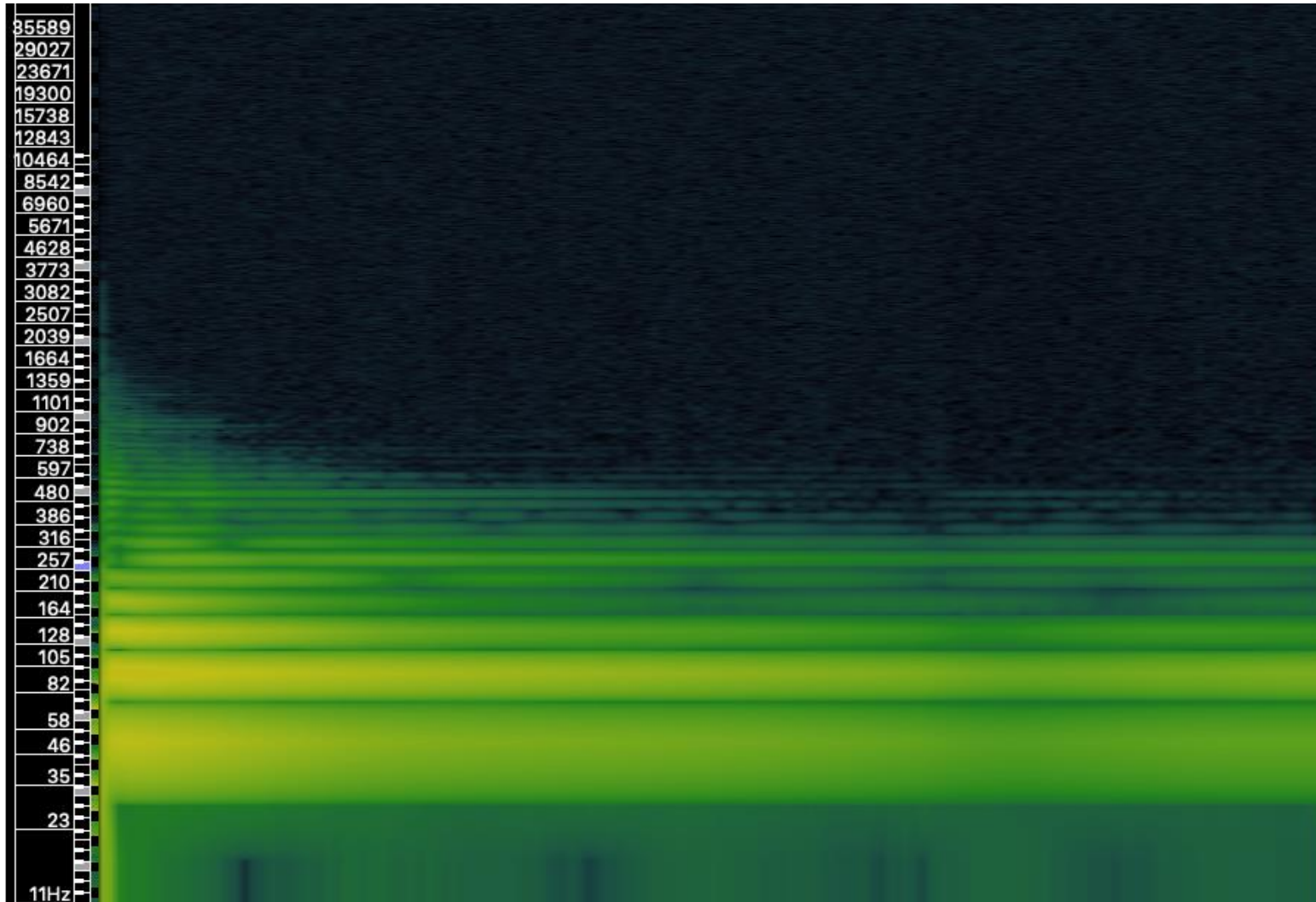


Figure 57. Test Circuit and Lundahl LL1582- Bass Sample- 0dB Gain

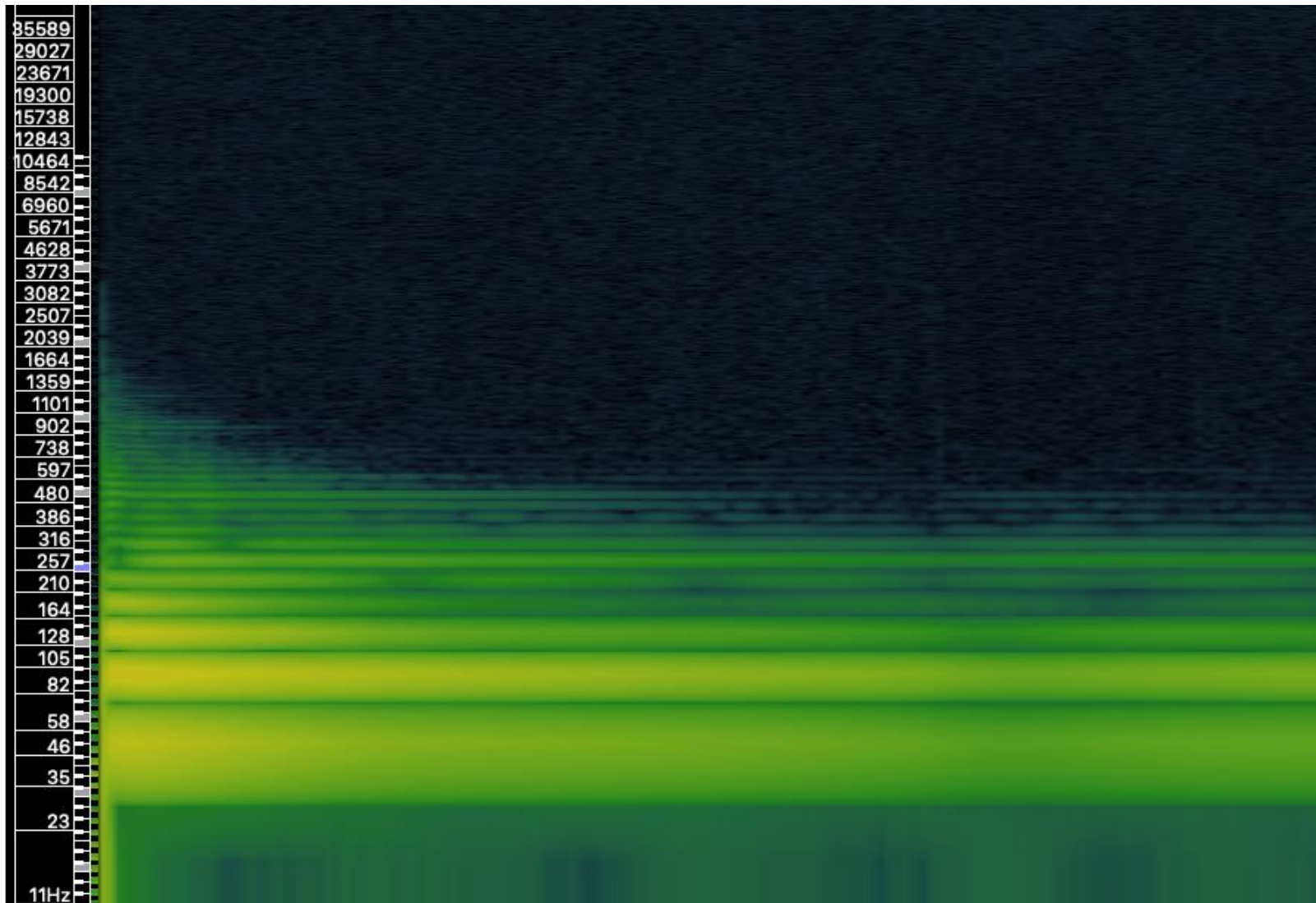


Figure 58. Test Circuit and Lundahl LL1582- Bass Sample- +6dB Gain

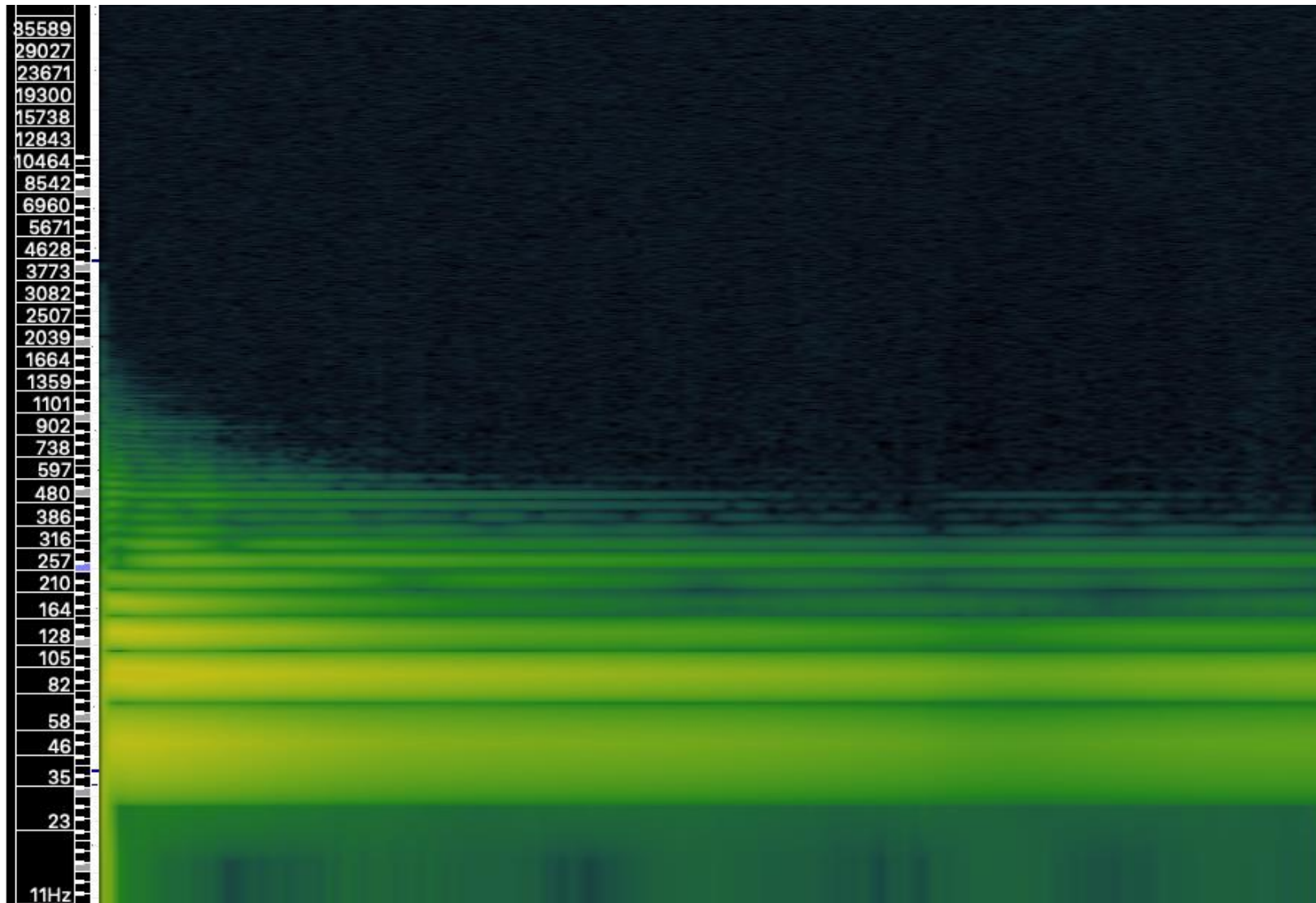


Figure 59. Test Circuit and Lundahl LL1582- Bass Sample- +16dB Gain

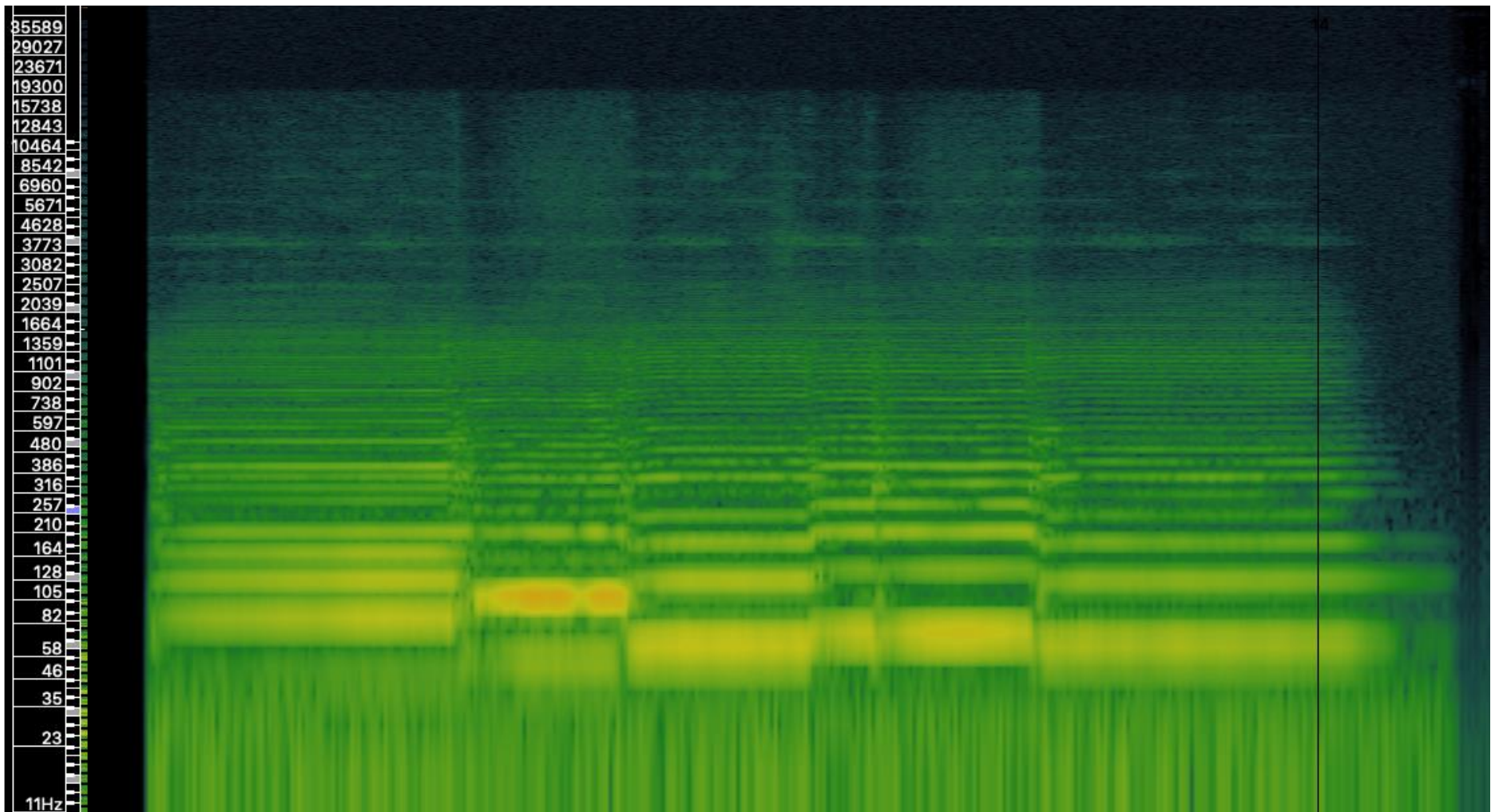


Figure 60. Test Circuit- Double Bass Sample- 0dB Gain

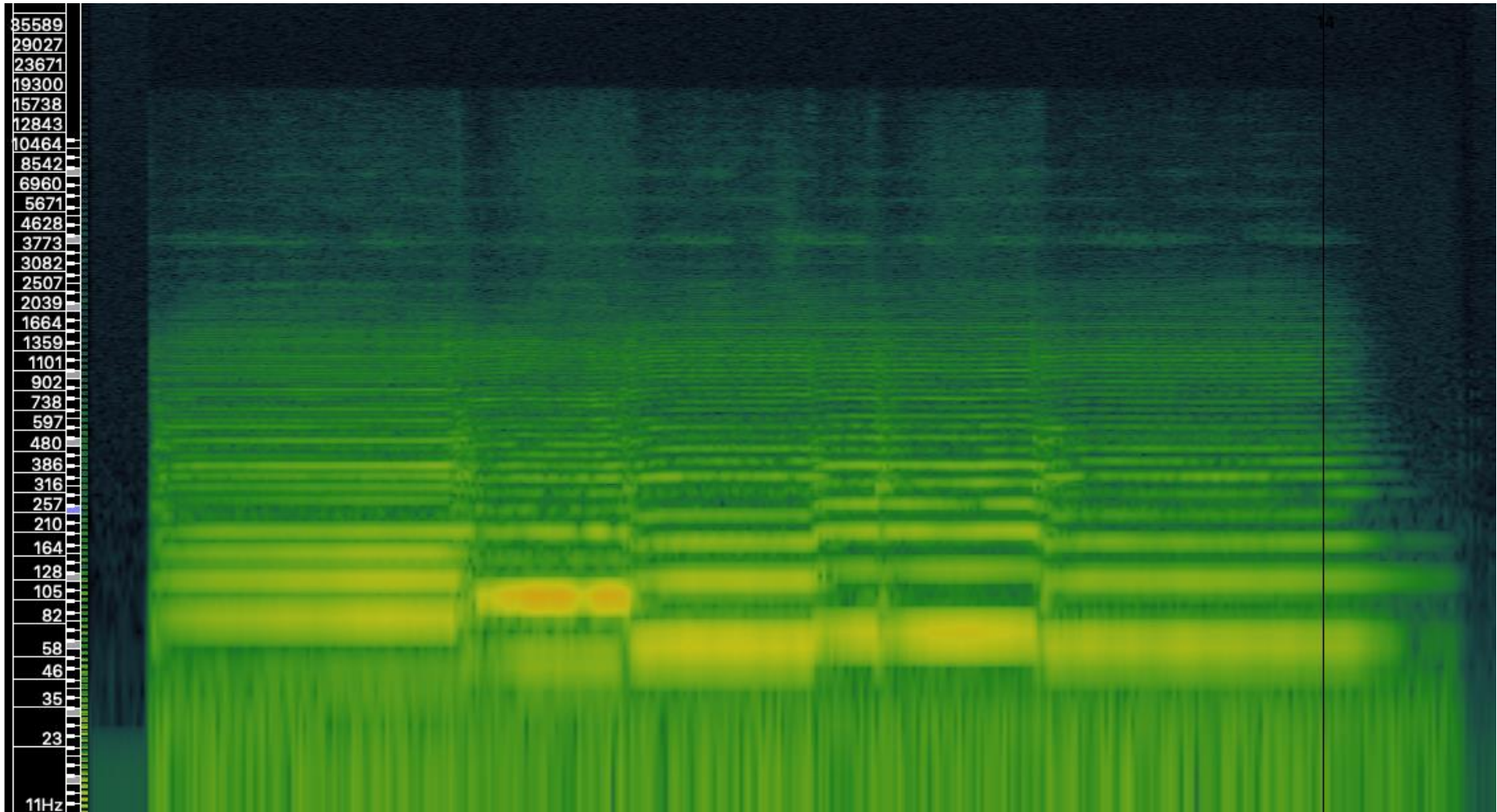


Figure 61. Test Circuit and Lundahl LL1582- Double Bass Sample- 0dB Gain

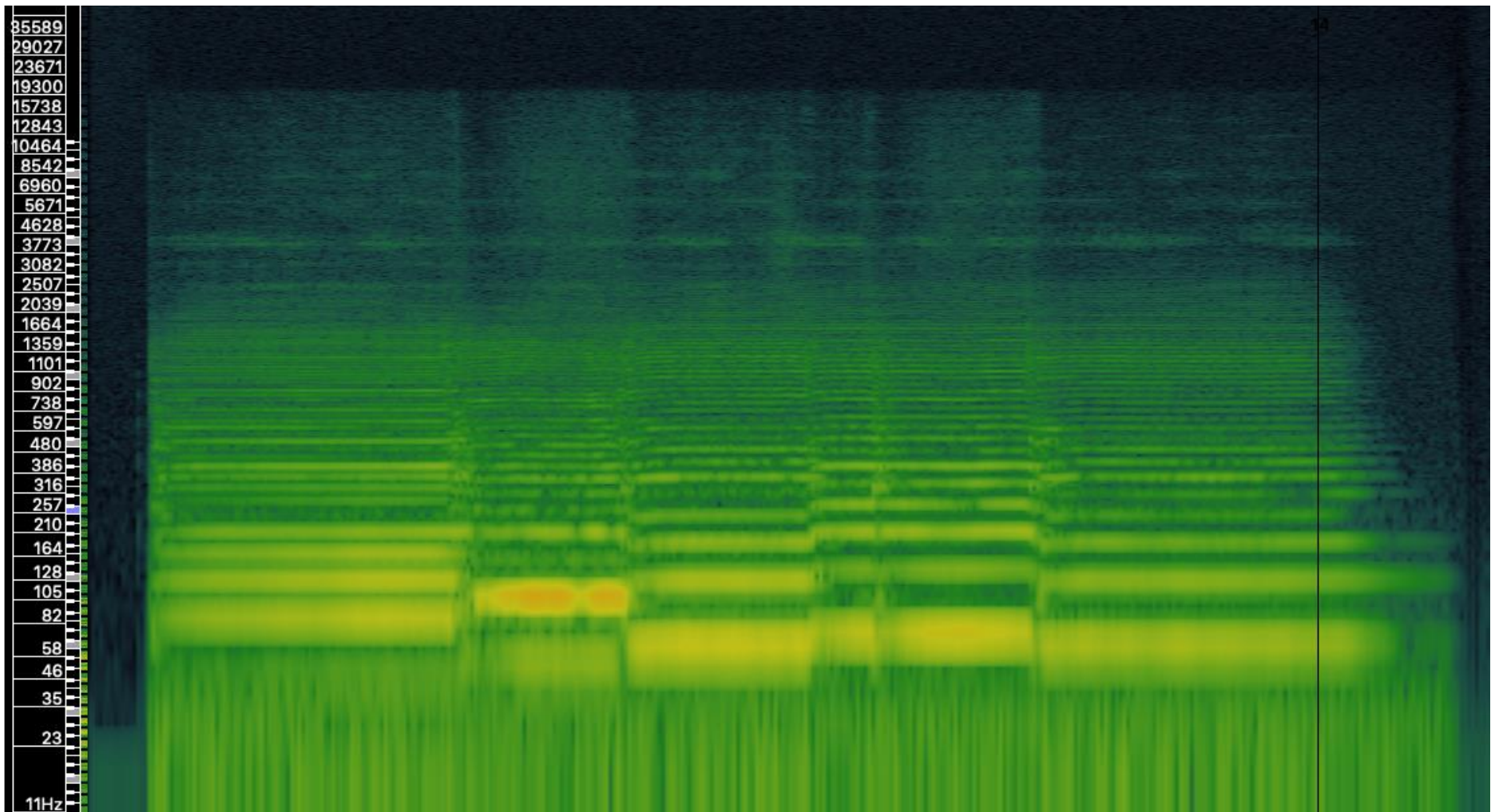


Figure 62. Test Circuit and Lundahl LL1582- Double Bass Sample- +6dB Gain

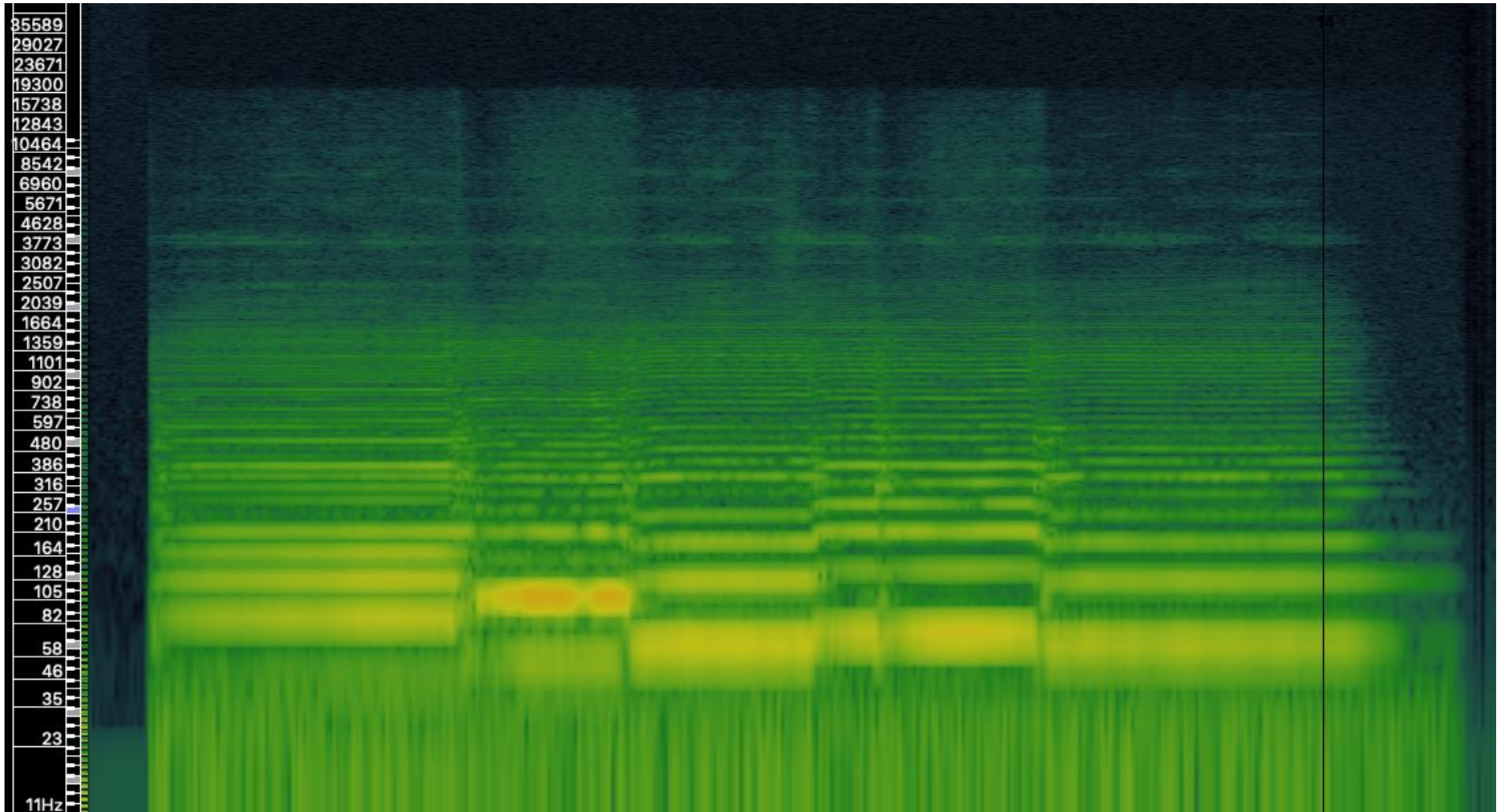


Figure 63. Test Circuit and Lundahl LL1582- Double Bass Sample- +16dB Gain

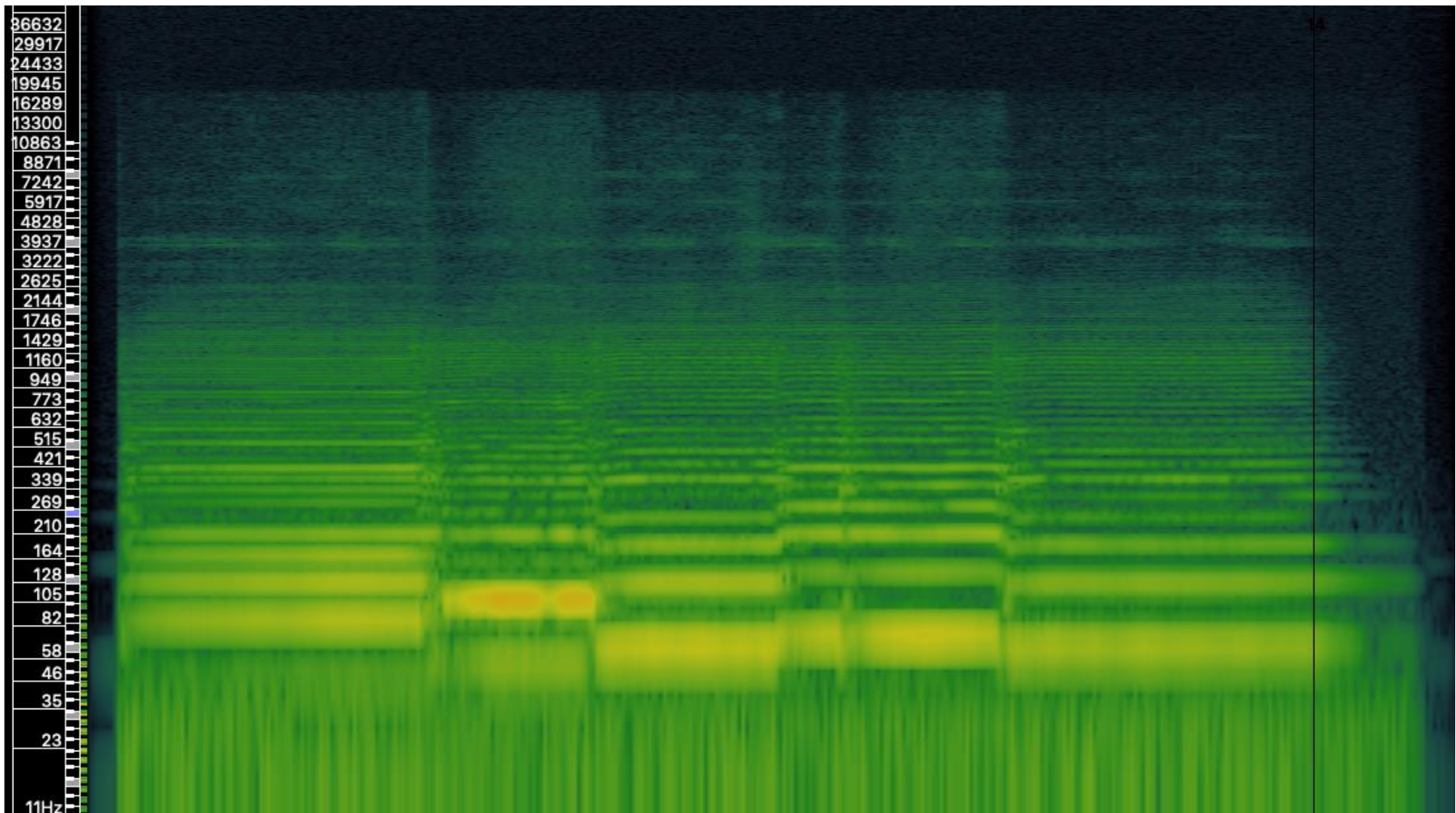


Figure 64. Test Circuit and Carnhill VTB1148- Double Bass Sample- 0dB Gain

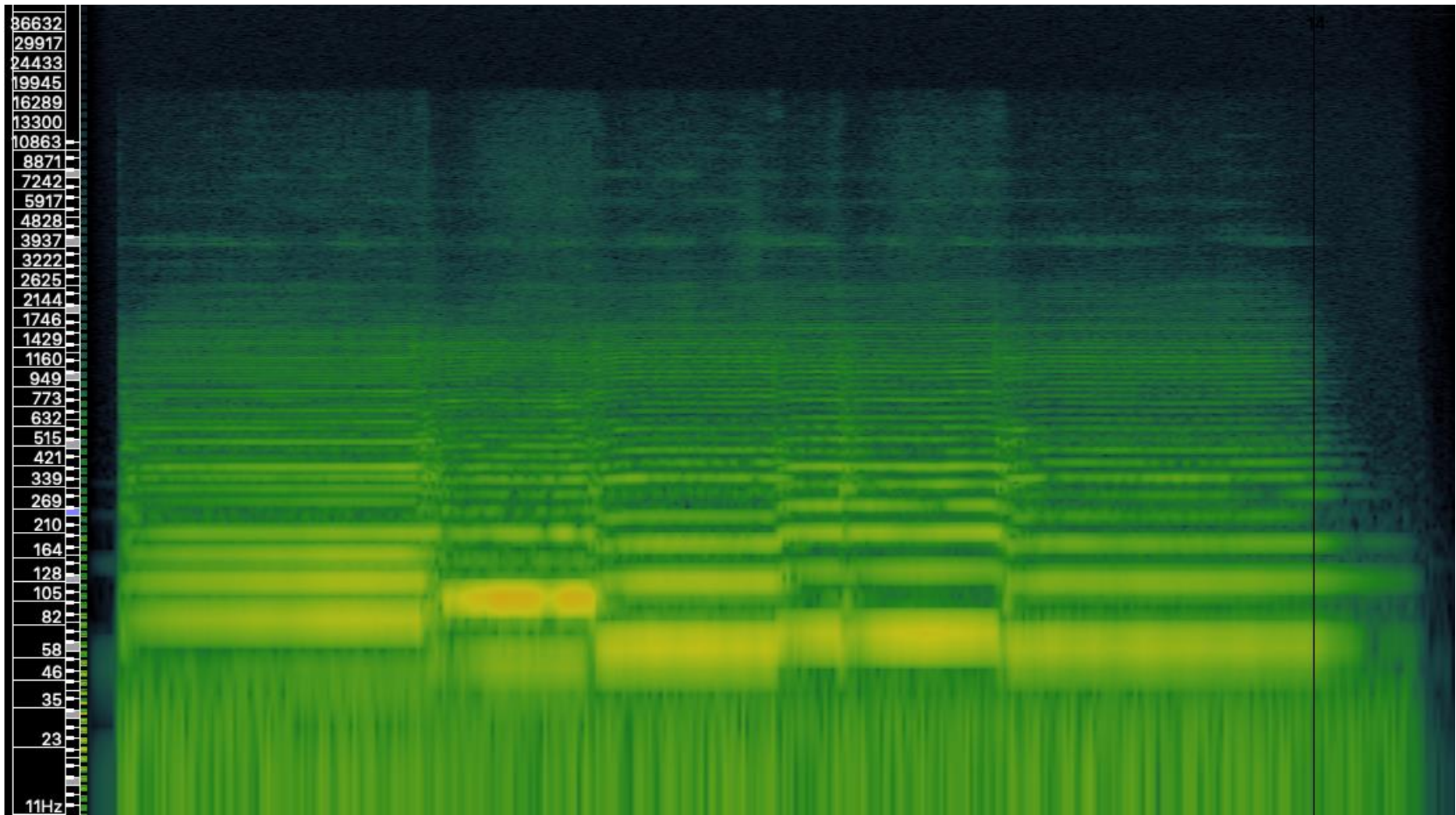


Figure 65. Test Circuit and Carnhill VTB1148- Double Bass Sample- +6dB Gain

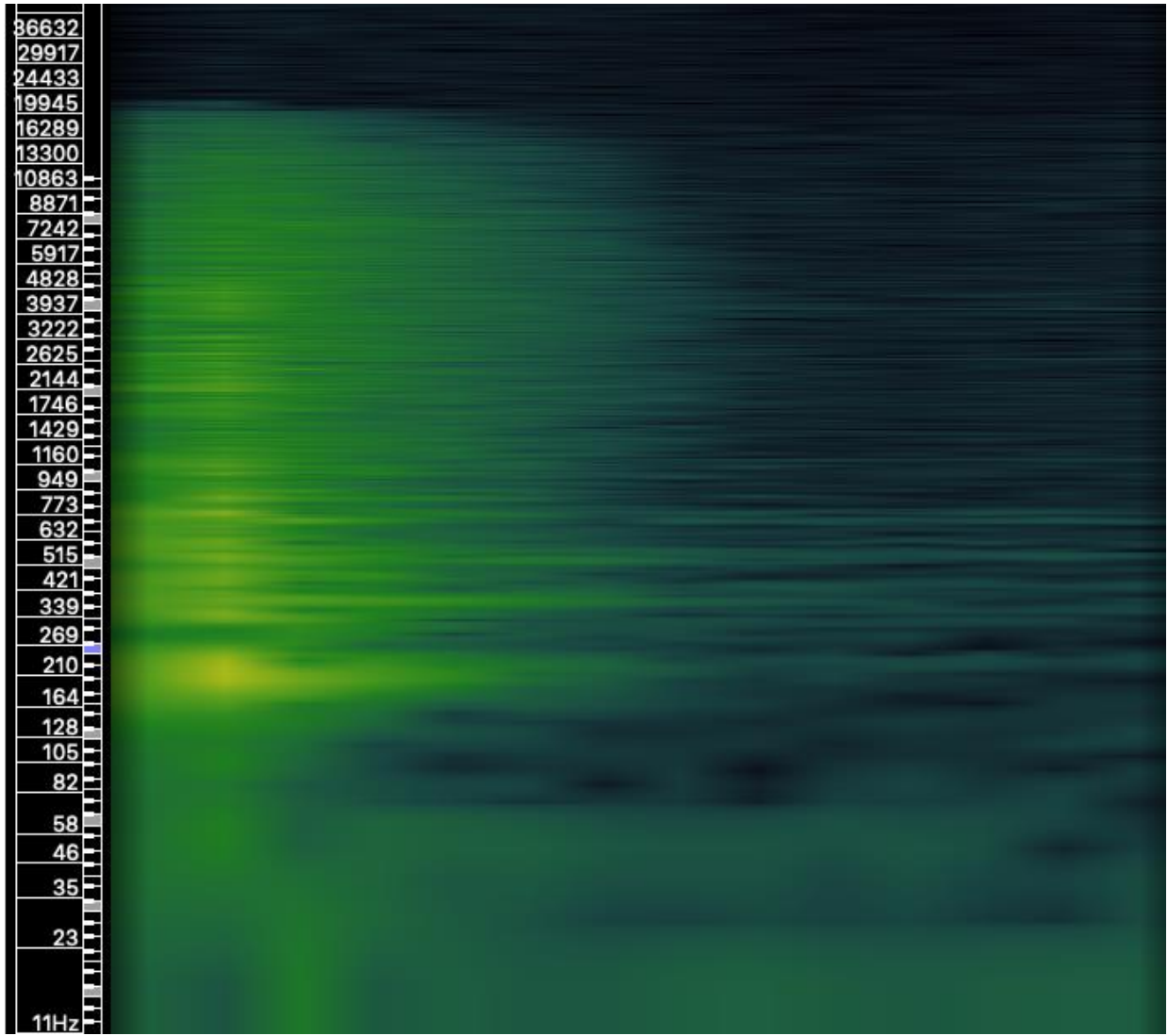


Figure 66. Test Circuit- Snare Drum Sample- 0dB Gain

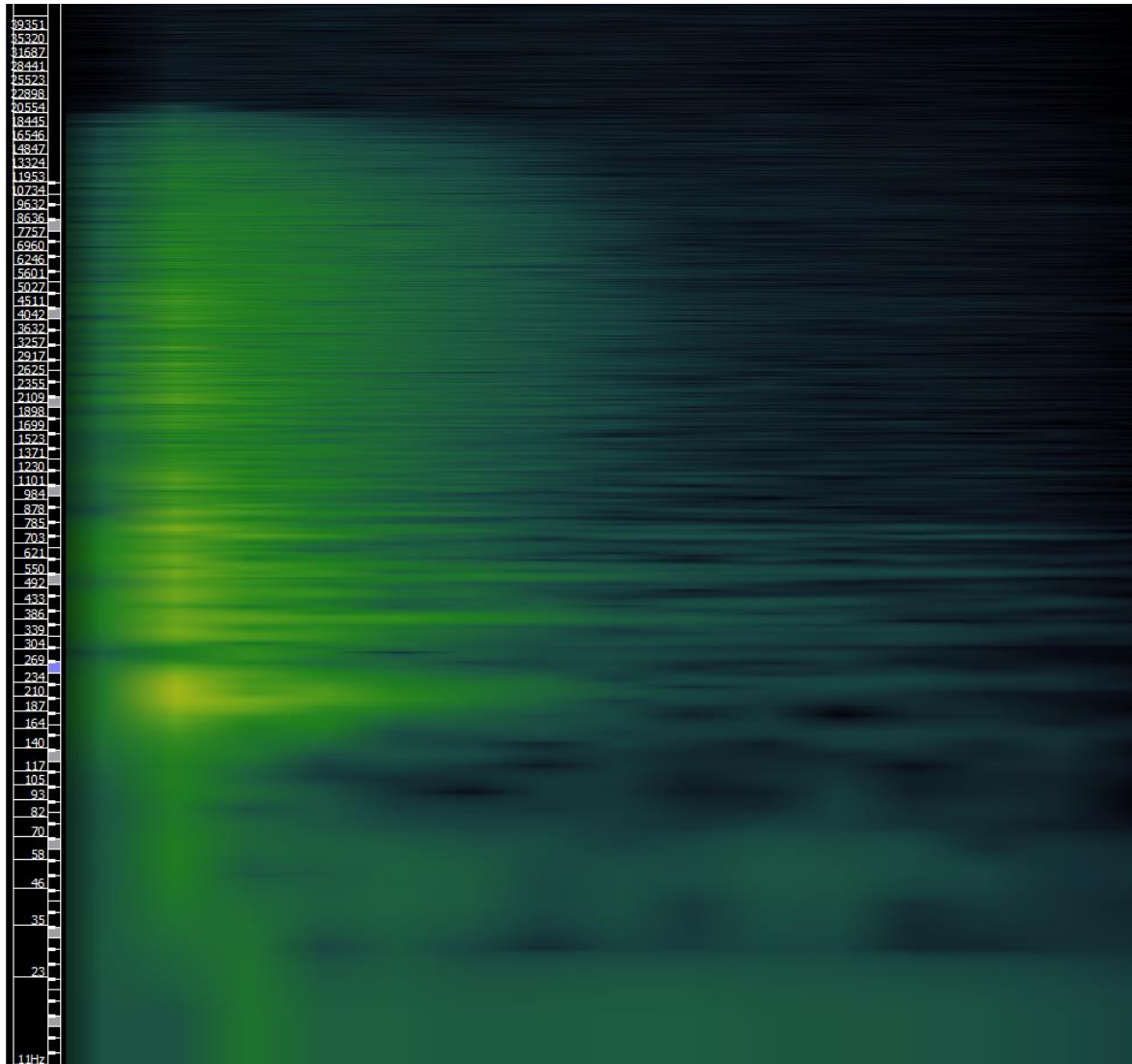


Figure 67. Test Circuit and Carnhill VTB1148- Snare Drum Sample- 0dB Gain

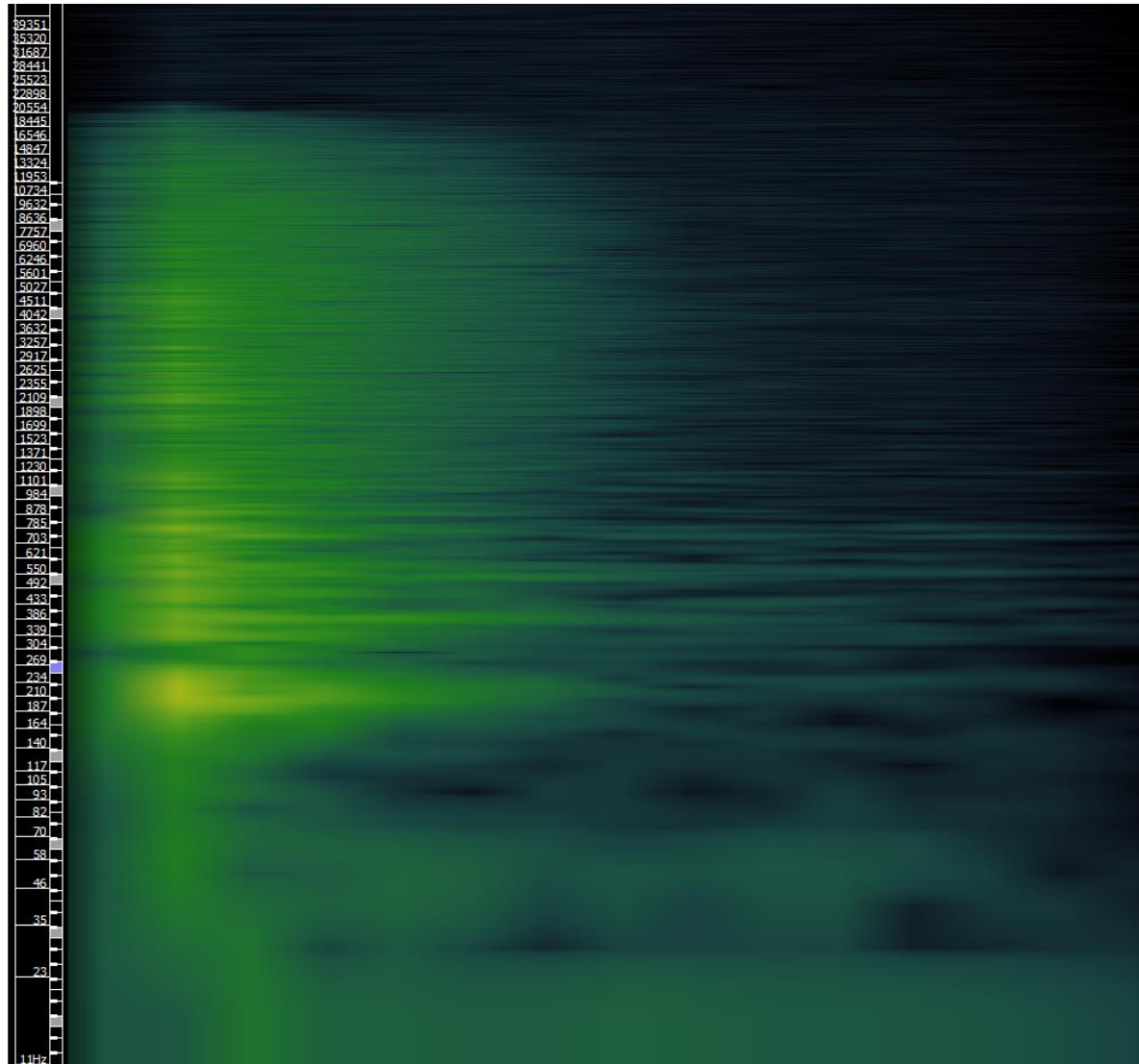


Figure 68. Test Circuit and Carnhill VTB1148- Snare Drum Sample- +6dB Gain